Record 2001/10

Gold Deposits of the Pilbara Craton:

Results of AGSO Research, 1998-2000

David Huston, Richard Blewett, Terrence Mernaugh, Shen-Su Sun and Julienne Kamprad

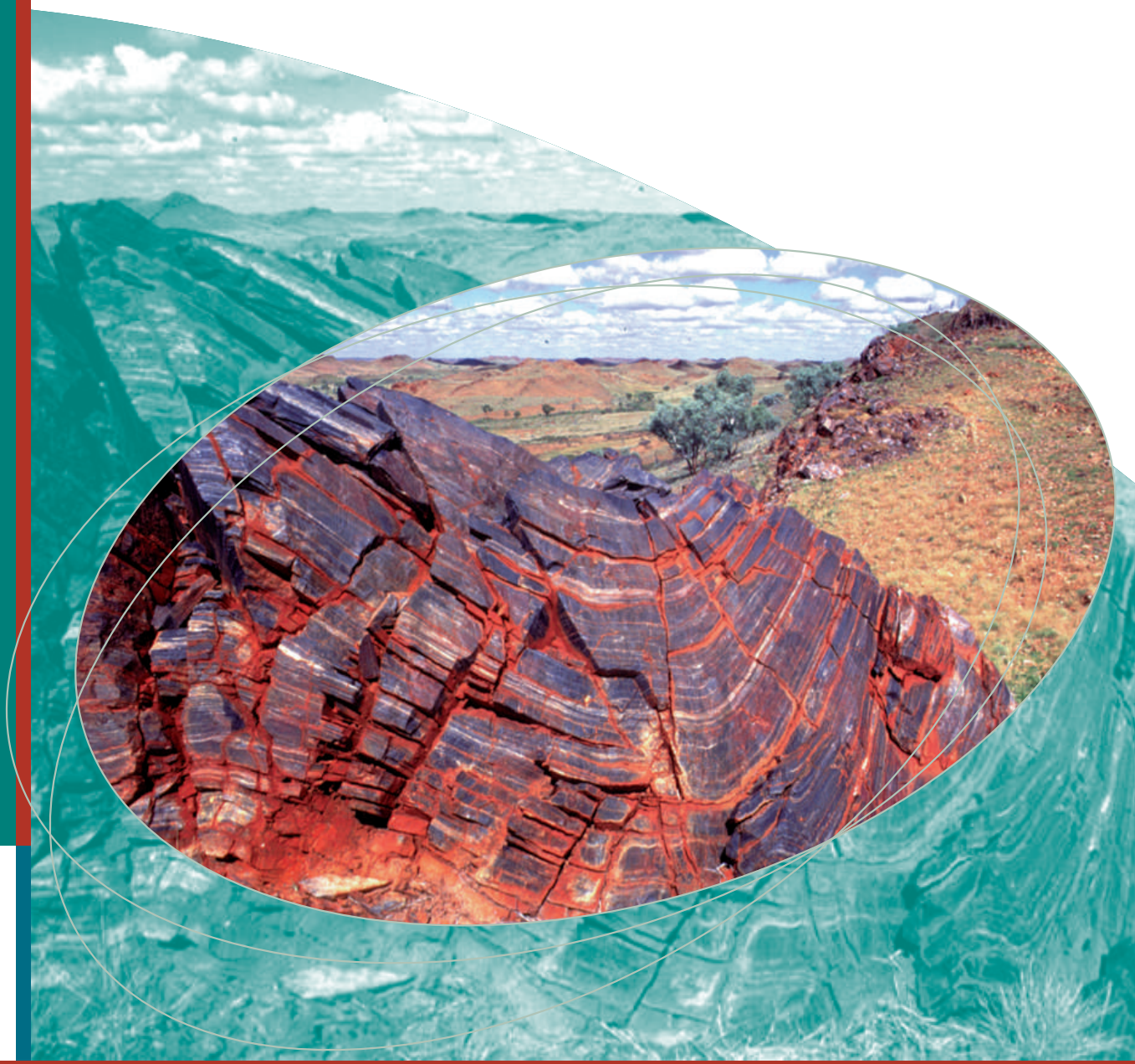

AGSO

AGSO
GEOSCIENCE AUSTRALIA

AGSO – GEOSCIENCE AUSTRALIA

Chief Executive Officer: Neil Williams

ISSN 1039–0073
ISBN 0 642 39888 7

Bibliographic reference: David Huston, Richard Blewett, Terrence Mernagh, Shen-Su Sun and Julienne Kamprad 2001. Gold Deposits of the Pilbara Craton: Results of AGSO Research, 1998-2000. AGSO – Geoscience Australia, Record 2001/10.

Table of Contents

Introduction

The Palaeo- to Mesoarchaean North Pilbara Terrane of the Pilbara Craton in Western Australia (**Fig. 1a**) has historically been a poor cousin to the Eastern Goldfields Province (Yilgarn Craton) in terms of Au production and perceived exploration potential. However, in recent years, significant amounts of Au have been produced at the Bamboo Creek deposit (7.05 t Au total production; Williams, 1998), the Golden Spec deposit (2.06 t Au to 1987) and the Lynas Find district (3.8 t). More importantly, however, significant Au resources have been defined at the Golden Eagle deposit (6.67 Mt @ 1.96 g/t Au for 10.1 t Au), the Klondyke deposit (9.95 Mt @ 1.0 g/t Au for 10.0 t Au) and the Indee area (4.96 Mt @ 2.08 g/t Au for 10.3 t Au).

As part of the North Pilbara NGMA Project, AGSO, together with Newcastle University and the Geological Survey of Western Australia (GSWA), have been conducting a research programme to document the geological setting, characteristics and genesis of Au deposits of the North Pilbara Terrane. This record summarises some results of this research programme. This research has concentrated on turbidite-hosted lode Au deposits in the Indee and Nullagine areas as well as basalt- and ultramafic-hosted deposits in the Mt York-Lynas Find area (**Fig. 1b**). In addition to these areas, AGSO's research also concentrated on epithermal deposits in the Indee area, and less detailed studies were undertaken on lode Au deposits at Gold Show Hill and Klondyke (**Fig. 1b**). This research programme was designed to complement recent (*e.g.*, Neumayr *et al.* [1993; 1998] on the Mt York deposits and Zegers [1996] on the Bamboo Creek deposits) and ongoing (*e.g.*, D. Baker, [University of Newcastle] at Mt York-Lynas Find) programmes conducted at the other institutions.

A total of 38 reports published by the Aerial Geological and Geophysical Survey, of Northern Australia (AGGSNA), the precursor to the Bureau of Mineral Resources and AGSO, have been digitally captured and reissued as a CD (AGSO Record 2000/05). These reports contain detailed descriptions, maps and sketches of the geology, mining history and methods, assays, water supply, and general economic geology. Maps of now removed lodes provide otherwise lost insights to the economic geology of the North Pilbara. The reports and maps can be viewed from a standard internet browser.

This Pilbara Gold Record is supported by an extensive GIS dataset, providing many new digital data sets, including a number of variations of the magnetics, gravity, and gamma-ray spectrometry. A solid geology map, and derivative maps, mineral deposits, geological events, and Landsat 5-TM provide additional views. This data set complements the 1:1.5 Million scale colour atlas (Blewett et al., 2000), both are available from the AGSO Sales Centre (sales@agso.gov.au). Low resolution gif files of the atlas plates are available on the Pilbara website.

Analytical techniques

Microthermometric studies of fluid inclusions were carried out on a Linkam THM 600 heating/freezing stage which was mounted on the laser Raman microprobe to allow simultaneous Raman microprobe analysis of the same fluid inclusions. Low-temperature measurements were conducted first because, during heating, many of the CO_2-rich inclusions decrepitated. Heating rates over the regions of interest were generally between 2 to 5 °C/min and low-temperature phase changes are accurate to ±0.2 °C and homogenisation temperatures are accurate to ± 2 °C.

Raman microprobe analyses were obtained from a Microdil 28 spectrometer using 50mW (at the sample) of 514.5 nm laser excitation from a Spectra Physics 2020 5W Ar^+ laser. Spectra were typically obtained after 10 accumulations with a 5 second integration time and approximately 3 cm^{-1} spectral bandpass. The Raman spectra were calibrated against the first order silicon line and are accurate to ±1 cm^{-1}.

0.5-3 kg rock chip samples were collected during mapping of veins for later geochemical analyses. Locations of the samples are good to within 20 m (or better) relative to each other at individual prospects, but the absolute accuracy is only 100 m. The samples were crushed at AGSO using a jaw crusher and then pulverised, in most cases using a chrome steel ring mill. A few samples were pulverised using a tungsten carbide ring mill. The samples were analysed at Analabs in Perth for a suite of elements (Au, Ag, Hg, As, Bi, Sb, Te, Tl, W, U, Cu, Pb and Zn) characteristic of the epizonal and mesozonal environment using a combination of AAS and ICP-MS techniques. Samples that were pulverised using a tungsten carbide ring mill were not analysed for W.

The geology and structure of the North Pilbara Terrane

The Pilbara Craton consists of the 3.6-2.8 Ga North Pilbara Terrane (**Table 1**), which is unconformably overlain by volcano-sedimentary sequences of the 2.77-2.42 Ga Hamersley Province (Arndt *et al.*, 1991; Trendall, 1983). The geological character and age of this terrane changes from east to west and can be subdivided into three domains: the East Pilbara Granite-Greenstone Terrane (EPGGT), the Central Pilbara Tectonic Zone (CPTZ), and the West Pilbara Granite-Greenstone Terrane (WPGGT; **Fig. 1a**).

The EPGGT, which formed between 3.6 and 2.85 Ga, is characterised by domal granitoid complexes that are separated by synclinal greenstone belts comprising volcano-sedimentary rocks. In contrast, the WPGGT is characterised by linear, NE-trending distributions that lack the dome-basin characteristic of the EGGT (**Fig. 1a**). Moreover, the WPGGT appears to be younger, with a maximum age of *ca* 3270 Ma (Hickman, 1997).

The CPTZ (Hickman, 1999), is the youngest component of the North Pilbara Terrane and comprises turbidites, volcanic rocks and granitoid complexes that range in age from 3.02 to 2.92 Ma. **Figure 2** summarises the geological evolution of the Pilbara Craton, and indicates the likely timing of Au mineralisation.

Supracrustal rocks

The oldest known supracrustal rocks in the Pilbara Craton are mafic and felsic volcanic rocks of the *ca* 3515 Ma Coonterunah Group (Buick *et al.*, 1995), which crops out in the central part of the EPGGT. These rocks are unconformably overlain by the *ca* 3490-3410 Ma Warrawoona Group (Thorpe *et al.*, 1992a; Nelson *et al.*, 1999). This unit, which comprises mainly basalt, with lesser high-Mg basalt and felsic units (*e.g.*, Hickman, 1983), occurs throughout much of the EPGGT and is one of the more important hosts to Au mineralisation.

The Warrawoona Group is unconformably overlain by rhyolitic volcanic rocks of the *ca* 3325-3307 Ma Wyman Formation and by basaltic to rhyolitic volcanic rocks of the *ca* 3255-3235 Ma Sulphur Springs Group (Hickman, 1983; Van Kranendonk & Morant, 1998; Barley & Pickard, 1998; Nelson *et al.*, 1999). The Gorge Creek Group, which consists mainly of sandstone and siltstone with lesser mafic volcanic rock disconformably overlies the Sulphur Springs Group in the EPGGT.

In the WPGGT, the oldest known unit is the *ca* 3250-3270 Ma Roebourne Group (Hickman, 1997), which is restricted to the north of the Sholl Shear Zone, a major east-trending structure that bisects the WPGGT. The Whundo Group, which is restricted to the southern margin of the Sholl Shear Zone, consists of mafic to felsic volcanic rock and has been dated at *ca* 3120 Ma (Hickman, 1997). The oldest rocks which cross the Sholl Shear Zone are in the Cleaverville Formation, which has been dated at *ca* 3015 Ma (Hickman, 1997). This unit was correlated across much of the North

Pilbara Terrane by Hickman (1983), and appears to be the first unit shared by both the EPGGT and WPGGT.

The Cleaverville Formation is unconformably overlain by the *ca* 3000-2940 Ma De Grey Group, which includes the Lalla Rookh Sandstone (Van Kranendonk & Morant, 1998), Constantine Sandstone, Mallina Formation (Smithies *et al.*, 1999) and, probably, the Mosquito Creek Formation. The De Grey Goup is characterised mainly by turbiditic rocks, although minor mafic volcanics are locally present, particularly in the Mallina Basin (Smithies *et al.*, 1999). Smithies *et al.* (1999) also demonstrated that felsic volcanics, mafic volcanics and sediments of the Whim Creek Group (Fitton *et al.*, 1975) correlate directly with the Mallina Formation and Constantine Sandstone of the De Grey Group. These rocks comprise the Mallina-Whim Creek Basin (or CPTZ), which separates the East and West Pilbara Granite-Greenstone Terranes. The Mosquito Creek Formation is present in the far south-eastern part of the East Pilbara Granite-Greenstone Terrane. Both the Mosquito Creek Formation and the Mallina Basin are important hosted to lode Au deposits.

Volcanic rocks associated with initial rifting form much of the Fortescue Group, the basal unit of the Hamersley Province. The Fortescue volcano-plutonic event initiated at *ca* 2775 Ma and continued, perhaps in two major volcanic episodes, until *ca* 2687 Ma (Arndt *et al.*, 1991; Nelson *et al.*, 1999). This event involved the deposition of up to 7 km of basalt with subordinate, although locally significant (*e.g.*, Lyre Creek Member of Hardey Formation), felsic units, which are more abundant towards the base (Hickman, 1983). After deposition of the Fortescue Group, the Hamersley Province was dominated by deposition of shale, banded iron formation and carbonate of the Hamersley Group (Hickman, 1983).

Granitoid complexes

Granitoid complexes (batholiths) of the EPGGT are 25-110 km in diameter, with centres spaced, on average, 60 km apart. The intrusion history of these bodies is long and complex, with many batholiths characterised by multiple intrusion events spaced over a period of more than 600 Ma. For example, the oldest phase of the Yule Granitoid Complex is *ca* 3450 Ma, but three additional events have been recognised, with the youngest event being at *ca* 2850 Ma (Bickle *et al.*, 1983; 1989; Williams *et al.*, 1983; McNaughton *et al.*, 1988; 1993; Williams & Collins, 1990; Buick *et al.* 1995; Dawes *et al.*, 1995; M. Van Kranendonk & D. Nelson, unpub. data). These older components were intruded by *ca* 3240 Ma granitoid in the Yule Granitoid Complex (M. Van Kranendonk & D. Nelson, unpub. data), which were, in turn, intruded by post-tectonic (*ca* 2850 Ma) monzogranites, which represent the final stages of cratonisation (Bickle *et al.*, 1989).

In contrast, granite complexes in the WPGGT tend to have a much simpler intrusive history: the longest history is 190 Ma (*e.g.*, Cherratta Granitoid Complex), and many have intrusion histories of less than 10 Ma (*cf.* Smithies & Champion, 1998). The oldest granitoid in the western Pilbara is the Karratha Granitoid, which has been dated at *ca* 3270 Ma. Major granitoid intrusion ceased at *ca* 2925 Ma (Smith *et al.*, 1998; Smithies & Champion, 1998).

The CPTZ saw extensive, almost continuous granitoid intrusion between *ca* 2955 and *ca* 2925 (Smithies *et al.*, 1999). A minor, but perhaps significant intrusion event in the CPTZ, occurred during the initiation of Fortescue Group deposition at *ca* 2765 Ma. The best example of this suite of intrusions is the Opaline Well Granite (Smithies, 1997). This last phase of granitoid intrusion is also present in the EPGGT and in the Gregory Ranges further to the east (**Fig. 1a**).

Regional Structural Geology

As might be expected in a craton that has a prolonged history of crustal evolution, the structural history of the Pilbara Craton is complex. Hickman (1983) initially recognised four events across the

Pilbara. Blewett (2000a) revised the four-fold division of Hickman (1983) using published descriptions of structural relationships and his own observations. He recognised thirteen deformation events that range in age from *ca* 3460 Ma to *ca* 2750 Ma. Moreover, there may have been additional events that were not recognised. **Table 2** shows Blewett's (2000a) correlation of local deformation events in the studied areas with his regional events.

An overview of gold mineralisation in the Pilbara

Although the quantity of Au produced from the North Pilbara Terrain does not even begin to approach that produced from the Eastern Goldfields Province, Au mineralisation in the Pilbara is highly variable in both its geological occurrence and age. **Table 3** summarises the characteristics of important Au deposits and districts of the Pilbara granite-greenstone terrane. Most of the important deposits and districts occur in either mafic to ultramafic volcanic sequences or in turbiditic sequences.

One of the most important hosts to Au mineralisation in the Pilbara are basaltic and ultramafic rocks of the Warrawoona Group, an observation first made by Hickman (1983). Important districts and deposits that are hosted within the Warrawoona Group include Marble Bar, Bamboo Creek, North Pole, Mt York-Lynas Find and Warrawoona. Production and resources from deposits of the Warrawoona Group totals 35.8 tonnes, or 41.3% of total production/resources (**Table 4**). Other mafic and ultramafic units, mainly in the West Pilbara Granite-Greenstone Terrane, have contributed a further 0.92 tonnes, or 1.1% of the total.

Turbiditic rocks, mainly of the De Grey Group, are also an important host to Au in the Pilbara granite-greenstone terrane. Districts hosted by these rocks include the Eastern Creek, Middle Creek, Mosquito Creek, Five Mile Creek, and Twenty Mile Sandy districts to the east of Nullagine, and the Indee district within the Mallina Basin. Some of the most important recent discoveries in the Pilbara have occurred in these districts. Production and resources of deposits hosted by turbiditic rocks account for 41.95 tonnes of Au, or 48.4% of the total (**Table 4**).

Relatively minor production has come from rocks units other than basalt, ultramafic rocks and turbiditic rocks in the North Pilbara Terrane. Mesoarchaean granitoids and porphyritic rocks host Au mineralisation at the Boodalyerie district and the Toweranna district. Production and resources from these districts total 1.62 tonnes and comprise only 1.9% of the total. Palaeoplacer Au also occurs in Neoarchaean conglomerates at the base of the Fortescue Group at Nullagine and to the south-southwest of Marble Bar. These deposits, and alluvial deposits derived from them, have production and resource totalling only 4.18 tonnes, or 4.8% of the total. A few small Au prospects such as Gold Show Hill also occur within felsic volcanic rocks along with minor Cu-Au prospects (*e.g.* Quartz Circle).

Additional information on Au deposits of the Pilbara may be found in the AGGSNA reports from the 1930's, which have been reissued as a CD AGSO Record (Blewett, 2000b).

Timing of mineralisation

Timing of mineralisation is one of the most difficult exercises in understanding the origin of mineral deposits. Very few direct age dating techniques apply, leaving age determination largely a function of Pb isotope model ages (*cf.* Thorpe *et al.*, 1992b) and the relationship of the mineralisation to other geological events. The only lode Au deposit in the Pilbara Craton for which a direct age of mineralisation has been determined is the Zakanaka deposit in the Mt York-Lynas Find district. This deposit was dated at 2888 ± 6 Ma using a Pb-Pb isochron of alteration minerals (Neumayer *et al.*, 1998). Other estimates of mineralisation ages are Pb model ages (**Table 5**). With the exception of

the Big Bertha deposit, which falls below the ^{208}Pb-^{206}Pb evolution curve, all analyses of lode Au deposits fall on the growth curves (**Fig. 3**). Although there is a broad spread in model ages, two distinct end members are present: (1) a group at 3431-3374 Ma from deposits hosted by mafic to ultramafic rocks of the Warrawoona Group, and (2) a group at 2954-2892 Ma from a suite of deposits hosted by turbidites of the DeGrey Group.

Model ages between these end members are quite varied, which led Blewett & Huston (1999) to infer the presence of four individual Au mineralizing events in the Pilbara Craton. However, additional data reported herein indicate that much of the variability in model ages is present in individual deposits or districts. For instance, the model age calculated from an ore-related K-feldspar analysis (Neumayr *et al.*, 1998) in the Zakanaka deposit is 3280 Ma, whereas a galena analysis from the nearby McPhees deposit yielded a model age of 3142 Ma. Similarly, analyses of galena from deposits in the Warrawoona district yield model ages of 3050 Ma, 3374 Ma and 3385 Ma (**Table 5**). The analysis of more samples may give an even a larger spread in Pb isotope ratios and calculated model ages between the two end members.

There are several processes whereby the observed spread of isotopic compositions and model ages could be produced: (1) intermediate mineralizing events between the two end-member events, as suggested by Blewett & Huston (1999), (2) the sourcing of Pb from regions with heterogeneous μ ($^{238}U/^{204}Pb$), and therefore Pb isotope, characteristics, and (3) the mixing of Pb introduced in an early hydrothermal event with Pb from a later, overprinting hydrothermal event. As the Warrawoona and Lynas Find districts have a large spread in model ages and model ages do not match the actual ages of mineralisation, the option of intermediate mineralizing events is unlikely. As both of the remaining processes produce linear or near-linear arrays on $^{207}Pb/^{204}Pb$ vs $^{206}Pb/^{204}Pb$ and on $^{208}Pb/^{204}Pb$ vs $^{206}Pb/^{204}Pb$ diagrams, distinguishing them solely on isotopic grounds is difficult.

However, analogies with the behaviour of Pb isotopes in Pilbara VHMS mineral systems and geological evidence suggest that the third option, introduction of Pb in two separate mineralizing events, best explains the observed Pb isotope systematics for many lode Au deposits. In all cases, the Pb isotope model ages calculated for VHMS deposits correspond closely with the ages of the host rocks and have similar μ (Thorpe *et al.*, 1992b). This suggests that the Pb in these deposits was derived from a broadly homogeneous source regime and suggests that heterogeneous Pb source regimes were not typical of the Pilbara Craton during the Archaean.

Secondly, all five deposits hosted by the *ca* 3000-2940 Ma De Grey Group have model ages of 2950-2890 Ma, whereas deposits hosted by the 3490-3410 Ma Warrawoona Group are the only deposits that have this range in model ages. If the source rocks had heterogeneities in U-Th-Pb isotope abundances, it is probable that the deposits hosted by the De Grey Group would also have anomalously young model ages, as in the Lynas Find district.

Thirdly, with the exception of the Big Bertha deposit, all lode Au deposits plot along the evolution curve on the $^{208}Pb/^{204}Pb$ *vs* $^{206}Pb/^{204}Pb$ diagram. If source regime heterogeneity in μ caused the observed scatter in the Pb isotopic compositions observed in the $^{207}Pb/^{204}Pb$ *vs* $^{206}Pb/^{204}Pb$ plot, extremely coherent behaviour between U and Th during the process(es) that caused the heterogeneity in μ would be required to produce the coherence in the $^{208}Pb/^{204}Pb$ vs $^{206}Pb/^{204}Pb$ diagram. We consider this to be less likely than mixing caused by two hydrothermal events.

Finally, two generations of galena are present in the Bamboo Creek deposit (S. White, pers. comm., 1999). Although Pb isotopes have not been determined from the younger generation of galena, this geological evidence is supportive of Pb introduction in two separate events.

Hence, it is our preferred interpretation that two broad lode Au events occurred in the Pilbara, the older at ca 3430-3370 Ma and the younger at *ca* 2950-2890 Ma. However, in detail there is a possibility of two events within the broad 2950-2890 Ma event. Of the four model ages from De Grey Group-hosted deposits, two (both from the Mallina Basin) had model ages of 2950 ± 5 Ma and two (one each from the Mallina Basin and the Mosquito Creek Basin) had model ages of 2900 ± 10 Ma. These model ages correspond to deformation events that affected most of the North Pilbara Terrane.

In addition to the above, three lode Au deposits/prospects gave model ages less than 2500 Ma (**Table 5**). Galena from an auriferous vein from the Upper Hardey River gave a model age of 2493 Ma, and samples from the Pilgrims Rest and Geemas deposits gave model ages of 1548 Ma and 1476 Ma, respectively, using the Western Superior model of Thorpe *et al.* (1992b). The latter two analyses plot above the ^{207}Pb-^{206}Pb growth curve but below the ^{208}Pb-^{206}Pb growth curve, which may indicate long term enrichment of U relative to Pb and Th and older true depositional ages.

As the Western Superior model has only been calibrated for ages in excess of 2.7 Ga, application of this model may not be appropriate for these "young" samples. Deb *et al.* (1989) proposed a Proterozic Pb isotope model based on syngenetic and diagenetic base metal deposits from Australia and North America This model gives model ages up to 320 Ma younger than the model of Thorpe et al (1992b). Using the model of Deb *et al.* (1989), the ages of all samples from the Pilbara Craton are in excess of 1.8 Ga. (**Table 5**). The significance of these young ages is not yet understood.

Lode Au and Sb-Au deposits of the Indee district

In 1997, Resolute Ltd commenced exploration in the Indee district (**Fig. 1b**). Although small Sb-Au deposits were known at Mallina and Peawah (Finucane & Telford, 1939), the discovery of deposits in the Indee district was the result of grassroots exploration. Lode Au and Sb-Au deposits in this area are hosted by turbidites of the *ca* 3000-2940 Ma De Grey Group, by mafic volcanics of the *ca* 3015-2950 Ma Whim Creek Group and by *ca* 2950-2930 Ma granitoids (**Fig. 4**; cf. Smithies, 1997, 1998, 1999; Smithies et al, 1999). The most significant deposits (Withnell and Camel) are hosted by shale, siltstone and fine-grained wacke of the Mallina Formation just to the north of the Mallina Shear Zone (Smithies, 1999). Smaller deposits are hosted by high-Mg basalts in the Whim Creek Group (Balla, Sherlock) and a *ca* 2950 ma granodiorite porphyry (Toweranna). Gold deposits, prospects and occurrences in the Central Pilbara (**Fig. 4**) are quite diverse in character, with three distinct styles of lode Au deposits recognised: (1) lode Au deposits associated with sericite-carbonate-pyrite alteration assemblages (*e.g.* Withnell), (2) lode Au deposits associated with pyrophyllite-bearing alteration assemblages (*e.g.* Camel 1), and (3) lode Sb-Au prospects (*e.g.*, Mallina and Peawah).

Structural Geology

Smithies (1998) recognised four separate deformation events that he termed D_1 to D_4. These events equate to D_{4a} to D_{4d} of Blewett's (2000a) synthesis of the North Pilbara Terrane (**Table 2**). The prefix *a* is used to distinguish the local deformation chronology from the regional chronology (*e.g.*, aD_1).

aD_1 deformation

The first phase of deformation in the Mallina Basin was the development of regional shortening in an approximately north-south orientation. Upright subhorizontal folds with east-west trending axes have an axial planar slaty cleavage. Evidence for aD_1 deformation in the vicinity of the Mallina Fault Zone is restricted to complex fold geometries of aF_2/F_3 fold interference. The main

approximately east-west penetrative fabric present in the Indee district is interpreted as a composite aS_1/S_3. The aD_1 deformation is inferred to be progressive and occurred at 3000-2950 Ma.

aD_2 deformation

The aD_2 deformation was the result of east-west oriented compression, which resulted in widespread macroscale refolding of the Mallina Basin about north-plunging upright folds. The aF_2 folds are associated with a well developed crenulation cleavage or pencil cleavage intersection with the folded aS_1 fabric. Smithies *et al.* (1999) interpret the intrusion of the Peawah Granodiorite (*ca* 2948 Ma; **Fig. 4**) as post- to syn-tectonic with respect to aD_2 folds, dating this event at *ca* 2950 Ma or older.

aD_3 deformation

The main fabric across much of the Mallina Basin is interpreted to be a composite of aS_1 and aS_3. The aS_3 fabric is commonly a crenulation cleavage associated with open to tight, upright, east-northeast to west-southwest plunging F_3 folds.

Extension

A major thermal event at *ca* 2780 Ma affected the entire Pilbara Craton and resulted in the development of the Hamersley Province. The effect of early rifting associated with this major basin was the development of normal fault movement on the Mallina Fault Zone and other linked faults.

aD_4 deformation

Minor crenulations, kink bands, faults, and folds are the result of aD_4 deformation. These structural elements also overprinted the Fortescue Group. Shortening was probably oriented approximately northeast-southwest and resulted in northwest trending folds. Tourmalinite veins are overprinted by aS_4 crenulations to the east of the Becher Au prospect.

Faults

In addition to the aforementioned folding events, the Indee district is also characterised by an east-trending, 1 km wide zone of shearing that Smithies (1999) termed the Mallina Shear Zone (**Fig. 4**). In the YULE 1:100 000 sheet this shear zone is characterised by a network of anastomosing faults that form a low ridge of calcreted and silicified rocks of the De Grey Group (Smithies, 1999). East of the Indee district, the Mallina Shear Zone is intersected by a northeasterly trending fault zone that may be part of the Wohler Shear Zone (**Fig. 4**). Interpretation of kinematic indicators (fold asymmetry) on the Mallina Fault Zone indicate that although a sinistral movement is the latest movement, a dip-slip, south-side up movement dominates (Smithies, 1999). The Mallina Fault Zone is an important structure in the Indee district as many of the more significant prospects occur just north of it and with a similar orientation.

Selected deposits of the Indee district

The Withnell deposit

The first group of lode Au deposits, those associated with a sericite-carbonate alteration assemblage, is best exemplifed by the Withnell deposit, which is also the most significant deposit discovered in the Central Pilbara Tectonic Zone. It is located just to the north of the Mallina Shear Zone (**Fig. 4**) within turbiditic sandstone and shale of the Mallina Formation. The Withnell deposit consists of a number of east-west striking, steeply south-dipping lenses that plunge moderately to the west.

Because of poor exposure, most geological information at the Withnell deposit is based on reverse circulation and diamond drilling. Two oriented diamond holes were drilled at the Withnell deposit, one through a mineralised lens (**Fig. 5**), and the second through a barren zone. The following discussion is based on core from these two holes.

Structural geology

All major structural elements observed in the core, which include bedding, foliation, fault and veins orientations, strike mainly to the east and dip steeply to the south and north. The foliation, interpreted as aS_3, generally is parallel to bedding.

Based on the oriented drill core, the majority of the faults and veins at Withnell dip steeply to the north and south (**Fig. 6**). The north- and south-dipping elements are interpreted to be conjugate with sigma 1 oriented vertically in an extensional regime, probably late in the aD_3 event.

Veining, mineralisation and alteration

The highest Au grades are associated with high abundances of locally pyritic, planar quartz-carbonate veins (**Fig. 7a**), particularly where these veins dip steeply to the south. Where the planar quartz-carbonate veins have a lower abundance and/or where they dip steeply north, Au grades are not elevated. With the possible exception of a lone ribbon quartz vein, which occurs along the margin of the high-grade zone, no other quartz vein types have a relationship to high Au grades. Mutual cross-cutting relationships and the occasional occurrence of a planar quartz-carbonate vein along south-dipping shears suggests an overlapping temporal relationship between these shears and veins.

Vein textures observed in drill core are characteristic of moderate depths, either in a slate belt or plutonic environment. This inference is supported by the lack of crustiform or colloform textures diagnostic of the epithermal environment and by the presence of ribbon quartz veins and deformed coarse-comb textures that are characteristic of deeper levels (*cf.* Dowling & Morrison, 1989).

Figure 5 also shows the relationship of the veins and Au grades to alteration and pyrite abundance as determined from core logging, petrography, PIMA analysis and XRD analysis. The ore and alteration assemblages at Withnell are relatively simple, comprising major quartz, carbonate, sericite and feldspar, variable pyrite and chlorite, and minor to trace arsenopyrite, rutile, chalcopyrite, electrum, galena, and sphalerite.

Quartz, carbonate (mainly dolomite, with some ankerite and siderite) and sericite are present as major minerals through the drill cores inspected, whereas chlorite is restricted, commonly occurring in finer-grained units or domains. Hydrothermal quartz mainly occurs in veins, whereas carbonate occurs both in veins and is pervasively disseminated through the wall rocks. Sericite occurs in the wall rocks, mainly as lepidoblastic grains that define the foliation.

Of the major minerals, pyrite has the closest correlation with Au-rich zones. Within these zones, pyrite content generally exceeds 1%, decreasing rapidly, away from ore, to background levels of trace to 0.5% (**Fig. 5**). Arsenopyrite was observed only in samples from the uphole part of the mineralised zone in hole INDD003.

Fluid inclusion studies.

In order to document fluid compositions, fluid inclusion plates were prepared from samples containing quartz/carbonate veins. Primary or pseudosecondary inclusions occur in relict growth bands within the quartz crystals. The inclusions are irregular to rounded in shape and exhibit

variable liquid/vapour ratios. Vapour-rich, liquid-rich and liquid+vapour CO_2-water inclusions were all commonly observed.

CO_2 melting temperatures are between -57.5 and -56.6°C indicating that they contain only small quantities of another gas (CH_4 ?). Salinities were low for inclusions with pure CO_2 (<0.5 eq. wt. % NaCl) but ranged up to 6.9 eq. wt. % NaCl for inclusions with depressed CO_2 melting temperatures with a mode around 3 eq. wt. % NaCl. The CO_2-bearing inclusions homogenised over a wide range of temperature, from 164 to 320°C with a mode at 280°C (**Fig. 8a**). The inclusions homogenising below 220°C all homogenised into the liquid phase, whereas those homogenising between 283 and 320°C all homogenised to the vapour phase. The homogenisation behaviour and the variable liquid/vapour ratios of the fluid inclusions suggest that phase separation may have occurred and that homogenisation temperatures are close to trapping temperatures. Aqueous inclusions had variable salinities ranging from 3.9 to 12.5 eq. wt. % NaCl and eutectic temperatures varied from -35.0 to -21.1°C. The inclusions homogenised between 107 and 210°C with a mode at 140°C (**Fig. 8a**).

The Camel deposits

The Camel deposits are located 3-5 km to the west of the Withnell deposit, along the northern margin of the Mallina Shear Zone (**Fig. 4**). The Camel 2 prospect is the best example of the second type of deposit, in which pyrophyllite is a significant alteration mineral. The ore zone is characterised by disseminated pyrite and other sulphide minerals within sheared, carbonate and pyrophyllite altered shale, siltstone and sandstone. The pyrophyllite was identified using PIMA. Bierwirth et al. (1999) mapped a broad zone of pyrophyllite alteration around the Camel deposits using airborne hyperspectal (HYMAP®) data.

Antimony-gold deposits.

Antimony, with minor Au, was produced from four historic mines in the Central Pilbara Tectonic Zone for a total of around 110 tonnes of stibnite concentrate (Hickman, 1983). The most significant production came from the Eastern Workings, which is located 0.5 km east-northeast of the Mallina Homestead (**Fig. 4**). The other deposits include the Peawah, Balla Balla (or Star) and Sherlock deposits (Finucane & Telford, 1939; Telford, 1939a; Hickman, 1983). In addition, recent exploration also identified several other Sb-Au deposits, including the Mirdawari prospect (**Fig. 4**).

The Sb was mined from quartz veins hosted by turbidites of the Mallina Formation (Eastern Workings and Peawah), by high-Mg basalt of the Louden Volcanics (Balla Balla and Sherlock) and by quartzite of the Constantine Sandstone (Mirdawari). Where the orientation is known, the veins strike east-northeast to east-southeast and dip steeply either to the north or south. Mineralogically the veins are simple, consisting of stibnite and quartz in varying proportions. Galena, which has been analyzed for Pb isotope ratios (see above), also occurs at the Sherlock River deposit. The stibnite is commonly oxidised to cervantite. Although significant Au occurs with the stibnite, no discrete Au minerals were recognised in this study.

At the Peawah deposit, stibnite is hosted by quartz veins that resemble tension gashes (**Fig. 7b**). These veins cut a well-developed aS_1 foliation, which strikes 100° and dips 80° to the north and east-plunging aF_3 folds. The veins strike 110° and dip 60° to the south. The tension gash geometry suggests south-side up normal faulting. The wall rocks adjacent to the veins are sericitically altered.

Fluid inclusion studies

Fluid inclusion studies were undertaken on quartz-stibnite veins from the Mirdawari and Peawah deposits. In the sample from Mirdawari, abundant fluid secondary fluid vapour-rich, liquid-rich and liquid+vapour CO_2 inclusions were observed. The CO_2-bearing inclusions all melted at –56.6°C indicating that CO_2 was the only gas present. Clathrate melting indicated salinities between 1 and 6

equiv. wt. % NaCl with a mode at 3 equiv. wt. % NaCl. The majority of CO_2-bearing inclusions homogenised to the liquid phase with two homogenising to the vapour phase and one exhibiting near-critical behaviour. Homogenisation temperatures varied between 179 and 331°C, with a mode around 260°C (**Fig. 8b**). The aqueous inclusions had salinities ranging from 3 to 14 equiv. wt. % NaCl with a mode at 4 equiv. wt. % NaCl. Homogenisation to the liquid phase occurred at temperatures ranging from 172 to 223°C with a mode at 175°C (**Fig. 8b**).

In the sample from the Peawah deposit, larger (1-3 mm) quartz crystals contain very small (<5 μm) inclusions in wispy trails, while smaller clear quartz crystals have rare, liquid-rich, primary or pseudosecondary fluid inclusions. The CO_2-bearing inclusions exhibit CO_2 melting between -57.7 and -57.3°C indicating the presence of another gas (CH_4?) and salinities were around 1 equiv. wt. % NaCl. Homogenisation temperatures ranged from 264 to 387°C with a mode at 280°C (**Fig. 8c**). The aqueous inclusions have salinities between 3 and 4 equiv. wt. % NaCl but eutectic melting temperatures around -37°C indicate that salts other than NaCl are present. These inclusions homogenise between 138 to 199°C with a mode at 155°C (**Fig. 8b**).

Other lode gold deposits

The most significant historic Au production was from the Station Peak and Toweranna centres, which are hosted by intrusions within the Mallina Formation (**Fig. 4**). In the Station Peak centre, which produced 360 kg of Au (Hickman, 1983), auriferous quartz veins are hosted mainly by a dolerite dyke (Finucane, 1937). This dyke has an age of *ca* 2950 Ma based on cross-cutting relationships to other intrusive rocks. The veins strike east-northeast to east and dip moderately to steeply to the south. The highest Au grades appear to increase as the dips of the veins flatten. Ore minerals in the hypogene zone include pyrite, arsenopyrite and chalcopyrite (Finucane, 1937).

Historical production at the Toweranna deposit amounted to 160 kg (Hickman, 1983) and a resource totaling 1130 kg has been defined by Swan Resources and Tindals Gold Mines. Pyritic, auriferous quartz veins are hosted by a coarse-grained feldspar-phyric granodiorite that intrudes the sheared axial region of the north-trending D_2 Croydon anticline. The granodiorite is interpreted to be co-magmatic with the *ca* 2950 Ma Peawah Granodiorite (Smithies, 1998a).

Like the Withnell deposit, the auriferous veins at Toweranna have both a northerly and an easterly strike. However, in this case, the north-trending veins, which strike 020° and dip moderately to the east, appear to be most significant, producing over 80% of the Au. The east-trending veins strike 080° and dip moderately to the north (Telford, 1939b).

Minor quantities of Au have also been extracted from folded Mallina Formation in the Croydon area and from carbonatised high-Mg basalt of unknown age in the Hong Kong and Teichmans areas (**Fig. 4**). Most of the prospects in these two latter areas trend east to northeast, with moderate dips to the southeast, but at the Annie's Gap workings, the veins strike north, with a moderate to steep easterly dip (Sullivan, 1939).

Epithermal vein deposits in the Central Pilbara Tectonic Zone

In 1997, Resolute Ltd recognised the presence of "epithermal", or high level, vein textures at the Becher prospect, 6 km southwest of the Withnell deposit (**Fig. 4**). Since this time, more detailed studies of this and other nearby prospects (Huston et al., 2000) and a review by Marshall (2000) indicate that high-level textured quartz veins occur extensively through the Pilbara Craton, particularly near the Pilbara-Fortescue unconformity, and in the overlying Hamersley Province. As Huston et al. (2000) described the geology of four of these deposits in detail, the results of that study are only summarised here.

Becher prospect

The Becher prospect is a zone of anastomosing quartz veins with an overall strike of 330º (**Fig. 9**). It comprises two vein sets, with the more dominant set striking 310º and the subordinate set striking 350º. The dip of the vein sets was difficult to establish, but where measured, it dipped moderately to steeply (60-90º) to the west. The veins vary in thickness from 10 cm to over 10 m, with the 350º trending veins being somewhat wider. The Becher area also contains earlier sets of buck quartz and quartz-tourmaline veins, both of which strike roughly east-west. The quartz-tourmaline veins, which locally carry up to 80% tourmaline, are the more prominent, with widths of 0.3-5 m.

The immediate wall rocks to the Becher vein system were altered to a quartz-sericite-(ex)pyrite assemblage, which is locally brecciated or cut by chalcedony veins. This assemblage can be traced up to 50 m from the vein system, where it grades into a quartz-sericite-chlorite assemblage (**Fig. 9**). More kaolinitic zones (either formed by primary alteration or by weathering) locally occur within the quartz-sericite-(ex)pyrite assemblage.

The major variety of quartz in the Becher vein system is chalcedony. Although generally massive, weakly banded chalcedony (**Fig. 10a**) is also present. Other types of quartz present include pseudoacicular (**Fig. 10b**), bladed pseudomorphs after carbonate or sulphate (**Fig. 10c**), and crustiform varieties (**Fig. 10d**). Bladed textures are also preserved by limonite pseudomorphs (**Fig. 10e**). The bladed mineral replaced by limonite appears to be paragenetically late as it fills the centre of individual veins and cross cuts high-level textured quartz. Crustiform textures (**Fig. 10d**) are relatively restricted. These textures differ from weakly-banded chalcedony, in that the quartz is more crystalline, and the bands better defined. The bands vary in colour from grey to white to pink; typically the banding is 2-20 mm in thickness and has a colloform habit. Breccias occur to varying degrees throughout the Becher vein system, and vary from wall rock breccias with chalcedony infill, to breccias in which crustiform clasts are surrounded by later crustiform quartz, and to breccias with complex clast and matrix types.

Fluid inclusion studies.

Fluid inclusion plates were prepared from samples containing chalcedony with small cockade quartz crystals, bladed quartz pseudomorphs, and crack-seal quartz veins. All samples contained abundant, small (<5 μm), primary fluid inclusions in growth bands within the quartz crystals. The inclusions were either liquid-only or liquid-rich and mostly irregular showing signs of necking-down, but rare equant shapes were also observed. No definitive evidence for boiling was found, but, in many cases, the vapour phase is not trapped in epithermal systems (Bodnar *et al.*, 1985). The large scatter in homogenisation temperatures reported below is probably due to necking down or other post entrapment modifications and temperatures near the minimum homogenisation temperature are most likely to represent trapping temperatures.

The inclusions in the bladed quartz pseudomorphs, and crack-seal quartz veins have salinities between 9 and 18 equiv. wt. % NaCl and eutectic melting temperatures between -50 and -16°C. However, inclusions in cockade quartz on the boundary of the chalcedony have salinities of less than 3 equiv. wt. % NaCl. Homogenisation occurred over a wide temperature range from 101 to 299°C with a distinct mode around 160°C (**Fig. 11a**).

Orange Rock prospect

The Orange Rock prospect is located 12 km west-southwest of the Becher deposit within high-Mg granodiorite of the *ca* 2950 Ma Peawah Granodiorite (**Fig. 4**). The Orange Rock vein system (**Fig. 12**), which can be traced for at least 2 km along strike, has an overall trend of 345º, but, like the Becher vein system, it is segmented, with two short segments in the northern and central parts of the

vein system having trends in the range from 350º to 015º. Although dips of the vein were difficult to establish, one measurement near a zone of bifurcation indicated a moderate east dip of 65º.

Most of the Orange Rock vein system is characterised by well developed vein breccias (**Fig. 10f**). These breccias typically contain 1-20 cm clasts of silicified granodiorite and chalcedony in a chalcedony matrix. Other textural types are much more restricted in their distribution. The most abundant of these textures occur near the northern extremity of the vein system within a ~50 m long, locally highly gossanous interval trending 345º (**Fig. 12**).

Textures present in the gossanous interval include breccia, bladed quartz psuedomorphs, and limonite pseudomorphs after a bladed mineral, possibly siderite. The breccias contain silicified granodiorite clasts set within a gossanous matrix. Bladed pseudomorphs of quartz are present within this zone and in a zone 1 km to the south where the vein system bifurcates.

The most unusual textures present in the gossanous zone are limonite pseudomorphs after a folded, bladed mineral (**Fig. 10g**). If these folds are tectonic, this suggests that mineralisation occurred prior to the development of the last deformation (i.e., aD_4).

Veins in the Opaline Well Granite

The 2765 Ma Opaline Well Granite (Nelson, 1997) is cut by 0.2-3 m quartz veins that trend 320-345º with strike lengths up to several hundred metres. These veins typically have well-developed high-level textures that are dominated by bladed pseudomorphs of quartz, with lesser, weakly banded chalcedony and minor crustiform and colliform quartz. An unusual characteristic of these bladed textures is that, locally, the blades are composed of fluorite rather than quartz. In outcrop the fluorite weathers recessively, leaving residual silica ridges (**Fig. 10h**). In thin section, the selvedges to some of the weakly banded chalcedony veins are comprised of potassium feldspar.

Fluid inclusion studies.

A thick section was prepared from a sample containing bladed quartz pseudomorphs that are separated by comb quartz which has grown symmetrically and perpendicular to the bladed crystals. The inclusions range in size up to 20 μm and are generally irregular in the bladed quartz crystals but are rounded to negative crystal shape in the comb quartz. The inclusions were primary in the bladed crystals and pseudosecondary in the comb quartz. All inclusions exhibited constant liquid/vapour ratios with vapour contents of around 10 vol. %.

The inclusions have salinities ranging from 16 to 21 equiv. wt. % NaCl with eutectic melting occurring between -56.1 and -27.9°C indicating the possible presence of calcium in the fluid. The inclusions homogenised between 108 and 135°C with a mode around 130°C (**Fig. 11b**). Fluid inclusions in the comb quartz homogenise at slightly lower temperatures than those in the earlier bladed quartz pseudomorphs.

The Sams Ridge vein system

The Sams Ridge vein system, located 35 km west-northwest of the Becher prospect, is hosted by high-Mg basalt of the Louden Volcanics. High-level textures were observed at various points over a 5 km strike length, including the Sams Ridge and Fisher Well prospects (Marshall, 2000). Although the vein is dominated by chalcedony, the vein also contains colloform quartz, crack-seal breccias and bladed quartz pseudomorphs. The Sams Ridge prospect consists of a 150 m wide, north-northeast-trending zone of quartz veining with both flat lying and steeply dipping veins. Gossanous zones, with some oxide Cu minerals are present at several places along the Sams Ridge vein system, and galena and stibnite have been observed at the Fishers Well prospect at the northern end of the vein system. Minor pyrite is also observed locally (Marshall, 2000).

Geochemistry of the high level veins

A total of 24 0.5-3 kg surface samples were selected for analysis (Appendix A). The samples were selected to be representative of the vein textures present at each deposit. The results are compiled in Appendix A, and **Table 6** summarises the results for the various vein systems.

The most anomalous samples were from the Becher prospect, where Au contents ranged upwards to 0.22 ppm. Arsenic, Bi, Sb, Te, W, Cu and Zn were also anomalous. Arsenic, Sb and Te were most elevated, with values to 6610 ppm, 178 ppm, and 3.3 ppm, respectively. Analyses from the Orange Rock prospect also gave anomalous values, although lower than Becher. The maximum for Au was 0.06 ppm, but As (to 208 ppm), Sb (to 14 ppm) and Te (to 0.6 ppm) were significantly elevated relative to average crustal abundances.

With the exception of weak Sb and Te anomalism, the assay results from the Opaline Well veins were low. In contrast, results from Sams Ridge vein sytem are enriched in Ag, Hg, As, Bi, Sb, Te and Cu, but Au assays are low (**Table 6**). However, Marshall (2000) reported highly anomalous results from the Sams Ridge vein system, with values up to 0.44 ppm Au, 15 ppm Ag, 90 ppm As, 8100 ppm Sb and 9800 ppm Cu. These latter results are the most significant reported for any high level prospect from the Central Pilbara Tectonic Zone.

The Mt York-Lynas Find district

The Mt York-Lynas Find district occurs in the Pilgangoora Syncline (**Fig. 13**) located in the western part of the EPGGT (**Fig. 1b**). Host rocks include mafic and ultramafic rocks of the ca. 3490-3410 Ma Warrawoona Group and iron formation of the <3240 Ma Gorge Creek Group (Neumayr, 1995). The Pilgangoora Syncline is a 20 km long, 6-8 km wide, north-trending belt of rocks between two lobes of the Carlindi Batholith. Deposits within the Mt York-Lynas Find occur through much of the Pilgangoora Syncline and ranged in size up 1.263 Mt at 2.19 g/t Au at the Iron Stirrup deposit. Total production from this district amounted to 3.82 tonnes, most of which was produced between 1994 and 1998 by Lynas Gold NL.

The purpose of this section is to describe the regional setting and history of the district and to present the results of pit mapping from two deposits (Zakanaka South and McPhees North) that illustrate local controls on the mineralisation. The results presented herein are intended to complement ongoing thesis work by Darcy Baker (Newcastle University) and previous thesis work by Neumayr (1995).

Regional geology

The Pilgangoora Belt (Hickman, 1983) is located in the east of the Wodgina and adjacent North Shaw and Wallaringa 1:100 000 Sheet areas. The belt contains greenstones of the Coonterunnah, Warrawoona, Strelley and Gorge Creek Groups (Van Kranendonk & Morant, 1998 and references therein), which range in age from 3515 Ma to <3240 Ma. These greenstone groups were intruded by a number of mafic and ultramafic bodies, some up to 10 km long. The structure of the belt is dominated by the Pilgangoora Syncline, a south-plunging regional F_{4b} fold in the north, which refolded shear zones and fabrics of older events. The western margin of the belt is variably sheared (by regional D_{4a} and D_{4c}) and was intruded by the Yule and Carlindi Granitoid Complexes (**Fig. 13**). The Pilgangoora Belt contains the Lynas Find district of Au deposits, some of which have been dated at *ca* 2890 Ma (Neumayer, 1995; Neumayr et al., 1998).

Structural Geology

The rocks of the Mount York-Lynas Find district were multiply deformed. A local deformation chronology pD_1 to pD_8 has been developed (Blewett, 2000a). The earliest fabric (pS_1) is found only in the 3515 Ma Coonterunnah Group, located along the northern and eastern part of the belt. The first fabric in the younger Warrawoona Group, which unconformably overlies the Coonterunnah Group, is a bedding-parallel pS_2 schistosity. The 'main' fabric of most of the Warrawoona Group is a composite, with pS_2 as an S-plane, or a crenulated fabric by pS_3 foliations. In the centre of the belt, the talc-chlorite-carbonate and talc-actinolite schists of the Lynas Find shear system (which is folded by a regional pF_5 fold), have pD_3 crenulation cleavages (pS_2 in microlithons) that are overprinted by coarse magnetite grains. These magnetite grains and foliations were all deformed by pD_4 shearing.

Sinistral pD_4 shear zones along the western margin of the belt deformed andalusite porphyroblasts in pelitic schist and clinozoisite porphyroblasts in mafic (chlorite) schist. Granitoid rocks of the Yule-Carlindi Granitoid Complexes have sinistral S-C planes, and associated stretching lineations are subhorizontal. In the Lynas Find shear system, muscovite defined C′ planes record sinistral shear.

North-striking pS_5 crenulations are axial planar fabrics to a series of south-plunging upright tight pF_5 folds. The pF_5 folds overprint an earlier schistosity (pS_2/pS_3 composite fabrics), earlier folds, shear zones and the Lynas Find alteration system associated with mineralisation. Metamorphic grade during pD_5 was, locally, high enough to form biotite.

Progressive deformation during pD_6 resulted in east-northeast oriented folds and reactiviation of the pD_4 shear zones. The pS_6 crenulations are generally coarser and more broadly spaced than the fine-spaced E–W oriented pS_7 crenulations that locally overprint the former. There are no macroscale examples of the relatively minor pD_7 deformation event that reflects minor north–south oriented shortening. The fold style is locally chevron-like, with moderately to steeply east-plunging hinges about steeply dipping crenulation axial surfaces. The intensity of the crenulation development varies considerably with the tightness of associated pF_7 folds. Fine-scaled pS_8, northwest striking, crenulations overprint all other fabric elements. Macroscale examples of the pD_8 folds refold the Pilgangoora Syncline.

Mineralisation

As discussed previously, mineralisation in the Mt York-Lynas Find district is hosted by mafic and ultramafic rocks of the Warrawoona Group and by banded iron formation at the base of the Gorge Creek Group. A Pb-Pb isochron on alteration and ore minerals at the Zakanaka deposit indicates that the mineralisation occurred at 2888 ±6 Ma (Neumayr *et al.*, 1998). The purpose of AGSO's investigations in this district was to establish local structural and lithological controls on mineralisation. Two deposits were chosen for this purpose, based on accessibility and geological characteristics, the Zakanaka South and McPhees North deposits. Pit mapping was conducted in May 1998 (**Figs. 14** and **15**), however, heavy rains in 1999 subsequently flooded the pits. In addition to these pits, the geology of the Birthday Gift and the Lynas Find quartz-fluorite-galena deposits are also described.

Zakanaka South deposit.

The Zakanaka deposit consists of two lenses (Zakanaka North and Zakanaka South) that occur within a northwest-striking sequence comprising mainly of tremolite-chlorite-talc schist, serpentinite and amphibolite (Neumayr, 1995). These rocks are part of the Warrawoona Group. At Zakanaka South, the ore lens occurs just to the west of a faulted contact between talcose rocks to the north (grid east) and amphibolitic rocks to the southwest (**Fig. 14a**). The amphibolitic unit is texturally and mineralogically quite varied. The easternmost facies consists of dark green biotite-quartz-amphibole schist, which grades to the west into a highly siliceous quartz-amphibole schist. Further

to the west, these rocks grade into a quartz-biotite-amphibole schist with lineated biotite augen, which then grades into massive amphibolite.

At Zakanaka South, Au enrichment forms a boomerang-shaped zone (**Fig. 14b**) that occurs almost exclusively within the dark green biotite-quartz-amphibole facies of the amphibolite. Two trends are evident: (1) a major, grid north trend that is 20-30 m wide and dips moderately to grid east, and (2) a subsidiary trend that strikes grid north-northest. These trends parallel the faulted contact with the talcose units.

Gold occurs in quartz-calcite±diopside±plagioclase±microcline±amphibole veins within the dark green biotite-quartz schist. Neumayr *et al.* (1993) note that Au is associated with sulphide minerals, mainly pyrrhotite and pyrite, and with microcline. The sulphide minerals are concentrated in the altered rocks adjacent to the veins.

McPhees North deposit
Mineralisation at McPhees mine occurs in small, elongate ore bodies that coincide with the distribution of mafic rock, suggesting a lithological control on mineralisation (**Fig. 15**). The mined high-grade ore bodies range in size from 150 m x 15 m to less than 10 m in length (**Fig. 15**). The ore bodies trend subparallel to the main regional composite foliation, and peak Au grades coincide the occurrence of amphibolite bodies (**Fig. 15**).

These amphibolite bodies consist of massive to foliated, fine-grained amphibole-quartz-carbonate±biotite rocks in which irregular sulphide-bearing carbonate, and quartz-carbonate veins up to 5-20 mm thick are commonly developed. The bodies are also cut by dark grey massive quartz veins with disseminated pyrite cubes. The amphibolites commonly have zoned margins, grading outwards to a more siliceous zone and into a thin zone comprised mainly of amphibole. These amphibolite bodies are surroundeed by talc schist.

Birthday Gift deposit
This small deposit illustrates a third type of deposit in the Pilgangoora belt (**Fig. 13**). The mineralisation is hosted by saccharoidal quartz veins within strongly foliated metabasalt. The other important unit within the area is strongly foliated granite of the Carlindi Batholith. At this location, the basalt forms a shallowly SSW-plunging anticlinorium which is defined by folding of the dominant foliation, which is interpreted to be pD_4. The workings at Birthday Gift appear to follow a mesoscale antiform (pF_5): one adit followed the hinge zone of the anticline, and crosscuts, visible from the shafts, appear to be directed toward this zone. The timing of mineralisation is uncertain. Is it located on a sheared (pD_4) contact between the greenstone and granite and has been folded (pF_5) into this geometry, or is mineralisation associated with a saddle reef control during pF_5 folding?

Lynas Find Pb-fluorite deposit
This deposit, hosted by sericitised foliated granite of the Carlindi Batholith, consists of a narrow quartz-fluorite-galena vein that can be traced over a distance of 10 m. This vein trends 145º and commonly contains coxcomb quartz on the interior of the vein with an and interior characterised by fluorite. The galena has been dated at about 2760 Ma (Thorpe *et al.*, 1992b). Pseudosecondary and secondary fluid inclusions in quartz indicate moderate salinities (12-18 eq wt % NaCl) and moderate to low homogenisation temperatures (150-230º; **Fig. 16**).

Lode gold deposits from the Warrawoona district

The Warrawoona district (**Fig. 17**), located 25 km southeast from Marble Bar, is one of the largest historical mafic-ultramafic-hosted goldfields outside of Marble Bar. This district has produced 745

kg of Au from 25 kt of ore, with an average grade of 29.6 g/t and an additional 22 kg alluvial and dollied Au (Hickman, 1983). More recently, a geological resource of 9.95 Mt at 1.0 g/t has been identified for the Klondyke deposit (**Fig. 17**).

The Warrawoona greenstone belt (Hickman, 1983) is a highly attenuated wedge-shaped belt between the Mt Edgar and Corunna Downs Granitoid Complexes (**Fig. 17**). The rocks include felsic volcanic rocks of the Duffer Formation (3470 Ma), mafic to ultramafic rocks of the younger Salgash Subgroup (Hickman, 1983), and slices of the 3325 Ma Wyman Formation (Thorpe *et al.*, 1992a). The Warrawoona area displays many of the early deformation events seen in the Pilbara, i.e., those developed in rocks between <3370 Ma and 3325 Ma.

Structural Geology

The structure of the Warrawoona belt is complex and contentious. Some workers suggest that diapirism from the adjacent granitoid batholiths (Mt Edgar and Corunna Downs) caused sinking in the intervening greenstone areas that host the lode Au deposits (Collins *et al.*, 1998). The geological evidence for this diapiric model is not considered strong by the authors, and the following provides an alternative view based on observations of structural elements in and around the Klondyke mine. The deformation chronology presented is a local one from wD_1 to wD_5 (Blewett, 2000a).

Boudins define low-strain zones in the Klondyke Shear Zone and multiple crenulation cleavages are preserved. The earliest noted fabric (wS_1) is an E-striking foliation in the Q-domains of N-striking wS_2 crenulation cleavages. These wS_2 crenulation cleavages were overprinted and crenulated by a batholith-parallel wS_3 fabric that is the main foliation through the Warrawoona Belt. This latter fabric is transected by the 3324 Ma Wilina Pluton of the Mt Edgar Granitoid Complex.

The main wS_3 shear fabric was refolded by several generations of mesoscale folds. Sinistral wF_4 drag folds with an S-shaped asymmetry plunge moderately to steeply to the NW, and overprint the main wS_3 shear fabric. These folds may record lateral escape of the greenstones from between Mount Edgar and Corunna Downs Granitoid Complexes. Elsewhere, dextral drag folds of the main wS_3 fabric record a north vergence and greenstone-up sense of shear, which also may be part of the tectonic escape.

The several generations of lineations include: 1) mineral lineations that plunge subvertically; 2) mineral lineations that plunge gently to moderately to the west, and: 3) an intense intersection lineation (L-tectonite) developed by N- to NE-trending wS_5 crenulation cleavage transecting the main wS_3 fabric. This latter intersection lineation has been interpreted as a stretching lineation related to diapirism (Collins *et al.*, 1998; Van Kranendonk, 1998).

There may be an element of dip-slip stretch (*e.g.*, local steep mineral lineation and pressure fringes on pyrite grains). This dip-slip movement was minor in the development of subvertical L-tectonites, as relatively unsheared quartz veins that are crenulated by wS_5 can be mapped across the zones of so-called sinking (*cf.* Collins *et al.*, 1998). Evidence for vertical and horizontal movements is present in quartz veins in the various pits of the Klondyke area. These veins show chocolate-tablet boudinage in both horizontal and vertical sections.

In summary, the structural geology can not easily be reconciled with a single diapiric movement of the granite batholiths. Successive horizontal shortening events across the Pilbara Craton were associated with both upward and lateral escape of the greenstones between the large granite batholiths.

Fluid inclusions

To establish the conditions of ore formation for this deposit, a reconnaissance fluid inclusion study was undertaken on four samples from drill core from this deposit. Lead isotope analyses were also undertaken (see above). A total of 117 fluid inclusions were examined in three doubly polished thick sections containing quartz/carbonate veining. In most cases the vein carbonate appears to have formed earlier than the vein quartz. Both 3-phase (liquid + vapour CO_2 and H_2O) inclusions and vapour-rich (CO_2-bearing) inclusions occur in the carbonate as primary inclusions and pseudosecondary trails. Inclusions in the vein quartz were less abundant with the majority occurring in strained or partly strained quartz as pseudosecondary arrays. The inclusions were mostly monophase but some aqueous inclusions with approximately 5 vol.% vapour were also observed.

Microthermometry

Fluid inclusions within individual healed microfractures within each vein are treated as separate fluid inclusion assemblages (FIA's) as these are assumed to have trapped only one generation of fluid. This method makes it easier to detect multiple generations of fluid or fluid re-equilibration processes. The volume % vapour of a selected number of inclusions from each sample was also accurately measured using the Quantimet 500 image analysis system.

Upon cooling the inclusions, a clathrate generally nucleated between -35 and -40ºC, and solid CO_2 nucleated below -93ºC. Upon warming the fluid inclusions in earlier vein carbonate, the solid CO_2 consistently melted at -56.6 ± 0.2ºC which is the temperature of the triple point of CO_2. A similar result was also obtained for the carbonic inclusions in the vein quartz. This indicates that the carbonic phase in both the carbonate and quartz contained pure CO_2.

The volume percent of the CO_2 phase in carbonate varied greatly from 10 to 100 % CO_2. However, inclusions in the vein quartz were mostly either monophase or liquid-rich with approximately 5 vol. % vapour. Since no other gases were detected in the CO_2-bearing inclusions, the method of Darling (1991) was used to determine the salinity of the aqueous phase from the clathrate final melting temperature. The salinity of the CO_2-rich inclusions in carbonate was generally below 3 equivalent wt.% NaCl while the salinity of CO_2-rich inclusions in quartz typically varied between 2 to 7 equivalent wt.% NaCl with three inclusions having salinities around 11 equivalent wt.% NaCl. The liquid-rich inclusions in quartz had salinities from 3 to 6 equivalent wt.% NaCl which is approximately the same as that of the CO_2-rich inclusions.

Most of the CO_2-bearing inclusions decrepitated before total homogenisation, however, with one exception, the remaining inclusions in carbonate exhibit a well defined mode at around 275 ºC (**Figure 18**). A much wider range of homogenisation temperatures are observed in quartz, which ranges from 160 to 380ºC with an average of 266ºC. The secondary, liquid-rich inclusions in quartz (not shown in **Figure 18**) homogenise over a narrower range from 120 to 180ºC with an average of 153ºC.

Raman microprobe analysis

Laser Raman detection limits are dependent on instrumental sensitivity and the partial pressures of each gas and are estimated to be about 0.15 Mpa for CO_2, O_2, N_2, and 0.03 Mpa for H_2S and CH_4 under the conditions of this study. The vapour phase of each inclusion was analysed for the presence of CO_2, N_2, H_2S, and CH_4 but in accord with the microthermometry results only CO_2 was detected.

Discussion

As most of the vein carbonate occurs on the outer selvedges of the veins, it appears to be earlier than the vein quartz. Although some vapour-rich inclusions occur within the carbonate, the majority of pseudosecondary trails contain only liquid-rich inclusions with constant liquid/vapour ratios. This

suggests that phase separation did not occur during carbonate precipitation and the vapour-rich inclusions may have resulted from leakage and post-entrapment modification of the inclusions. As shown in **Figure 18**, homogenisation temperatures around 275 ºC are consistent with a low salinity fluid containing low amounts of CO_2. However, if the inclusions trapped fluid in the one-phase region, the homogenisation temperature gives us only a minimum trapping temperature and an independent estimate of pressure is required to give us the true trapping temperature.

The fluid inclusions in the vein quartz have a much larger scatter in homogenisation temperature than those in carbonate. The inclusions in quartz have an average homogenisation temperature of 266 ºC but the homogenisation temperature of only two vapour-rich inclusions could be measured as the rest decrepitated before homogenisation. Once again the homogenisation temperatures from the liquid-rich inclusions are consistent with those expected from a fluid with approximately 6 wt.% NaCl and low CO_2 contents. The increase in salinity in the inclusions in quartz could possibly result from phase separation during quartz precipitation which would be consistent with the higher proportion of vapour-rich inclusions observed in the quartz. If phase separation is assumed to have occurred, then no pressure correction is required and the fluids in quartz would have been trapped between 160 and 380 ºC at pressures ranging from 4 to 6 kbar (Brown & Hagemann, 1995).

The CO_2 content of the fluids, the salinity and the homogenisation temperatures and pressures are all similar to those of lode Au deposits such as those commonly found in the Yilgarn Craton in Western Australia. Therefore, this deposit appears to be a similar style of lode Au deposit.

Selected deposits of the Warrawoona district

At the Gauntlet deposit, Jones (1938) described a small pipelike orebody that pitched north at a very steep angle. The ore body was formed at the intersection between an east-west striking reef and a reef striking 322°. At the surface, the ore shoot was 5 m long, broadening at depth to be 10 m long with an average width of 60 cm. Jones (1938) reports little drop off in grade.

Along strike to the east-southeast, the Klondyke Queen mine produced almost 5,000 oz Au from 1898 to 1936 (Jones, 1938). The mineralised zone, which strikes 290°, contains a fuchsite-pyrite-quartz alteration assemblage. Quartz veins are boudinaged in a chocolate-tablet manner (vertical and horizontal). A 15 cm wide black chert band, termed the Kopkes Leader by early miners, is exposed along the southern edge of the fuchsite altered zone. This chert band is laterally persistent and provides an indication of the location of mineralisation.

Age of mineralisation

Galena from the Warrawoona district returned a large range of model ages (**Table 5**). As discussed previously, this range of ages is interpreted to result from the mixing of Pb from two separate hydrothermal events. If so, the maximum model age of 3385 Ma is considered as the minimum age of gold mineralisation. The most likely age, by analogy with Bamboo Creek and Normay (Zegers, 1996; Thorpe et al., 1992b), is in excess of 3400 Ma.

Lode gold deposits of the southwest Mosquito Creek Belt

Introduction

Until recently, the Archaean Mosquito Creek Formation was the only known metasedimentary host for lode Au and Au-Sb deposits in the Pilbara Craton. In excess of 5 t of Au have been extracted from the Mosquito Creek Belt (**Fig. 1a**), with an average, in the early days, of 3.0 oz/t (Maitland, 1908). The Mosquito Creek Belt hosts four mining centres, Eastern Creek, Middle Creek, Mosquito Creek, and Twenty Mile Sandy. Gold production to the end of 1988 was 4819 kg. Identified resources at the time of writing amount to 11.57 Mt grading 2.27 g/t, making a production and

remaining resource total of 31.8 t Au (**Table 7**). Deposits in these mining centres are aligned onto two east-west arcuate lineaments. The northern Blue Spec Line (Au-Sb), and southern Middle Creek Line (Au), can both be traced for 40 km along strike in the southwest part of the Mosquito Creek Belt (**Fig. 19a**).

This paper describes five deposits from the westernmost 20 km of the arcuate Middle Creek Line (**Fig. 19a**) to illustrate the large diversity in deposit style over a short distance. Although this diversity in deposit style creates a challenge for exploration, there may be a common origin, and deposit style differences may be simply a function of structural control.

Regional Geology

The Mosquito Creek Belt is exposed in an elongated belt 120 km by 60 km in the east Pilbara Craton (**Fig. 19a**). Geophysical data indicate that these rocks extend under the Hamersley Province, 20 km to the east, and 20 km to the southwest of the exposed portion. The extension of this rich Au-bearing belt under cover offers unexplored potential for mineralisation.

The Middle Creek Line defines the northern extent of upper greenschist facies metamorphic rocks in the Mosquito Creek Belt. These higher grade rocks include mylonite, phyllite, mica schist, and chlorite ± magnetite schist, as well as mafic and felsic intrusive rocks. To the north of the Middle Creek Line, the Mosquito Creek Formation is dominated by poorly sorted wacke-siltstone and wacke-sandstone interbedded with more pelitic rock types. Coarser grained rock types, including conglomerate and pebbly sandstone are also present.

Hickman (1983) estimated the stratigraphic thickness of rocks of the Mosquito Creek Belt to be ~5000 m, although he acknowledged the difficulties in this estimation due to tectonic thickening from isoclinal folding. Along the northern margin of the belt, the base of the Mosquito Creek Formation lies unconformably on the Warrawoona Group. The Kurrana Shear Zone defines the southern margin of the belt (**Figs. 1, 19a**).

The deposits in the southwest part of the Mosquito Creek Belt are overlain on a reduced-to-pole magnetic image in **Figure 19b**. The Mosquito Creek Belt rocks are mostly low- to non-magnetic, and the textured body to the south is the Kurrana Granite. Of particular interest are the two linear magnetic highs in the mostly low-magnetic Mosquito Creek Belt rocks that define part of the trace of the Middle Creek Line (see later discussion).

Structural Geology

As the structural setting of the deposits along the Middle Creek Line is variable, knowledge of the structural evolution is needed to understand the mineral deposit style. Rocks of the Mosquito Creek Belt record at least six phases of penetrative deformation. The style of deformation becomes progressively more brittle through time, reflecting the unroofing and inversion of the Mosquito Creek basin.

The uncertainty in the age of the Mosquito Creek Formation makes the precise correlation of this belt's relative structural chronology with other areas of the Pilbara somewhat tentative (**Table 2**). The deformation chronology presented here is local.

mD_1

In the metamorphic rocks to the south of the Middle Creek Line, the first event recognised is an mS_1 fabric that is mostly parallel to bedding and most easily recognised in the fold closures of later tight to isoclinal mF_2 folds. mD_1 structural elements are not found in the rocks to the north of the Middle Creek Line.

mD$_2$

To the north of the Middle Creek Line, the earliest fabric in the Mosquito Creek Formation is a strong penetrative slaty cleavage, interpreted as *m*S_2, that strikes east-northeast across the belt. This element may correlate with the first main fabric (*a*S_1) in the Mallina Basin (Blewett, 2000a). Mesoscale *m*F_2 folds are mostly tight to isoclinal and inclined, with an axial-plane *m*S_2 slaty cleavage. Most *m*F_2 plunge shallowly to the east-northeast (**Fig. 20a**). A reclined macroscale *m*F_2 anticline-syncline pair defines the structure of the North and South Dromedary hills in the far southwest part of the belt (**Fig. 21**). The northern limb of this macroscale fold is right-way up and dips moderately to gently to the north, while the southern limb is overturned, and dips steeply to the north. To the south of Middle Creek Line, an *m*S_2 crenulation cleavage overprints andalusite porphyroblasts (*m*M_1?) and are, in turn, overprinted by north-plunging *m*F_3 folds.

mD$_3$

Widespread *m*D_3 deformation resulted in approximately north trending, upright folds and associated crenulation cleavage, as well as dextral reworking of the main *m*S_2 fabric in response to a regional east-west shortening event.

Many of the *m*D_3 shear zones trend sub-parallel to the *m*S_2 cleavage and contain shear bands (*m*S_3) with a dextral sense of shear (northeast–southwest). The dextral shear couple is a result of east-west coaxial compression acting on a pre-existing east-northeast-oriented anisotropy (*m*D_2). Stretching lineations (*m*L_3), defined by chlorite, plunge steeply to the north-northeast. The pitch of the lineation on the shear plane and the accompanying kinematic indicators (S-C fabrics) imply normal-dextral oblique-slip shearing. Along the southern margin of the Mosquito Creek Belt, the *m*D_3 shear bands are defined by chlorite, which record a dextral sense of movement.

mD$_4$

The *m*D_4 structures include north- to northwest directed reverse faulting and shearing, and east-northeast-trending upright folds and associated crenulations. Shearing is particularly intense and complex along parts of the Middle Creek Line, which contains many of the lode Au mineral occurrences in the belt. The *m*D_4 deformation event reflects northwest-southeast oriented shortening.

mD$_5$

Despite the apparent ‘stratabound’ alignment of workings along the Middle Creek Line, in detail most deposits were influenced by cross-cutting structures. North-trending *m*D_5 faults were developed under high-level, brittle conditions, with maximum compression oriented north-south. Most faults dip steeply and have sinistral and dextral strike-slip offsets, as well as normal-oblique movements. Late-stage conjugate quartz veins that trend northwest and northeast are interpreted to fill *m*D_5 structures.

mD$_6$

The last penetrative fabrics to develop were *m*S_6 crenulations and kinks. The crenulation is commonly a fine-spaced, steeply dipping fabric that strikes northwest-southeast and generally dips steeply to the southwest. No macroscopic folds have been observed to be associated with this minor fabric, despite its common appearance in the more pelitic and least competent units. Additional to these fine-spaced crenulations is an unknown generation of gently dipping to subhorizontal crenulations. Steeply dipping conjugate faults were also developed during *m*D_6, with north-northwest- to north-trending dextral faults and reworking of the east-northeast-trending structural grain by sinistral faults.

Selected lode gold deposits.

In the following section the Golden Eagle, Otways-Shearers, and Bartons-Hopetoun North (**Fig. 19a**) deposits are described to illustrate the diversity of lode Au mineralisation in the Mosquito Creek Belt.

Golden Eagle

Geology and host rocks

At the Golden Eagle deposit, the westernmost deposit on the Middle Creek Line (**Fig. 19a**), a resource totalling 10.1 t Au has been established (**Table 7**). Deformed metaturbiditic rocks of the Mosquito Creek Formation host the Golden Eagle deposit. The metamorphic grade is low greenschist facies. The deposit lies on the eastern end of a weak magnetic anomaly, which can be traced to the southwest under cover rocks (**Figs. 19a, 19b**).

Examination of RC cuttings indicate that two broad units are present at Golden Eagle (**Fig. 22a**), a lower psammitic unit with a 20 m thick pelitic lens towards its base, and an upper pelitic unit with only narrow psammite-bearing lenses. These units dip 30° to the north-northwest.

Structural geology

The Golden Eagle deposit lies on the northern, upright, limb of a major reclined, easternly plunging. Bedding is consistently at more shallow attitudes than the mS_2 slaty cleavage. Mesoscale mF_2 folds are reclined and verge south, consistent with the geometry of the major structure (**Fig. 20a**). A weak mL_2 chlorite mineral lineation plunges to the northwest, perpendicular to the mF_2 fold hinge and within the axial-plane mS_2 cleavage. A fine-scaled mS_6 crenulation cleavage, with crenulation fold axes plunging to the northwest, is the only visible overprinting penetrative fabric other than quartz veins and joints.

Mineralisation

The original Golden Eagle deposit is exposed in a small open cut (**Fig. 20b**), and was mined from 1898 to 1901, producing 15.4 kg of Au from ore grading 144.6 g/t (Maitland, 1908). Extremely high Au grades (to 102 g/t; Kismet Gold Mining Prospectus) are associated with narrow ferruginous quartz veins that cut highly weathered and cleaved (mS_2) siltstone with minor, disseminated pyrite casts, particularly adjacent to the veins.

The present Golden Eagle resource occurs within an east-northeast-trending zone just north of the historic mine as broadly stratiform zones. The most significant zone, which occurs mainly in the upper part of the psammitic unit has a maximum thickness of ~50 m (**Fig. 22b**). Many of the highest values within this zone occur within 10 m of the surface, indicating possible supergene upgrading. A second, narrower (5-10 m) zone occurs within pelitic rocks in a lens toward the base of the lower psammitic unit. This zone is separated from the main zone by 15-20 m of relatively low grade rock. Gold is slightly enriched in psammitic and mixed psammite-pelite intervals relative to pelitic intervals, and gold grades are also enhanced in zones with abundant pyrite and quartz, particularly in psammitic intervals.

The concentration of vein quartz and pyrite in psammitic relative to pelitic units may be a function of their behaviour during deformation. Being more competent, psammitic units take up strain by fracturing, whereas pelitic units take up the strain by more ductile mechanisms. As a result of more intense fracturing, psammitic intervals concentrate mineralising fluids, leading to more intense veining and pyritisation, and hence, Au mineralisation.

The most abundant ore mineral at Golden Eagle is pyrite, which is present at levels up to 5% in drill cuttings. Other ore minerals present at Golden Eagle include rutile, magnetite, chalcopyrite, gold,

sphalerite, galena, and altaite. Magnetite occurs as in abundances up to 5%, which may explain the aeromagnetic anomaly (**Fig. 19b**), and the high magnetic susceptibility (up to 1680 x 10^{-5} SI units) near the base of some drill holes.

Alteration

Although variations in alteration facies are subtle, general relationships indicate that the basal, more psammitic, part of the sequence tends to be more strongly silicified in comparison with the upper, more pelitic, part of the sequence, which tends to be more sericitic (**Fig. 22c**). Examination of thin sections from the more silicified intervals suggests that the silicified zone also contains abundant tourmaline. Albite and K-feldspar are also stable in the silicified zone, they occur both in the wall rock and in quartz-feldspar veins. This quartz-tourmaline±feldspar altered zone is broadly associated with disseminated pyrite that locally comprises 5% of the rock. The zone of pyritisation dies out towards the north, which may relate to the major grade drop off in the northern-most hole in the fence (**Fig. 22b**).

Chips from a total of 83 composite (4 m) samples were analysed using PIMA which identified chlorite and sericite as the major phyllosilicate minerals present. Other minor minerals identified include montmorillonite and biotite. The biotite is restricted to the psammitic lower sequence and does not have any observable relationship to Au grades.

Of the quantitative parameters measured, only two, the depth of the H_2O feature and the wavelength of the Al-OH feature (**Fig. 22d**), showed systematic variations. As the depth of the H_2O feature increases markedly near the surface and towards a low hill to the south (not shown), this feature is interpreted to reflect weathering processes. The wavelength of the Al-OH feature, which measures the phengicity of sericite, increases within the psammitic unit, suggesting that it is lithologically controlled. No systematic relationship to Au grades was observed for any of the parameters measured from the PIMA spectra.

The alteration assemblages associated with the Golden Eagle deposit are unusual in that they lack widespread carbonate, a feature commonly present in lode Au deposits in the Eastern Goldfields Province (Groves, 1993), turbidite-hosted Au deposits in Victoria (Bierlein, *et al.*, 1998) and deposits from the Pilbara Craton (Zegers, 1996; see above). Carbonate is present in small quantities, usually in quartz veins, but wall rock carbonate alteration was not observed at Golden Eagle.

Fluid inclusion studies

Four samples of vein quartz were selected for fluid inclusion studies. Although the vein quartz has been largely recrystallised, which has destroyed most the early inclusions or moved them to grain boundaries, there are many trails of secondary inclusions. These secondary inclusions range up to 30 μ in size and are irregular to rounded. Three types of inclusions were recognised: (1) vapour-rich, carbonic inclusions that did not freeze upon cooling to -194ºC, (2) vapour-rich, carbonic inclusions that froze upon cooling, with CO_2 melting temperatures of -63.6 to -62.6ºC; and (3) aqueous inclusions with eutectic melting temperatures of -59.1 to -24.5ºC. Some liquid-rich inclusions contained only about 2 vol.% vapour and a small needle-like, opaque solid. One sample contained some relict quartz crystals with apparent pseudosecondary, liquid-rich inclusions, but the inclusions with solids appear to be late secondary inclusions.

Homogenisation temperatures of the carbonic phase of type (1) inclusions ranged from -71.1 to -63.2ºC, implying a very high methane (or nitrogen) content. Clathrate melting temperatures were around 20ºC and salinities were not determined.

The low CO_2 melting temperatures of type (2) inclusions indicate that they contain a significant quantity of another gas (CH_4?). Assuming that methane was the other gas, salinities range between 2.3 and 3.0 eq. wt. % NaCl. As most inclusions decrepitated before total homogenisation, only three homogenisation temperatures were recorded. Two inclusions homogenised to the vapour phase at 311.9 and 373.9ºC, respectively, while the other inclusion homogenised to the liquid phase at 283.7ºC.

The low eutectic temperatures of type (3) aqueous inclusions indicate the presence of other salts besides NaCl, probably including $CaCl_2$. The salinities of these inclusions are bimodal, with one mode at 9.5-21.7 eq. wt. % NaCl and the second with salinities below 5 eq. wt. % NaCl. The moderate to high salinity inclusions homogenised between 100 and 198ºC with a mean of 140ºC (**Fig. 23**). The lower salinity fluid inclusions homogenised between 99 and 263ºC with a mean of 130ºC.

The high $CH_4(\pm N_2)$ content of type (1) inclusions is similar to metamorphic fluids generated during the late stages of a continental collision (Mullis *et al.*, 1994), and are interpreted to be regional metamorphic fluids. The more CO_2-rich, type (2) fluids have characteristics similar to ore-bearing fluids from lode Au deposits (Groves *et al.*, 1998) and hence, are thought to be related to Au mineralisation. If phase separation (i.e., boiling) occurred during mineralisation, then this may have lead to an increase in the salinity of the aqueous phase and to the trapping of the moderate-high salinity fluid inclusions reported above. The low salinity inclusions most likely represent the late influx of meteoric fluids.

Shearers and Otways

Geology and host lithology

The outermost unit in the Shearers-Otways area consists of chloritic schist with interlayered amphibolite, psammite and minor talc schist. The amphibolite generally occurs as 10-50 m thick, strataform lenses that extend up to 300 m along strike. These rocks may not be part of the Mosquito Creek Formation, rather they may be correlates of the Gorge Creek Group (3240 Ma) or even older units found to the west (Wouter Nijman, pers comm, 1999). Shearing accommodated within these chlorite schists marks the trace of the Middle Creek Line.

The chlorite schists are in contact to the north with a 20-80 m thick, lenticular, conglomerate, with the thickest section just to the west of the Shearers deposit, but thinning further to the west. The conglomerate is lithologically and stratigraphically similar to conglomerate exposed at the North and South Dromedaries (**Fig. 19a**). A 10-70 m thick psammitic unit, that thickens to the west, overlies the conglomerate. The pelitic schist that forms the base of the central pelitic unit of Thom *et al.* (1973) overlies this psammitic unit. These rocks dip sub-vertically and young to the north.

Structural geology

This stratigraphy (**Fig. 24**) has been cut by two north-trending dextral faults that have offset the steeply north-dipping stratigraphy by 60 m (eastern fault) and 170 m (western fault). As the thickest accumulation of conglomerate is just to the west of the western fault, it is possible that this fault was initially a growth fault. This western fault is marked in places by a 0.2-1 m thick quartz vein. Minor north-trending dextral faults are common, with mm to cm offsets (**Fig. 20d**).

The Otways–Shearers sequence, particularly the chloritic schist, talc schist and pelitic units, is deformed by an east-northeast-trending foliation, which is locally overprinted by a north-trending crenulation. The east-northeast-trending foliation is interpreted to be a composite of the regional mS_2 and mS_4 foliations, whereas the north-trending foliation is inferred to be mS_3. The chlorite schists south of the Shearers deposit are overprinted by the main mS_1 schistosity, which is

isoclinally folded by east-plunging mF_2 folds. Although the north-trending faults cannot be traced into this southern, chloritic unit, the southern extensions of these faults are characterised by an increase in the frequencey and intensity of mS_5 crenulations..

Mineralisation

The Shearers deposit occurs as a north-trending zone of quartz veins and stockworks near the western fault (**Fig. 24**). Although broadly associated with this fault, in detail, much of the Shearers mineralisation occurs in a stockwork zone of quartz veins that is about 1 m wide at the surface and extends for nearly 200 m 10-20 m to the east of the fault. At the surface, the host to the mineralised stockwork is pelitic rock types. A sample from this zone assayed 0.38 ppm Au, whereas a sample from the quartz vein that marks the fault assayed only 0.08 ppm Au (Appendix A). To the south of this stockwork zone, the vein which marks the fault is variably, but weakly, mineralised. One sample assayed 0.18 ppm Au and a second sample assayed 0.06 ppm Au.

At the Otways prospect which is located 50 m south of the 'Otways' diggings (**Fig. 24**), the mineralisation, which is patchy, occurs in east-northeast- to northeast-trending (040-065º), subvertical to steeply northwest-dipping (70-90º) veins that are hosted by conglomerate. The easternmost mapped vein in the Otways prospect area, which strikes 065º, is intersected by a 5 m long, 005º-trending vein. The east-northeast-trending vein assayed 0.32 ppm Au, whereas the north-trending vein assayed only 0.06 ppm Au. Samples of other east-northeast-trending veins assayed 0.66 and 0.68 ppm Au, respectively, which confirms that Au is associated with the north-northeast- to northeast-trending veins. These mineralised veins appear to be controlled by the conglomerate: on either side of the conglomerate, these veins rapidly pinch out. The veins are typically 0.2-1 m in width and extend 40-100 m in strike length. The Otways 'diggings' were developed on an east-northeast-trending silicified zone within pelites to the north of the conglomerate. However, two samples from these silicified zones assayed <0.01 and 0.02 ppm Au, respectively, suggesting that silicification did not bring in significant Au.

Alteration

At the Shearers deposit, the alteration zones associated with the mineralised veins and stockworks are narrow, extending at most 1 m away from the mineralised zone. These alteration zones are characterised by silicification and sericitisation. At the surface, these narrow zones are weakly to moderately ferruginous.

Geochemistry

In addition to Au, only As, Sb and Te are systematically and significantly elevated with respect to average crustal values at the Shearers deposit. The Te values, although elevated relative to crustal abundances, are not elevated relative to samples from other prospects analysed (*e.g.*, Bartons). Of the other elements determined, most Ag values of Au-bearing quartz are also significantly elevated, and, locally, Bi is also significantly elevated. One sample also was elevated in Pb. Mercury, Tl, W, U, Cu and Zn were below or near crustal abundances in all samples. The geochemical suite that characterises the Otways and Shearers deposits is Au-As-Sb±Ag±Bi. The Bartons deposit veins have a similar trace element suite, but their levels of As, Sb and Te anomalism are significantly higher than those at Otways and Shearers.

Bartons and Hopetoun North

Geology and host rocks

Unlike the more simple structural geology of the Golden Eagle deposit, the Bartons and Hopetoun North deposits have a complex structural history of folding, refolding, and several generations of shearing (**Figs. 20e, f, g, h**). Greenschist facies metasedimentary rocks host the Bartons and the Hopetoun North deposits. The host rocks are sheared and all display well-developed penetrative

fabrics. To the south of the deposits, chlorite schists crop out and are characterised by an additional, earlier fabric, which is interpreted to be mS_1.

Structural geology
Chlorite schists to the south of the Hopetoun North deposit are characterised by isoclinal mF_2 folds of the mS_1 cleavage. However, the main fabric, which is present throughout, is an east-northeast-trending schistosity to slaty cleavage that is axial planar to isoclinal mF_2 folds. North-south trending mS_3 crenulations that overprint the this fabric, and mD_4 shear zones with steep south-block up reverse movement deform mS_3 crenulations.

Mineralisation
The Barton mine was one of the most productive mines in the central part of the Middle Creek Line, producing 239 t of Au, with additional identified resources of 820 t (**Table 7**). The production, which mainly occurred early last century came from ore averaging 37 g/t (Finucane, 1939). The Hopetoun deposit was much smaller, producing only 8 t from 890 t of ore.

The Barton mine contains three north-northeast- to northeast-trending quartz reefs, with an overall strike-length of ~300 m. The West and Main reefs dip on average 60°E, and strike 030 (**Fig. 20g**). The East reef strikes 040, and dips 70-75°SE. Finucane (1939) reported that four ores shoots were worked on the Main reef. These shoots pitch north at 30° to 40°, parallel to the intersection between the schistosity/cleavage and the reef.

The Hopetoun North deposit contains six short (30 m), north-northeast-trending, steeply dipping quartz veins in highly sheared pelite. The main fabric is a phacoidal mS_2 schistosity that has been extensively reworked by mD_3 and mD_4 shearing (**Figs. 20e, f**). The shear fabrics strike north-northeast and dip steeply to the east (**Fig. 20g**). Quartz veins were transposed into parallelism with the mS_2 fabric and boudinaged by the shearing. Shear sense indicators suggest a southeast down (normal) dextral shear (mD_3) overprinted by a northwest-directed mD_4 thrusting event (**Fig. 20f**).

Auriferous quartz veins at the Bartons and Hopetoun North deposits are folded by mF_4 folds, which plunge moderately northeast and verge northwest (**Fig. 20h**). Pyrite grains, which overprint fine mS_3 crenulation cleavages, have pressure fringes developed during *m*D4 deformation that locally record a south-block up shear movement. This sense of movement is consistent with the vergence and asymmetry of the mF_4 folds.

Timing and genesis of lode gold deposits in the southwest Mosquito Creek Belt
The descriptions above illustrate the great diversity of deposit styles along a relatively short section of the Mosquito Creek Line in the southern Mosquito Creek Belt. This diversity makes developing unifying genetic models of mineralisation difficult. One of the most difficult elements to determine for a mineral system is the timing of mineralisation, both in an absolute sense, and relative to other geological events.

Timing of mineralisation
Although the actual timing of ore deposition at Golden Eagle relative to structural elements could not be determined, geological relationships can be used to constrain the relative ages of the Shearers, Barton and Hopetoun North deposits.

At Shearers, the age of the dextral faulting, and therefore mineralisation, postdates the mS_4 cleavage. However, mineralisation could have occurred during the last stages of mD_4, with maximum compression oriented almost north-south to generate the dextral offsets on the faults. Alternatively,

mineralisation could be younger; the mD_5 event also involved north-south shortening. Another alternative is an early Fortescue (*ca* 2760 Ma) age.

At Bartons mineralisation postdates mD_3 but predates or is synchronous with mD_4 as pyrite cubes overprint the mS_3 crenulation cleavage but have pressure shadows that grew during north-directed shearing. Gold is also hosted in sheared mF_4 folded quartz veins (**Fig. 20h**). Mining at the Hopetoun North deposit was also concentrated along mD_4 shears. The mF_4 fold vergence, pyrite pressure shadows, and the shear sense indicators on the mD_6 shear zones, are consistent with tectonic transport to the north-northwest and northwest. These observations suggest that mineralisation is syn mD_4.

In summary, the relationships at Shearers, Bartons and Hopetoun North suggest mineralisation is syn- to late-mD_4, although relationships at Shearers are also consistent with a later timing, either syn-mD_5 or early Fortescue. These relative timings are similar to that demonstrated in the Indee district, where mineralisation is also interpreted to have formed late during an north-northwest-directed compressional or transpressional event.

As discussed earlier, a Pb-Pb model age of 2905 Ma (Thorpe *et al.*, 1992b) was obtained from Au-bearing quartz veins from further east in the Mosquito Creek Belt. This age is consistent the D_{4c} regional event elsewhere in the Pilbara Craton (i.e. in the Indee district, **Table 2**; Blewett, 2000a). The timing of gold mineralisation in the Mosquito Creek Group favoured here is for Au deposition during mD_4 (regional D_{4c}) and local remobilisation and concentration during later mD_5 deformation.

Ore controls

Lithology as well as pyrite and quartz abundance control Au distribution at Golden Eagle. A possible reason for the concentration of vein quartz and pyrite in psammitic relative to pelitic units is their relative behaviour during deformation. Being more competent, psammitic units take up strain by fracturing and cleavage development, whereas pelitic units take up strain by flow. As a result of more intense fracturing, psammitic intervals concentrate mineralising fluids, leading to more intense veining and pyritisation, and hence, Au mineralisation. Or, the competence allows the development of lower pressure, dilatational zones that facilitate fluid effervescence and quartz and Au to precipitate.

Along the western end of the Mosquito Creek Belt, the mD_4 strain was partitioned mostly to the south along the Middle Creek Line. At the Golden Eagle deposit, the mD_4 strain was distributed over a pre-existing north-dipping anisotropy, resulting in subhorizontal tension-like dilation within the more competent horizons (**Fig. 20c**). The north-northwest oriented shortening also resulted in more steeply dipping northeast and northwest conjugate vein sets, that were exploited in the original mining operations. Alternatively, the steeper veins were later, associated with north-south shortening during mD_5, which remobilised mD_4 Au into high-grade veins.

The unifying theme to the Otways and Shearers deposits is the close association of mineralisation and conglomerate (**Fig. 24**). The Otways veins are hosted by, and do not extend far outside of, the conglomerate unit. The Shearers vein, although not entirely hosted by conglomerate, occurs where the conglomeratic unit is offset by a north-trending dextral fault. These relationships suggest that the relative competency of the conglomerate relative to surrounding rock units was an important control on mineralisation.

The north trend of the Shearers prospect is also unusual as other deposits in the Mosquito Creek Formation generally have trends from 060º in the west to 110º in the east (Huston *et al.*, 1999). Other deposits that have north-trending ore lenses include the All Nations and Onion mines

(Finucane, 1939). Huston *et al.* (1999) interpreted north-trending faults present at Shearers as second-order Reidel faults developed under the latest stages of the mD_4 deformation. Alternatively these veins were developed under north-south compression during mD_5. Another alternative interpretation is that the dextral faults were related to Fortescue age extension, with the north-trending dextral faults developed during ESE oriented extension.

The Blue Spec Line
The Blue Spec Line is located about 6 km north of, and parallel to, the Middle Creek Line. The Blue Spec Line is developed in sheared pelitic rocks of the Mosquito Creek Formation. The Blue Spec deposit like others along strike the Blue Spec Line, hosts Sb-Au mineralisation on steeply southeast-dipping bifurcating shears (Gifford, 1990). An unknown question is "are these Sb-Au deposits part of the same lode Au mineral system of the Middle Creek Line, such as in the Murchison Province of South Africa?" The continuum model (Groves, 1993) would place the Sb-Au deposits at a higher level in the system. More work is needed to address this question.

Summary of gold events of the Pilbara Craton

Evidence presented herein suggests that lode Au mineralisation in the Pilbara occurred in two main events, one at *ca* 3400 Ma and the second at *ca* 2900 Ma. Both of these events coincide with major craton-wide deformation events and postdate the deposition of major supracrustal rock packages.

The *ca* 3400 Ma event is restricted mainly to mafic and ultramafic rocks of the Warrawoona Group and seems to be associated with faults and shear zones that now ring major granitoid complexes in the East Pilbara Granite-Greenstone Terrane. In contrast, the *ca* 2900 Ma event is hosted by turbiditic rocks of the DeGrey Group, mafic-ultramafic rocks of the Warrawoona and possibly other units older than 2900 Ma. These deposits are associated with east-northeast-trending, terrane-scale faults and shear zones such as the Mallina Shear Zone.

The association of lode Au deposits with ring faults around granitoid complexes seems to unique to the Pilbara. Rather, in most Archaean terranes, lode Au are related to province-scale, broadly linear structures such as the Boulder-Lefroy Fault in the Eastern Goldfields Province in the Yilgarn Craton (Vearncombe et al., 1989). The association of the *ca* 2900 Ma deposits with terrane-scale structures such as the Mallina Fault Zone is most similar to the relationship demonstrated in the Eastern Goldfield Province and in the Abitibi Subprovince in the Superior Province (Hodgson and Hamilton, 1989). The Middle Creek and Blue Spec Lines may be manifestations of such structures in the Mosquito Creek Belt. Recognition of such terrane-scale structures bodes well for the potential of the *ca* 2900 Ma lode Au event.

Local controls on lode gold mineralisation

Much of the gold mineralisation in the Pilbara is associated with shear zones and the faulted contacts between units of contrasting competencies and lithology. These shear zones and faults range in strike length, throw, geometry and structural level now exposed. The important control of tensional zones in regional faults is illustrated at the Withnell deposit. This deposit appears to be hosted in a tension-gash array developed during normal faulting with a downthrow to the north.

Sheared contacts between units with a marked competency contrast controlled mineralisation in the Mt York-Lynas Find district, where deposits are commonly hosted by altered, competent mafic rocks near sheared contacts with ultramafic rocks.

In the Warrawoona district, Au is hosted mostly by boudinaged quartz veins that strike subparallel to the main west-northwest oriented tectonic fabric of the greenstone belt. A more tabular set of later

quartz veins intersect the main trend at a high angle. The intersection of these two trends results in very steeply north-plunging ore shoots, so that gold may have been introduced during two different events. These ore shoots are a subparallel to a pervasive lineation (L-tectonite) formed by the intersection of two tectonic foliations. The later fabric may be the regional S_{4b} or S_{4c} fabrics.

In the Mosquito Creek Belt, Au mineralisation along the Middle Creek Line is located just to the north of the contact between chloritic schist to the south and metasedimentary rocks to the north. The deposits are oriented both parallel to this contact and at a high angle to this contact. The controls on mineralisation along the Middle Creek Line appear to be related to competency (Golden Eagle, Shearers, and Otways deposits), and shear zones (Bartons and Hopetoun North deposits).

Tectonic controls on lode gold mineralisation

Lode Au mineralisation in the Pilbara was probably introduced during two separate events, the first at ca 3400 Ma, and the second at ca 2900 Ma. Blewett (2000a) identified a multiphase deformation history for the Pilbara Craton, and interpreted these two mineralising events to possibly correlate with the regional D_{2a}, and the regional D_{4c} events respectively.

The ca 3400 Ma lode Au event was probably associated with the regional D_{2a} deformation event. This event is only found in the Warrawoona and Coonterunnah Groups Greenstones. Maximum compressive shortening during D_{2a} is interpreted to have been from the northeast-southwest.

The ca 2900 Ma event appears to be associated with northwest-southeast convergence (D_{4c}; Blewett, 2000a) that developed east-northest-trending structural elements in the Mallina Basin and in the Mosquito Creek Belt. At Mount York-Lynas Find, Au deposition was associated with renewed D_{4c} sinistral shear, many of the shear zones being reworking of earlier D_{4b} faults.

Epithermal mineralisation

Epithermal vein systems have been recognised in the Central Pilbara Tectonic Zone (e.g. Becher and Orange Rock). Marshall (2000) indicates that these vein systems are probably more widespread, including Pb-Ag deposits in the Braeside district in Fortescue Group rocks just to the east of the East Pilbara Granite-Greenstone Terrane. R. Smithies (pers. comm., 2000) has observed epithermal textures in Fortescue Group rock on the SATIRIST and WHITE SPRINGS 1:100 000 sheet areas, well southeast of the occurrences herein, which are on the YULE and SHERLOCK 1:100 000 sheet areas.

The deposits described as part of this study trend to the north and are interpreted to be associated with phases of the opening of the Fortescue Basin at 2780-2700 Ma. Evidence for this timing includes geological relationships and some Pb isotope data as described above. To the authors' knowledge these deposits are the best preserved examples of old epithermal vein systems. Data from this study indicates that these veins contain zones with anomalous Au, but elements of the epithermal suite, including As, Sb, W and Te, are characterised by stronger, more widespread anomalism.

Acknowledgements

Resolute Ltd, Lynas Gold NL and Welcome Stranger NL are all thanked for allowing access to the various deposits during this study. Additional assistance in the form of logistical support and access to data are appreciated. Sean Armstrong, John Backo, John Bunting, Nigel Cranley, Andrew Eaddows, Brett Keillor, Bruce Morrin, Steve Shelton, and Jon Standing are thanked for introducing the authors to the various deposits, their assistance at various times and their discussions in the field. Our field assistants Peter Taylor, Olli Muellenhoff, Holger Przibytzin, Lasslo Beckman, and Olli

Bigge are gratefully acknowledged. We thank Darcy Baker, David Champion, Bill Collins, Arthur Hickman, Hugh Smithies, Wouter Nijman, Martin Van Kranendonk, Peter Wellman, and Stan White for the opportunity to discuss the great geology of the Pilbara.

References

Arndt NT, Nelson DR, Compston W, Trendall AF & Thorne AM. 1991. The age of the Fortescue Group, Hamersley Province, Western Australia, from ion microprobe zircon U-Pb results. Australian Journal of Earth Sciences; 38:261-281.

Barley ME & Pickard AL. 1999. An extensive, crustally-derived, 3325 to 3310 Ma silicic volcanoplutonic suite in the eastern Pilbara Craton: evidence from the Kelly Belt, McPhee Dome and Corunna Downs Batholith. Precambrian Research; 96:41-62.

Bickle MJ, Bettenay LF, Barley ME, Chapman HJ, Groves DI, Campbell IH & De Laeter, JR. 1983. A 3500 Ma plutonic and volcanic calc-alkaline province in the Archaean East Pilbara Block. Contributions to Mineralogy and Petrology; 84:25-35.

Bickle MJ, Bettenay LF, Barley ME, Chapman HJ, Groves DI, Campbell IH & De Laeter JR. 1989. The age and origin of younger granitic plutons of the Shaw batholith in the Archaean Pilbara Block, Western Australia. Contributions to Mineralogy and Petrology; 101:361-376.

Bierlein FP, Fuller T, Stuwe K, Arne DC & Keays RR. 1998. Wallrock alteration associaed with turbidite-hosted gold deposits. Examples from the Palaeozoic Lachlan Fold Belt in central Victoria. Ore Geology Reviews; 13:345-380.

Bierwirth P, Blewett R & Huston D. 1999. Finding new mineral prospects with HYMAP: early results from a hyperspectral remote-sensing case study in the west Pilbara. AGSO Research Newsletter; 31:1-3.

Blewett RS. 2000a. North Pilbara 'Virtual' Structural Field Trip. Australian Geological Survey Organisation record 2000/45.

Blewett RS. 2000b. Facsimile copy of the Aerial Geological and Geophysical Survey of Northern Australia (AGGSNA) Reports 1 to 26, 28, 46 to 48, 51 to 59 for Western Australia Pilbara Goldfield. Canberra. Australian Geological Survey Organisation record 2000/05.

Blewett RS & Huston DL. 1999. Deformation and gold mineralisation of the Archaean Pilbara Craton Western Australia. AGSO Research Newsletter; 30:12-15.

Blewett RS, Wellman P, Ratajkoski M & Huston DL. Atlas of North Pilbara geology and geophysics. Canberra. Australian Geological Survey Organisation record 2000/04.

Bodnar RJ, Reynolds TJ & Kuehn CA. 1985. Fluid-inclusion systematics in epithermal systems. Reviews in Economic Geology; 2:73-97.

Brown PE & Hagemann SG. 1995. MacFlinCor and its application to fluids in Archaean lode-gold deposits. Geochimica et Cosmochimica Acta; 59:3943-3952.

Buick R, Thornett JR, McNaughton NJ, Smith JB, Barley ME & Savage M. 1995. Record of emergent continental crust ~3.5 billion years ago in the Pilbara Craton of Australia. Nature; 375:575-577.

Collins WJ, Van Kranendonk MJ & Teyssier C. 1998. Partial convective overturn of Archaean crust in the east Pilbara Craton, Western Australia: driving mechanisms and tectonic implications. Journal of Structural Geology; 20:1405-1424.

Dawes PR, Smithies RH, Centofani J, & Podmore DC. 1995. Sunrise Hill unconformity: a newly discovered regional hiatus between Archaean granites and greenstones in the northeastern Pilbara Craton. Australian Journal of Earth Sciences; 42:635-639.

Deb M, Thorpe RI, Cumming GL & Wagner PA. 1989. Age, source and stratigraphic implications of Pb isotopic data for conformable, sediment-hosted, base metal deposits in the Proterozoic Aravalli-Delhi orogenic belt, northwestern India. Precambrian Research; 43:1-22.

Dowling K & Morrison G. 1989. Application of quartz textures to the classification of gold deposits using north Queensland examples. Economic Geology; monograph 6:342-355.

Finucane KJ. 1936. The Lalla Rookh mining centre, Pilbara Goldfields. Canberra: Aerial Geological and Geophysical Survey of Northern Australia, Western Australia report 3.
Finucane KJ. 1937. Station Peak mining centre, Pilbara Goldfield. Canberra: Aerial, Geological and Geophysical Survey of Northern Australia, Western Australia report 12, 7 p.
Finucane KJ. 1939. Mining centres east of Nullagine, Pilbara Goldfields. Canberra: Aerial Geological and Geophysical Survey of Northern Australia, Western Australia report 19.
Finucane KJ & Telford RJ. 1939. The antimony deposits of the Pilbara Goldfield. Canberra: Aerial Geological and Geophysical Survey of Northern Australia, Western Australia report 46.
Fitton MJ, Horwitz RC & Sylvester CG. 1975. Stratigraphy of the early Precambrian of the west Pilbara, Western Australia. Sydney: CSIRO Australia Mineral Research Laboratory report FP11.
Gifford AC. 1990. Blue Spec–Golden Spec gold-antimony deposit. Australian Institute of Mining and Metallurgy monograph; 16:155-158.
Groves DI, Goldfarb RJ, Gebre-Mariam M, Hagemann S & Robert F. 1998. Orogenic gold deposits: A proposed classification in the context of their crustal distribution and relationship to other gold deposit types. Ore Geology Reviews; 13:7-27.
Groves DI. 1993. The crustal continuum model for late Archaean lode-gold deposits of the Yilgarn Block, Western Australia. Mineralium Deposita; 28:366-374.
Hickman AH. 1983. Geology of the Pilbara Block and its environs. Perth: Western Australia Geological Survey bulletin 127.
Hickman AH. 1997. A revision of the stratigraphy of Archaean greenstone successions in the Roebourne-Whundo area - west Pilbara. Western Australian Geological Survey annual review; 1996-97:76-81.
Hickman AH. 1999. New tectono-stratigraphic interpretations of the Pilbara Craton, Western Australia. In: GSWA '99 extended abstracts: New geological data for WA explorers. Geological Survey of Western Australia record 1999/6:4-6.
Hodgeson CJ & Hamilton JV. 1989. Gold mineralization in the Abitibi greenston belt: end-stage results of Archean collisional tectonics? Economic Geology; monograph 6:86-100.
Huston DL, Blewett RS, Baker D & Smithies RH. 1999. The diverse origin of Archaean lode gold in the North Pilbara, Western Australia: a field excursion. Unpublished field guide. Australian Geological Survey Organisation.
Huston DL, Keillor B, Standing J, Blewett R & Mernagh TP. 2000. Epithermal deposits of the Central Pilbara tectonic zone, Pilbara Craton: description and exploration significance. AGSO Research Newsletter; 32:34-39.
Jones FH. 1938. The Warrawoona Area, Pilbara Goldfield. Canberra: Aerial Geological and Geophysical Survey of Northern Australia, Western Australia, Report 20.
Maitland AG. 1908. The geological features and mineral resources of the Pilbara Goldfield. Perth: Western Australia Geological Survey bulletin 40.
Marshall AE. 2000. Low temperature-low pressure ('epithermal') siliceous vein deposits of the North Pilbara granite-greenstone terrane, Western Australia. Canberra: Australian Geological Survey Organisation record 2000/1.
McNaughton NJ, Green MD, Compston W & Williams IS. 1988. Are anorthositic rocks basement to the Pilbara Craton? Geological Society of Australia, Abstracts; 21:272-273.
McNaughton NJ, Compston W & Barley ME. 1993. Constraints on the age of the Warrawoona Group., eastern Pilbara Block, Western Australia. Precambrian Research; 60:69-98.
Mullis, J, Dubessy, J, Poty, B, & O'Neil, J. 1994. Fluid regimes during late stages of a continental collision: physical, chemical, and stable isotope measurements of fluid inclusions in fissure quartz from a geotraverse through the Central Alps, Switzerland. Geochimica et Cosmochimica Acta; 58:2239-2267.
Nelson, DR., 1997, Compilation of SHRIMP U-Pb zircon geochronology data, 1996. Perth: Western Australia Geological Survey record 1997/2.

Nelson, DR, Trendall, AF & Altermann, W. 1999. Chronological correlations between the Pilbara and Kaapvaal cratons. Precambrian Research; 97:165-189.

Neumayr P. 1995. The nature and genesis of Archaean, syn-amphibolite-facies gold mineralisation in the Mt York district, Pilbara Craton, Western Australia. Perth: Unpublished Ph. D. thesis, University of Western Australia.

Neumayr P, Groves DI, Ridley JR & Koning CD. 1993. Syn-amphibolite facies Archaean lode gold mineralisation in the Mt. York district, Pilbara Block, Western Australia. Mineralium Deposita; 28:457-468.

Neumayr, P, Ridley, JR, McNaughton, NJ, Kinny, PD, Barley, ME, & Groves, DI. 1998 Timing of gold mineralisation in the Mt. York district, Pillgangoora greenstone belt, and implications for the tectonic and metamorphic evolution of an area linking the weatern and eastern Pilbara. Precambrian Research; 88:249-265.

Richards JR, Fletcher IR & Blockley JG. 1981. Pilbara galenas: precise isotopic assay of the oldest Australian leads; model ages and growth-curve implications. Mineralium Deposita; 16:7-30.

Smith, JB, Barley, ME, Groves, DI, Krapez, B, McNaughton, NJ, Bickle, MJ & Chapman, HJ. 1998. The Sholl Shear Zones, West Pilbara. evidence for a domain boundary structure from integrated tectonic analyses, SHRIMP U-Pb dating and isotopic and geochemical data of granitoids. Precambrian Research; 88:143-171.

Smithies, RH. 1997. Sherlock, W.A. Sheet 2456. Perth: Western Australia Geological Survey 1:100 000 Geological Series Explanatory Notes.

Smithies, RH. 1998. Mount Wohler, W.A. Sheet 2455. Perth: Western Australia Geological Survey 1:100 000 Geological Series Explanatory Notes.

Smithies, RH. 1999. Yule, W.A. Sheet 2556. Perth: Western Australia Geological Survey 1:100 000 Geological Series Explanatory Notes.

Smithies RH, & Champion DC. 1998. Secular compositional changes in Archaean Granites of the west Pilbara. Western Australia Geological Survey Annual Review 1997-98:71-76.

Smithies RH, Hickman AH & Nelson DR. 1999. New constraints on the evolution of the Mallina Basin, and their bearing on relationships between the contrasting eastern and western granite-greenstone terranes of the Archaean Pilbara Craton, Western Australia. Precambrian Research; 94:11-28.

Sullivan CJ. 1939. The Hong King, Pilbara and Egina mining centres, Pilbara gold-field. Canberra: Aerial, Geological and Geophysical Survey of Northern Australia report 52.

Telford RJ. 1939a. The Mallina and Peawah Mining Centres. Canberra: Aerial Geological and Geophysical Survey of Northern Australia, Western Australia report 47.

Telford RJ. 1939b. The Toweranna mining centre, Pilbara gold-field. Canberra: Aerial, Geological and Geophysical Survey of Northern Australia Report 53.

Thom R, Hickman AH & Chin, RJ. 1973. Nullagine (SF 51-5). Perth: Western Australia Geological Survey 1:250 000 series geological map.

Thorpe RI, Hickman AH, Davis DW, Mortensen JK & Trendall AF. 1992a. U-Pb zircon geochronology of Archaean felsic units in the Marble Bar region, Pilbara Craton, Western Australia. Precambrian Research; 56:169-189.

Thorpe RI, Hickman AH, Davis DW, Mortenson JK & Trendall AF. 1992b. Constraints to models for Archaean lead evolution from precise zircon U-Pb geochronology for the Marble Bar region, Pilbara Craton, Western Australia. Perth: Geology Department (Key Centre) & University Extension, The University of Western Australia, publication; 22:395-407.

Trendall AF. 1983. The Hamersley Basin, In Trendall AF & Morris RC, eds. Iron formations — facts and problems. Amsterdam: Elsevier:69-129.

Van Kranendonk MJ. 1997. Results of field mapping, 1994-1996, in the North Shaw & Tambourah 1:100,000 sheet areas, eastern Pilbara Craton, northwestern Australia. Canberra: Australian Geological Survey Organisation record 1997/23.

Van Kranendonk MJ & Morant P. 1998. Revised Archaean stratigraphy of the North Shaw 1:100 000 sheet, Pilbara Craton. Western Australia Geological Survey Annual Review 1997-98:55-62.

Vearncombe JR, Barley ME, Eisenlohr BN, Groves DI, Houstoun SM, Skwarnecki MS, Grigson MW & Partington GA. 1989. Structural controls on mesothermal gold mineralization: examples from the Archean terranes of southern Africa and Western Australia. Economic Geology Monograph; 6:124-134.

Williams IR. 1998. Muccan, W.A Sheet 2956. Perth: Western Australia Geological Survey 1:100 000 Geological Series Explanatory Notes.

Williams IS & Collins WJ. 1990. Granite-greenstone terranes in the Pilbara Block, Australia, as coeval volcano-plutonic complexes; evidence from U-Pb zircon dating of the Mount Edgar batholith. Earth & Planetary Science Letters; 97:41-53.

Williams IS, Page RW, Froude D, Foster JJ & Compston W. 1983. Early crustal components in the Western Australian Archaean: zircon U-Pb ages by ion microprobe analysis from the Shaw Batholith and Narryer Metamorphic Belt. Geological Society of Australia Abstracts; 9:169.

Woodall, R., 1990. Gold in Australia Blue. Australian Institute of Mining and Metallurgy monograph; 16:155-158.

Zegers, TE 1996. Structural, kinematic and metallogenic evolution of selected domains of the Pilbara granitoid-greenstone terrane. Utrecht: Faculteit Aardwetenschappen, Universiteit Utrecht, Geologica Ultraiectina; 146.

Table listing

Table 1. Stratigraphic relationships in the Pilbara Craton.

Ages [Ga]	Stratigraphy	Supracrustal lithological assemblages	Plutonic units and domain
c.2.47	Hamersley Group: Boolgeeda Iron Formation Wongarra volcanics Weeli Wolli Iron Fm Brockman Iron Formation	 felsic volcanics banded ironstones-tuff-shale	
c.2.603 c.2.56	McRae Shale Mt Sylvia Formation Carawine Dolomite Wittenoom Formation	sedimentary carbonates and clastics	
c.2.63	Marra Mamba Formation	banded ironstones and shale	
c.2.68-2.67	Jeerinah Formation	shale, tuff, greywacke	
unconformity			
c.2.76-2.69	Fortescue Group Maddina Basalt Kuruna Siltstone Nymerina Basalt Tumbiana Formation (>2.715 Ga) Kylena Basalt Hardy Sandstone Mount Roe Basalt	massive and amygdaloidal basalts, minor pillowed basalts, pyroclastics, sandstone/conglomerate lenses	Cooya Pooya dolerite, Gidley gabbro/granophyre lopolith complex; leucogranite, and epithermal mineral system Gregory Range granitoids
unconformity			
c.2.85			Moolyella and Cooglegong granites - high-K Sn-Ta granites within the older batholiths.
c.2.925			West and Central Pilbara Munni Munni layered intrusion and equivalents (Millindina Complex); Bookingarra Granite
c.3.0-2.925	Kialrah Rhyolite Louden Volcanics Mount Negri Volcanics	Rhyolite, tholeiitic and high-Mg basalts, amygdaloidal basalts	
>3.0-2.94	De Grey Group Mallina, Lalla Rookh and Mosquito Creek Basins	Rifting (strike-slip) and deposition of coarse-grained clastic sediments and conglomerates (including granite clasts).	Peawah and Portrea granitoids in central Pilbara (sanukatoids)
c.3.01-2.99	Whim Creek Group Rushall Slate Cistern Formation Mons Cupri Volcanics Warrambie Basalt		Pilbara-wide isotopic resetting of Rb-Sr and Pb-Pb systematics
unconformity			
c.3.014	Cleaverville Formation	Pilbara-wide deposition of banded ironstone/silica - shale formations	West and Central Pilbara
unconformity			
c.3.12	Whundo Group, west Pilbara, south of the Sholl shear zone.	Calc-alkaline felsic and mafic volcanics volcanogenic sediment and chert	Central Pilbara only Granitoids in the Chirrata-Whundo belt, south of the Sholl shear zone. Caines Well Granitoid complex
unconformity			
c.3.24-3.25	Gorge Creek Group Sulphur Springs Group	Basalts and dacites; chert clastic sediments volcanics and clastic sediments	East Pilbara - Strelley granite sill; granitic phases in the Yule batholith.
>3.24	Golden Cockatoo Formation	Metapelite and quartzite, BIF, rhyolite	Abydos Belt East Pilbara
3.27-3.26	Roebourne Group Regal Formation (undated) *tectonic contact* Nickol River Formation Ruth Well Formation (3.27)	Basalt, peridotite, chert, BIF, felsic volcanogenic metasediment	West Pilbara only Karratha and Harding Granitoid Complexes (ca 3.26)

Table 2. Structural events in the Pilbara Craton (after Blewett, 2000a).

Regional events this study	Hickman (1983)	Mallina Basin	Northern Pilgangoora Belt	Warrawoona Belt	Mosquito Creek Belt
D_1	D_1		D_1		
D_{2a}	D_2			D_1	
D_{2b}	D_2			D_2	
D_{2c}	D_2		D_2	D_3	
D_{2d}	D_2				
D_{3a}	D_2		D_3	D_4	D_1
D_{3b}	D_2				
D_{3c}	D_2				
D_{4a}	D_2	D_1	D_4		D_2
D_{4b}	D_2	D_2	D_5	D_5	D_3
D_{4c}	$?D_3$	D_3	D_6		D_4
D_{4d}	$?D_3$	D_4	D_7		D_5
D_5	D_4		D_8		D_6

Table 3. Characteristics of important gold deposits of the Pilbara granite-greenstone terrane.

District-deposit	Host rocks	Structural controls	Structural level	Absolute age (Ma)	Interpreted structural age
Bamboo Creek	Komatiite, Warrawoona Group	E-W trending mylonitic shear zones (sinistral NE up shear)	Moderate to deep	3410	Syn-D_2
North Pole-Normay	Mafic schist, Talga Talga Subgroup	E-W striking, N-dipping veins		3405	Syn-D_2
Warrawoona-Klondyke	Mafic and ultramafic schists	Subvertical lineation caused by intersection of S_2 and S_{3a}.	Moderate to deep	>3385	?
Lalla Rookh-Lalla Rookh	Basalts, basal part of Salgash Subgroup	Dilational zones in axial regions of E-W oriented 'kink' folds	Moderate ?	?	Syn-D_3?
North Shaw-Big Bertha	Metabasalts, Warrawoona Group	Moderately east-dipping veins		?	?
Nullagine-Golden Eagle	Turbiditic sediments, Mosquito Creek Group	Upright limb of reclined, south-verging F_4 fold	Moderate to deep	?	Syn-D_{4a} or D_{4c}
Mt York/Lynas Find	Amphibolite, and talc schist, Warrawoona Group	Highly sheared contact (thrusted?) between amphibolite and ultramafic schist	Deep	2890	Syn- or post-D_{4c}
Indee-Withnell	Turbiditic sediments, Mallina Formation	Steeply dipping shears with S-side sense of movement	Moderate	?	Syn- to post-D_{4c}
Indee-Peawah	Turbiditic sediments, Mallina Formation	Tension gash array developed on E-W normal (S-side up) faults	Moderate	?	Syn- to post-D_{4c}
Indee-Becher	Turbiditic sediments, Mallina Formation	N-S veins	High	?	Syn- to post-D_{5a}

Sources of data: This study; Finucane (1936); Hickman (1983); Neumayr (1995); Thorpe *et al.* (1992b); Zegers (1996)

Table 4. Gold production and resources of the North Pilbara granite-greenstone terrane based on host rock (data from Hickman [1983], Register of Australian Mining, Woodall [1990] and Gifford [1990]).

Host rocks	Production (tonnes)	Resources (tonnes)	Total (tonnes)	Portion of total (%)
Ultramafic/mafic volcanic rocks				
EPGGT	22.58	13.19	35.76	41.3
WPGGT	0.18	0.74	0.92	1.1
Turbiditic rocks	5.11	36.83	41.95	48.4
Palaeoplacers	0.50	3.68	4.18	4.8
Felsic volcanic rocks/granitoids	0.43	1.18	1.62	1.9
Other	2.16	0.00	2.16	2.5
Total	30.96	55.62	86.59	

Table 5. Lead isotope analyses of galena, gossanous material and K-feldspar from Au-bearing and related deposits of the Pilbara Craton.

Occurrence	Easting	Northing	Sample	Description	$^{206}Pb/^{204}Pb$	$^{207}Pb/^{204}Pb$
Lode gold deposits-hosted by Warrawoona Group						
Bamboo Creek						
Bamboo Creek	120.238	-20.951	110008	Galena from quartz vein in Warrawoona Group.	12.116	13.843
Bamboo Creek	120.238	-20.951		Galena in quartz vein in Warrawoona Group.	12.012	13.790
Bonnie Doon	120.220	-20.942	110004	Galena from quartz vein in Warrawoona Group.	12.013	13.798
Bonnie Doon	120.220	-20.942	110003	Galena from quartz vein in Warrawoona Group.	12.013	13.805
Kitchener	120.218	-20.938	K1	Galena in quartz vein in Warrawoona Group.	12.036	13.798
Prophecy-Perseverance	120.211	-20.930	PP10	Galena in quartz vein in Warrawoona Group.	12.086	13.819
Prophecy-Perseverance	120.211	-20.930	PP1	Galena in quartz vein in Warrawoona Group.	12.031	13.794
Lalla Rookh						
Lalla Rookh	119.274	-21.053	Pb401 (GSWA 44963)	Galena in auriferous quartz-pyrite-galena vein cutting basaltic schist of Salgash Subgroup.	12.548	14.173
Mt York-Lynas Find						
McPhees	118.937	-21.000	256-98	Galena in quartz cutting amphibole talc rock.	12.6157	14.1949
Zakanaka	118.900	-21.093	8514/48	Microcline in auriferous alteration selvedges to quartz-calc silicate veins. Analysis of residue after acid leach.	12.337	14.030
North Pole						
Normay	119.403	-21.099	94772	Galena from quartz vein cutting basalt of Warrawoona Group.	12.126	13.904
Normay	119.403	-21.099	49A	Galena from quartz vein cutting basalt of Warrawoona Group.	12.121	13.912
Normay	119.403	-21.099	49B	Galena from quartz vein cutting basalt of Warrawoona Group.	12.115	13.908
Normay	119.403	-21.099	49C	Galena from quartz vein cutting basalt of Warrawoona Group.	12.115	13.908
North Shaw						
Big Bertha	119.393	-21.341		Galena in quartz vein cutting schistose amphibolite in Talga Talga Subgroup.	13.068	14.524
Talga Talga						
North Star	119.824	-21.017	64817	Galena in epigenetic quartz vein in North Star Basalt.	12.239	13.946
Warrawoona						
Klondyke	119.885	-21.337	98042043A	Galena in quartz vein cutting quartz-sericite-fuchsite schist.	12.8104	14.3067
Klondyke	119.885	-21.337	KL138-140	Galena in 40 cm quartz zone in brecciated fuchsite-carbonate rock. Low grade (0.10 g/t Au) zone within zone of higher grades.	12.0766	13.8168
Klondyke	119.885	-21.337	98042046A	Galena in 10 cm quartz vein that cuts sericite-quartz schist.	12.0422	13.7845
Lode gold deposits-hosted by DeGrey Group						
Mosquito Creek						
Mosquito Creek North	120.456	-21.707	86250	Galena in auriferous quartz vein in pelitic schist from Mosquito Creek Formation.	13.206	14.571
Mallina-Whim Creek						
Geemas	117.775	-20.982	870150	Pulp of gossanous rock chip. 3800 ppm Pb	16.2184	15.5992
North of North Calvert	118.243	-20.853	876726	Pulp of gossanous rock chip. 3700 ppm.	13.0890	14.4956
Sherlock River	117.605	-21.023	110030	Galena.	13.081	14.495
West Yule North	118.296	-19.341	810649	Pulp of gossanous rock chip. 2250 ppm Pb	13.1806	14.5252
Station Peak						
Station Peak	118.181	-21.162	110001	Galena in quartz vein in dolerite and metasedimentary rocks, Mallina Formation.	16.229	15.692
Lode gold deposits-hosted by other units						
Upper Hardey River			53275	Galena in auriferous quartz vein cutting Fortescue Group.	14.033	14.905

[1]Calculated using model of Thorpe et al. (1992b). Values in parentheses are calculated using model of Deb et al. (1990).

$^{208}Pb/^{204}Pb$	Analytical technique	Model age (Ga)[1]	μ[1]	Source of data
32.052	Conventional	3.355	8.77	This study
31.932	Conventional	3.420	8.91	Thorpe et al. (1992b)
31.966	Conventional	3.426	8.96	This study
32.088	Conventional	3.431	8.99	This study
31.921	Conventional	3.402	8.86	Zegers (1996)
31.990	Conventional	3.367	8.77	Zegers (1996)
31.938	Conventional	3.404	8.86	Zegers (1996)
32.427	Conventional	3.188	8.91	Richards et al. (1981)
32.5114	Double spike	3.142	8.83	This study
32.291	Conventional	3.280	8.54	Neumayr et al. (1998)
31.953	Conventional	3.392	9.06	I.R. Fletcher in Thorpe et al. (1992b)
31.991	Conventional	3.403	9.12	Thorpe et al. (1992b)
31.982	Conventional	3.406	9.12	Thorpe et al. (1992a)
31.982	Conventional	3.406	9.12	Thorpe et al. (1992a)
32.617	Conventional	2.987	9.08	Thorpe et al. (1992a)
32.129	Conventional	3.311	8.84	This study
32.6194	Double spike	3.050	8.80	This study
31.9950	Double spike	3.374	8.79	This study
31.9525	Double spike	3.385	8.76	This study
33.020	Conventional	2.905	8.98	I.R. Fletcher in Thorpe et al. (1992b)
35.6254	Double spike	1.476 (1.809)	9.25 (11.15)	This study
32.9535	Double spike	2.948	8.93	This study
32.984	Conventional	2.954	8.94	This study
32.9594	Double spike	2.892	8.86	This study
34.665	Conventional	1.548 (1.916)	9.44 (11.71)	This study
33.729	Conventional	2.493 (2.672)	8.90 (10.91)	This study

Table 6. Summary of geochemical analyses from epithermal vein deposits from the Central Pilbara and from lode Au deposits in the Mosquito Creek Basin (all values in ppm).

Deposit	No.	Au	Ag	Hg	As	Bi	Sb	Te	Tl	W	U	Cu	Pb	Zn
Becher	12	<0.01-0.22	<0.1-1.8	<0.005-0.36	15-6610	0.2-3.3	2.6-178	0.2-3.3	<0.5-0.6	1.6-34.9	<0.05-11.9	4-740	<5-170	<4-409
Orange Rock	7	<0.01-0.06	<0.1-0.3	0.012-0.024	6-208	0.2-1.1	5.7-13.5	0.5-0.6	<0.5	1.1-2.4	0.08-2.9	5-13	<5-22	5-26
Opaline Well	2	<0.01	<0.1-0.2	0.012	8-27	0.4-0.5	6.2-8.4	0.5-0.8	<0.5	1.3-1.6	<0.05-0.07	4-5	16-23	4-5
Quartz Hill	1	<0.01	<0.1	0.035	13	0.5	14.3	0.7	<0.5	0.8	0.05	6	5	5
Sams Ridge	2	<0.01-0.02	2.3-4.5	1.64	73-868	0.3-7.9	69-131	0.6-0.8	<0.5	1.0-1.3	0.16-4.3	1135-2820	<5-187	39-40
Bartons	7	0.04-9.10	0.1-0.8	0.012-0.047	23-1730	0.3-4.5	5.4-30.8	0.8-1.6	<0.5	1.9-5.1	0.06-3.15	7-89	23-76	11-246
Shearers	4	0.06-0.38	0.1-1.8	0.012-0.29	8-275	0.5-0.9	3.9-12.8	0.5-0.7	<0.5	1.4-3.6	0.07-0.35	<4-83	19-59	6-22
Otways	6	<0.01-0.68	<0.1-1.2	0.023-0.105	39-264	0.2-11.9	4.8-15.5	0.5-0.7	<0.5	0.8-3.7	0.18-0.61	12-155	<5-120	<4-15

Table 7. Gold production and geological resources of the Mosquito Creek Belt (data from Hickman [1983], Gifford [1990] and the Registry of Australian Mining).

	Production (kg)	Geological resources	Production and resources (tonnes)
Middle Creek line	1053	8.97 Mt @ 1.96 g/t Au	18.6
Golden Eagle	15	6.67 Mt @1.96 g/t Au	13.1
Barton	239	0.331 Mt @ 2.5 g/t	1.06
Hopetoun	8		0.008
Blue Spec line	2953	2.60 Mt @ 3.36 g/t	11.9
Blue Spec/Golden Spec	2356	0.167 Mt @ 21.4 g/t Au	5.92
Golden Gate	—	2.43 Mt @ 2.12 g/t Au	5.15
Mosquito Creek area	525	—	0.525
Eastern Creek area	358	—	0.358
Nullagine Common	374	—	0.374
Total	5263		31.8

Appendix A. Results of geochemical analyses for vein deposits in the Central Pilbara Tectonic Zone and in the Mosquito Creek Basin (all values in ppm).

Sample	Deposit	Description	Easting	Northing	Zone	Datum	Au	Ag	Hg	As	Bi	Sb	Te	Tl	W	U	Cu	Pb	Zn
98042016G	Becher	Quartz breccia	621238	7683986	50	GDA94	<0.01	0.5	0.024	20	3.3	12.4	1.0	<0.5	2.9	<0.05	6	13	7
99042008A	Becher	Quartz with disseminated pyrite	621243.5	7684006.5	50	GDA94	0.22	0.4	0.012	847	0.2	43.0	1.5	<0.5	2.6	0.22	12	11	5
99042012A	Becher	Gossanous quartz vein	621266.7	7683956.4	50	GDA94	0.10	0.4	0.024	2410	0.5	51.0	1.7	<0.5	8.8	5.60	83	72	152
99042013A	Becher	Brecciated banded quartz	621330.5	7683975.9	50	GDA94	0.05	0.5	0.020	35	1.8	10.9	0.3	<0.5		0.14	22	67	16
99042013AS	Becher	Sulfidic part of brecciated quartz	621330.5	7683975.9	50	GDA94	0.16	1.8	0.360	84	1.2	19.3	0.2	0.6		0.15	28	170	45
99042015A	Becher	Quartz vein	621391.7	7683739.9	50	GDA94	0.02	<0.1	0.012	28	1.2	20.5	2.2	0.6	2.8	<0.05	5	<5	4
99042015B	Becher	Gossanous quartz vein	621391.7	7683739.9	50	GDA94	<0.01	<0.1	0.024	6610	0.3	178.0	3.3	<0.5	11.0	11.90	740	17	409
99042027A	Becher	Pseudoacicular quartz vein	621420.3	7683710.2	50	GDA94	<0.01	<0.1	<0.005	15	2.1	2.6	0.3	<0.5		<0.05	4	7	4
99042030A	Becher	Ferrugenous casts/gossan	621473.9	7683527.5	50	GDA94	<0.01	0.1	0.035	3400	0.6	38.2	0.9	<0.5	6.1	8.60	424	22	67
99042031A	Becher	Stockwork quartz veins in sericitic grit	621456.5	7683517.5	50	GDA94	<0.01	0.3	0.012	250	0.4	23.8	1.0	<0.5	34.9	1.05	50	5	8
99042032B	Becher	Ex-pyritic, banded, chalcedonic quartz	621497.8	7683472.1	50	GDA94	0.02	0.1	<0.005	53	2.4	10.2	1.2	0.5	4.4	0.14	21	8	<4
99042034B	Becher	Coarse bladed quartz	621546.2	7683442.3	50	GDA94	0.02	0.3	0.012	131	0.5	7.4	0.6	<0.5	1.6	0.10	34	<5	4
99042026A	Orange Rock	Bladed quartz	610250	7678900	50	AGD66	<0.01	<0.1	0.024	7	0.2	10.9	0.6	<0.5	1.1	0.08	5	7	6
99042026B	Orange Rock	Chalcedonic quartz	610250	7678900	50	AGD66	0.06	0.3	0.024	96	0.2	13.5	0.6	<0.5	2.4	0.71	13	<5	12
99042039A	Orange Rock	Chalcedonic quartz	610250	7679900	50	AGD66	<0.01	0.2	0.012	18	1.1	7.0	0.5	<0.5	1.9	0.67	7	22	5
99042039C	Orange Rock	Bladed quartz	610250	7679900	50	AGD66	<0.01	<0.1	0.012	6	0.3	5.7	0.5	<0.5	1.4	0.12	5	6	7
99042039D	Orange Rock	Gossanous breccia	610250	7679900	50	AGD66	<0.01	<0.1	0.012	115	0.3	10.1	0.6	<0.5	2.3	2.90	11	15	26
99042039E	Orange Rock	Gossanous bladed quartz	610250	7679900	50	AGD66	<0.01	<0.1	0.012	146	0.2	7.8	0.6	<0.5	2.0	2.35	9	<5	22
99042040A	Orange Rock	Brecciated chalcedonic quartz	610150	7679400	50	AGD66	0.04	0.2	0.023	208	0.2	13.3	0.6	<0.5	1.6	0.35	7	8	5
99042036B	Opaline Well	Bladed quartz	574700	7679050	50	AGD66	<0.01	<0.1	0.012	27	0.4	8.4	0.8	<0.5	1.6	0.07	5	16	4
99042038A	Opaline Well	Chalcedonic quartz with trace pyrite	575550	7679450	50	AGD66	<0.01	0.2	0.012	8	0.5	6.2	0.5	<0.5	1.3	<0.05	4	23	5
99042025A	North of Sholl Shear	Quartz breccia	578700	7708000	50	AGD66	<0.01	<0.1	0.035	13	0.5	14.3	0.7	<0.5	0.8	0.05	6	5	5
99042020A	Sams Ridge	Weakly gossanous quartz	590300	7706900	50	AGD66	0.02	4.5	1.640	73	0.3	130.5	0.6	<0.5	1.0	0.16	2820	<5	39
99042023A	Sams Ridge	Gossan	590200	7706700	50	AGD66	<0.01	2.3	1.640	868	7.9	69.3	0.8	<0.5	1.3	4.30	1135	187	40
99042035A	Roberts Hill	Tourmalinite	610050	7693100	50	AGD66	<0.01	0.3	0.012	15000	7.8	16.6	2.7	<0.5	25.9	1.82	74	41	106
99042035B	Roberts Hill	Quartz vein	610050	7693100	50	AGD66	<0.01	0.3	0.012	628	1.9	6.4	1.3	<0.5	10.4	0.52	85	7	36
99042001A	Bartons	Folded, white quartz vein	219082	7577573	51	AGD66	2.05	0.2	0.024	23	0.4	5.4	0.8	<0.5	5.1	0.06	7	66	11
99042001B	Bartons	Anastomosing, ferruginous quartz veins along shear	219082	7577573	51	AGD66	0.08	0.3	0.035	645	0.3	25.5	1.2	<0.5	2.8	2.05	73	25	150
99042001C	Bartons	Folded, ferruginous quartz vein	219082	7577573	51	AGD66	9.10	1.1	0.035	1170	0.6	18.0	1.0	<0.5	2.1	1.20	25	49	83
99042001D	Bartons	Anastomosing, ferruginous quartz veins developed along shear	219082	7577573	51	AGD66	5.25	0.8	0.047	1730	0.6	20.6	1.2	<0.5	2.4	1.31	89	76	246
99042001E	Bartons	Ferruginous banding	219082	7577573	51	AGD66	0.04	0.1	0.024	1240	0.5	20.1	1.4	<0.5	3.1	3.15	80	28	190
99042001F	Bartons	Ferruginous quartz stockwork	219082	7577573	51	AGD66	1.76	0.2	0.012	691	1.2	30.8	1.6	<0.5	3.1	1.06	35	23	67
99042001G	Bartons	Weakly ferrigenous quartz vein	219082	7577573	51	AGD66	0.68	0.2	0.012	486	4.5	8.7	1.6	<0.5	1.9	0.20	13	43	41
99042113A	Otways	Ferrugenous N-trending quartz vein	212400	7573320	51	AGD66	0.06	1.2	0.105	49	11.9	11.0	0.7	<0.5	1.6	0.42	155	120	15
99042113B	Otways	Ferrugenous E-trending quartz vein	212400	7573320	51	AGD66	0.32	<0.1	0.023	264	1.5	8.4	0.6	<0.5	3.7	0.48	36	75	13
99042114A	Otways	Ferrugenous silicified shale	212300	7573390	51	AGD66	<0.01	0.1	0.023	52	0.3	15.5	0.5	<0.5	1.9	0.61	21	12	<4
99042115A	Otways	Ferrugenous quartz vein	212160	7573270	51	AGD66	0.66	0.5	0.023	274	2.5	4.8	0.5	<0.5	1.5	0.48	36	38	5
99042116A	Otways	Ferrugenous quartz vein	212130	7573240	51	AGD66	0.68	0.5	0.058	98	0.6	4.6	0.5	<0.5	3.2	0.18	17	11	8
99042117A	Otways	Ferrugenous silicified shale	212030	7573320	51	AGD66	0.02	0.3	0.035	39	0.2	7.9	0.5	<0.5	0.8	0.41	12	<5	15
99042120A	Shearers	Ferrugenous quartz vein	211720	7573230	51	AGD66	0.18	1.8	0.035	275	0.9	12.8	0.7	<0.5	3.6	0.35	83	49	22
99042121A	Shearers	Ferrugenous quartz vein	211740	7573320	51	AGD66	0.06	0.1	0.012	106	0.5	7.0	0.6	<0.5	2.4	0.21	12	19	6
99042122A	Shearers	Quartz vein	211750	7573450	51	AGD66	0.38	0.7	0.059	11	0.7	9.9	0.5	<0.5	3.8	0.20	<4	19	9
99042123A	Shearers	Quartz vein	211730	7573420	51	AGD66	0.08	0.7	0.290	8	0.6	3.9	0.5	<0.5	1.4	0.07	12	59	12
98042041B	Lynas Find	Quartz-fluorite-galena vein; ~5% galena	699950	7678500	50	AGD66	0.02	42.5	0.094	4	75.9	3.7	0.7	<0.5	0.9	0.74	132	59600	67
Method							P649	A649	H110	M104	M104	M104	M104	M104	M104	M104	A104	A104	A104
DL							0.01	0.1	0.005	1	0.1	0.1	0.2	0.5	0.1	0.05	4	5	4
Crustal abundance (Levinson, 1980)							0.004	0.07	0.08	1.8	0.17	0.2	0.001	0.45	1.5	2.7	55	12.5	70
Crustal abundance x 5							0.020	0.35	0.40	9.0	0.85	1.0	0.005	2.25	7.5	13.5	275	62.5	350

Figure 1a. Simplified outcrop geology of the North Pilbara region, Western Australia.

Figure 1b. Solid geology of the North Pilbara granite-greenstone terrane showing the location of gold deposits and the areas studied: A) Indee district; B) Pilgangoora Belt; C) Warrawoona Belt; D) SW Mosquito Creek Belt.

Figure 2. Event chart for the Pilbara Craton from 3600 Ma to 2600 Ma showing correlation of penetrative deformation events and Au mineralising events through time.

Figure 3. The Pb isotope composition of galena and Pb-rich gossan from lode Au deposits in the Pilbara Craton. The evolution curves shown are the "Western Superior" model of Thorpe *et al.* (1992b). Data with model ages above 2.5 Ga are plotted.

Figure 4. Geology of the Central Pilbara area showing the location of deposits studied (modified after Smithies, 1997; 1998; 1999).

Figure 5. Graphical log of INDD003.

Figure 6. Structural elements of the Withnell deposit (based on oriented drill cores INDD003 and INDD004): (a) π-diagram showing poles to faults, (b) rose diagram showing fault orientations and (c) Bedding plotted as great circles, dips steeply north and south.

Figure 7. Photographs of textures from the Withnell and Peawah deposits: (a) planar quartz-carbonate veins (Withnell); (b) south-dipping quartz veins (Peawah).

Figure 8. Histograms showing the homogenisation temperatures of fluid inclusions from lode Au deposits from the Central Pilbara: (a) Withnell, (b) Mirdawari, and (c) Peawah.

Figure 9. Geology of the Becher vein system.

Figure 10. Photographs of vein textures from the Becher (a-e), Orange Rock (f-g) and Opaline Well (h) vein systems: (a) weakly banded chalcedony; (b) pseudoacicular quartz; (c) bladed quartz pseudomorphs after a carbonate or sulphate mineral; (d) crustiform quartz; (e) bladed limonite pseudomorphs after a carbonate or sulphate mineral; (f) vein breccias; (g) limonite pseudomorps after a folded, bladed mineral; and (h) recessively weathered, bladed fluorite.

Figure 11. Histograms showing the homogenisation temperatures of fluid inclusions from epithermal vein deposits: (a) Becher, and (b) Opaline Well.

Figure 12. Geology of the Orange Rock vein system

Figure 13. Geology of the Pilgangoora showing the location of Au deposits from the Mt York-Lynas Find district.

Figure 14. Plans showing (a) geology and (b) grade distribution of the Zakanaka open cut.

Figure 15. Geology of the North McPhees open cut.

Figure 16. Histograms showing indicating the salinities and homogenisation temperatures from fluid inclusions from the Lynas Find Pb-fluorite deposit.

Figure 17. Geology of the Warrawoona Syncline.

Figure 18. Histogram showing the homogenisation temperatures of fluid inclusions from the Klondyke deposit.

Figure 19. Plans showing the southwest Mosquito Creek Belt: (a) Simplified geological map showing the alignment of mineral deposits, vein orientations, and location of Golden Eagle, Otways-Shearers, Barton's, and Hopetoun deposits along the Middle Creek Line; and (b) reduced to the pole first vertical derivative aeromagnetic image from the SW Mosquito Creek Belt. Positions of the deposits discussed in the text are adjacent to, or along, significant magnetic anomalies in an otherwise low magnetic belt.

Figure 20. Photographs from the Mosquito Creek Belt: (a) F_2 reclined fold with axial-plane mS_2 cleavage in the Golden Eagle deposit. View east; (b) the original Golden Eagle pit (note cleaved Mosquito Creek Formation host rock and steep veins; (c) diamond drill hole core from Golden Eagle deposit with low angle quartz veins. (the sketch illustrates how a dipping psammite develops low-angle tension gash like veins under horizontal shortening); (d) coarse-grained polymict conglomerate with thin north-trending quartz vein (arrow) at Shearers deposit; (e) view east into Hopetoun deposit pit showing northwest-directed shearing (mD_4) (note phacoidal S_2 fabric dips steeply southeast); (f) mS_2 phacoidal cleavage overprinted by normal-sense mS_3 shear bands (C' planes), all transposed by strong S_4 shearing fabric at Hopetoun deposit; (g) view northeast along the main reef of the Bartons deposit; and (h) view southwest onto a mF_4 folded auriferous vein of the East reef of the Bartons deposit (note the northwest vergence of the mF_4 fold and the strong mS_4 fabric).

Figure 21. Schematic diagram showing the relationship of bedding and cleavage in the inferred reclined fold at the Dromedaries. Note cleavage steeper than bedding in right-way up limb.

Figure 22. Cross sections of the Golden Eagle deposit showing: a) geology; b) variations in Au grades; c) alteration facies; and d) variations in the wavelength of the PIMA Al-OH feature. Note the association of psammitic rocks with quartz-chlorite alteration, and higher Au grades.

Figure 23. Histogram showing the homogenisation temperatures for low- and high-salinity, aqueous fluid inclusions from Golden Eagle. The low-salinity inclusions have an average around 130ºC while the high salinity inclusions have an average around 140ºC (see text for details).

Figure 24. Geological map of the Otways and Shearers deposits. Note the development of mostly north-trending veins in the conglomerate, and the association with dextral faults.

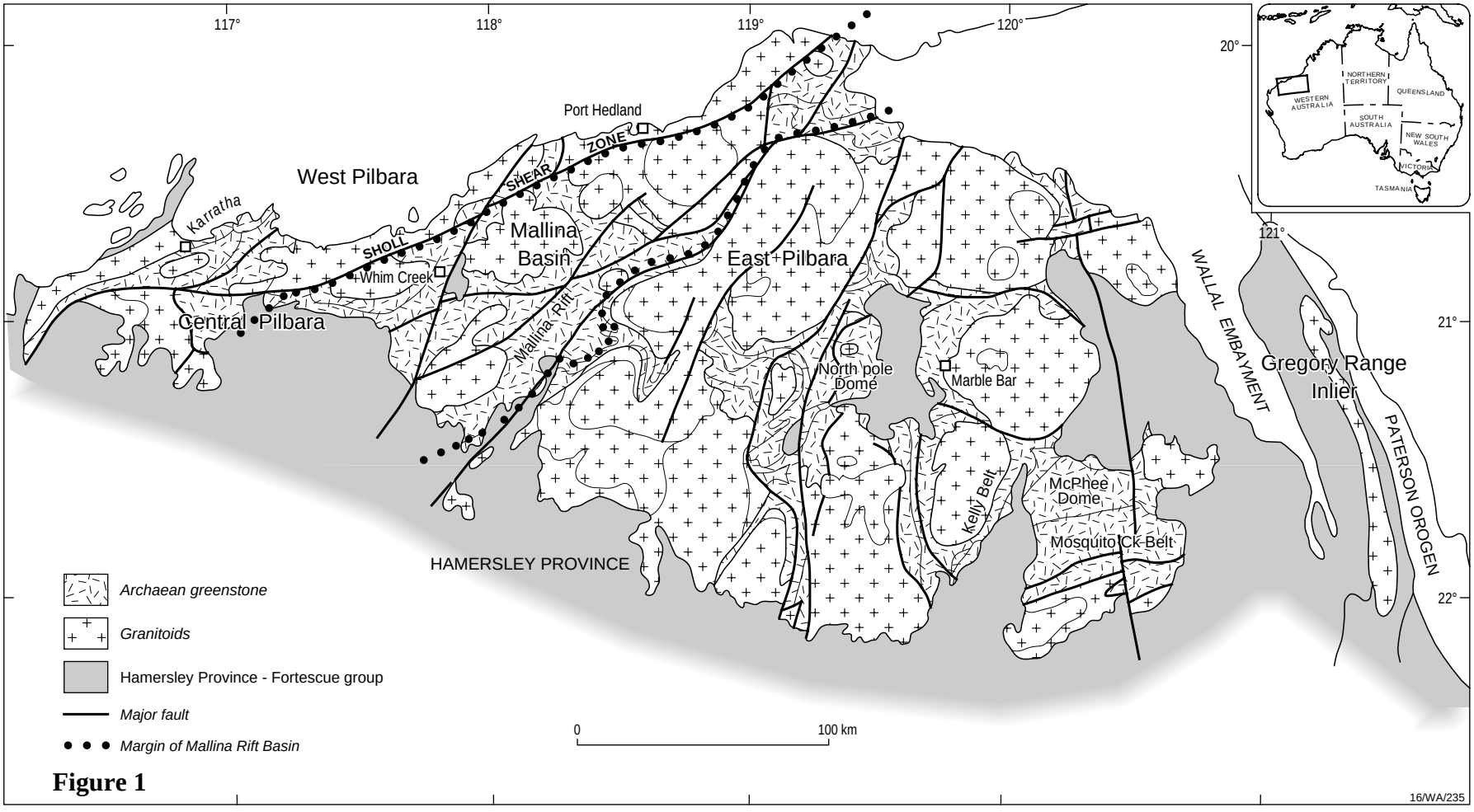
117°
118°
119°
120°
121°
20°
21°
22°
Port Hedland
West Pilbara
SHEAR ZONE
Karratha
SHOLL
Whim Creek
Mallina Basin
East Pilbara
Central Pilbara
Mallina Rift
North pole Dome
Marble Bar
WALLAL EMBAYMENT
Gregory Range Inlier
PATERSON OROGEN
Kelly Belt
McPhee Dome
Mosquito Ck Belt
HAMERSLEY PROVINCE
WESTERN AUSTRALIA
NORTHERN TERRITORY
QUEENSLAND
SOUTH AUSTRALIA
NEW SOUTH WALES
VICTORIA
TASMANIA
Archaean greenstone
Granitoids
Hamersley Province - Fortescue group
Major fault
Margin of Mallina Rift Basin
0
100 km
16/WA/235

Figure 1

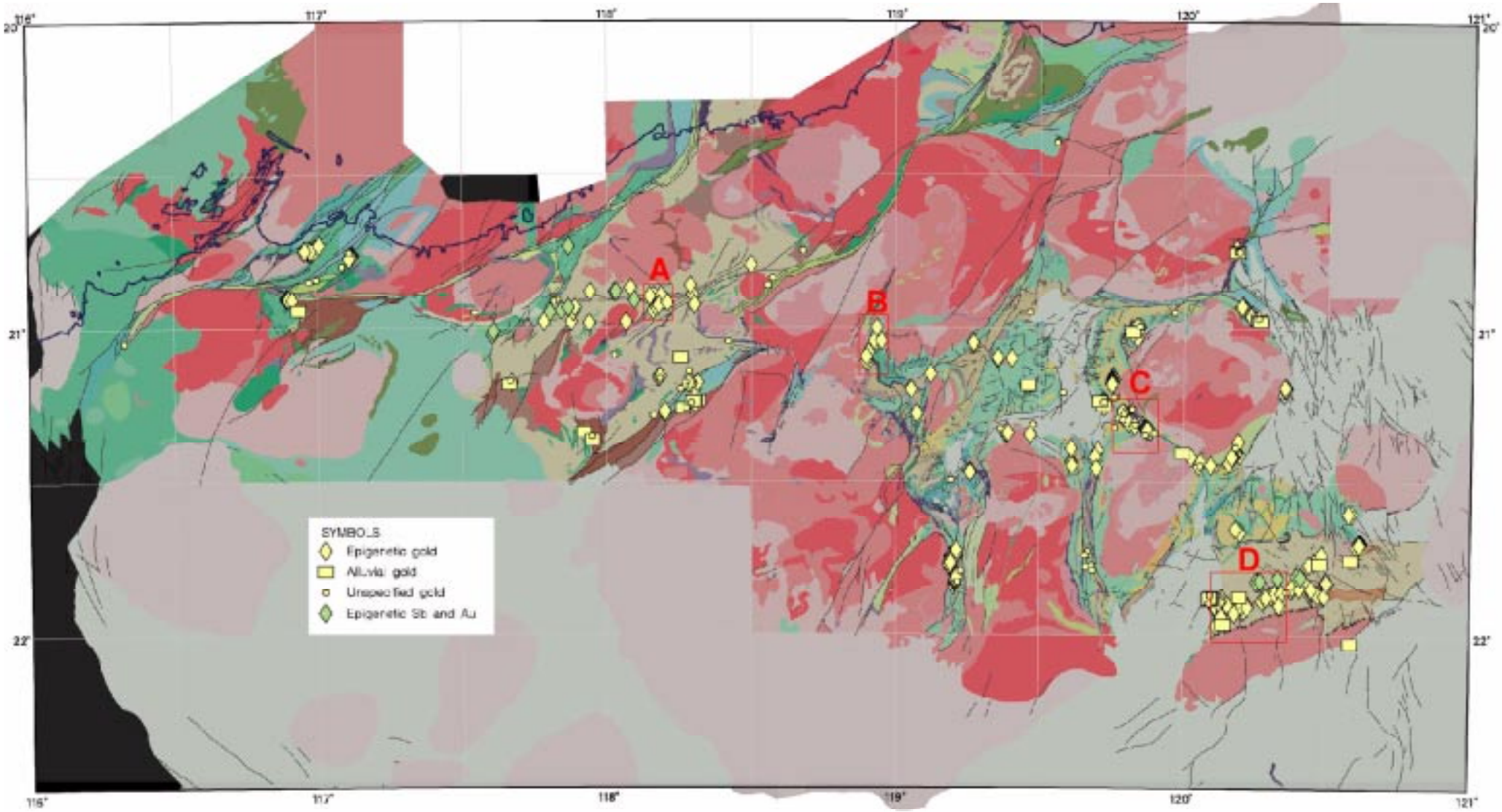
SYMBOLS
Epigenetic gold
Alluvial gold
Unspecified gold
Epigenetic Sb and Au
A
B
C
D

Figure 1b

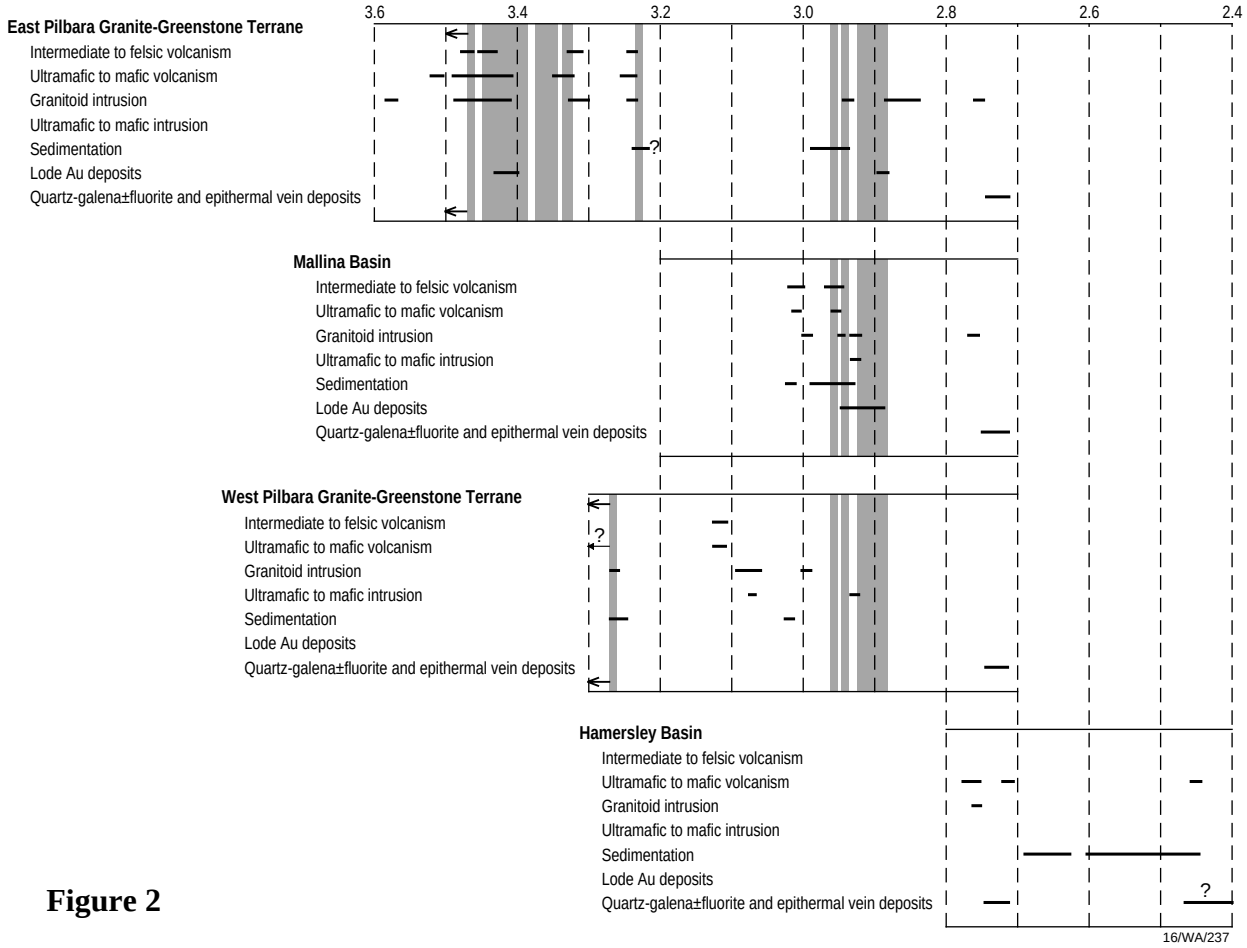
3.6
3.4
3.2
3.0
2.8
2.6
2.4
East Pilbara Granite-Greenstone Terrane
Intermediate to felsic volcanism
Ultramafic to mafic volcanism
Granitoid intrusion
Ultramafic to mafic intrusion
Sedimentation
Lode Au deposits
Quartz-galena±fluorite and epithermal vein deposits
?
Mallina Basin
Intermediate to felsic volcanism
Ultramafic to mafic volcanism
Granitoid intrusion
Ultramafic to mafic intrusion
Sedimentation
Lode Au deposits
Quartz-galena±fluorite and epithermal vein deposits
West Pilbara Granite-Greenstone Terrane
Intermediate to felsic volcanism
Ultramafic to mafic volcanism
Granitoid intrusion
Ultramafic to mafic intrusion
Sedimentation
Lode Au deposits
Quartz-galena±fluorite and epithermal vein deposits
?
Hamersley Basin
Intermediate to felsic volcanism
Ultramafic to mafic volcanism
Granitoid intrusion
Ultramafic to mafic intrusion
Sedimentation
Lode Au deposits
Quartz-galena±fluorite and epithermal vein deposits
?
16/WA/237

Figure 2

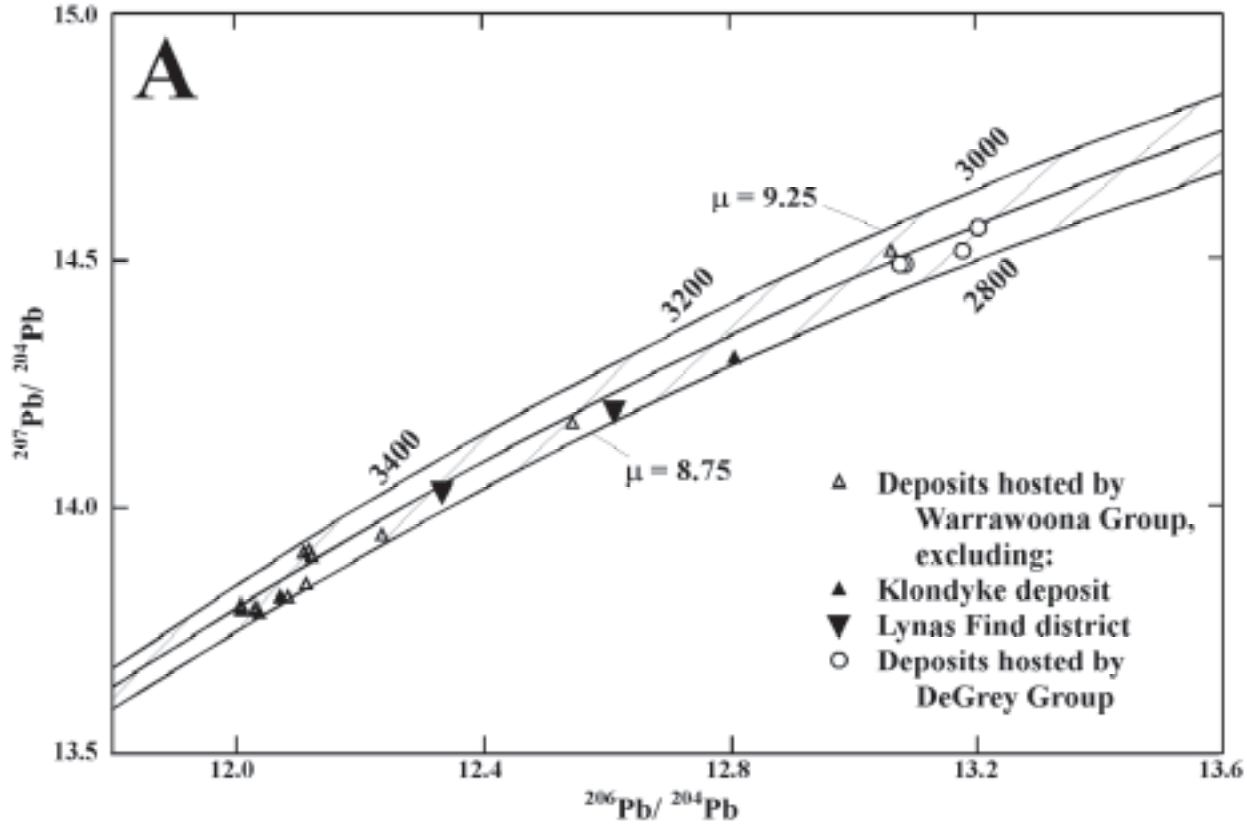
A
15.0
14.5
14.0
13.5
12.0
12.4
12.8
13.2
13.6
$^{207}Pb/^{204}Pb$
$^{206}Pb/^{204}Pb$
μ = 9.25
μ = 8.75
3000
3200
2800
3400
Deposits hosted by Warrawoona Group, excluding:
Klondyke deposit
Lynas Find district
Deposits hosted by DeGrey Group

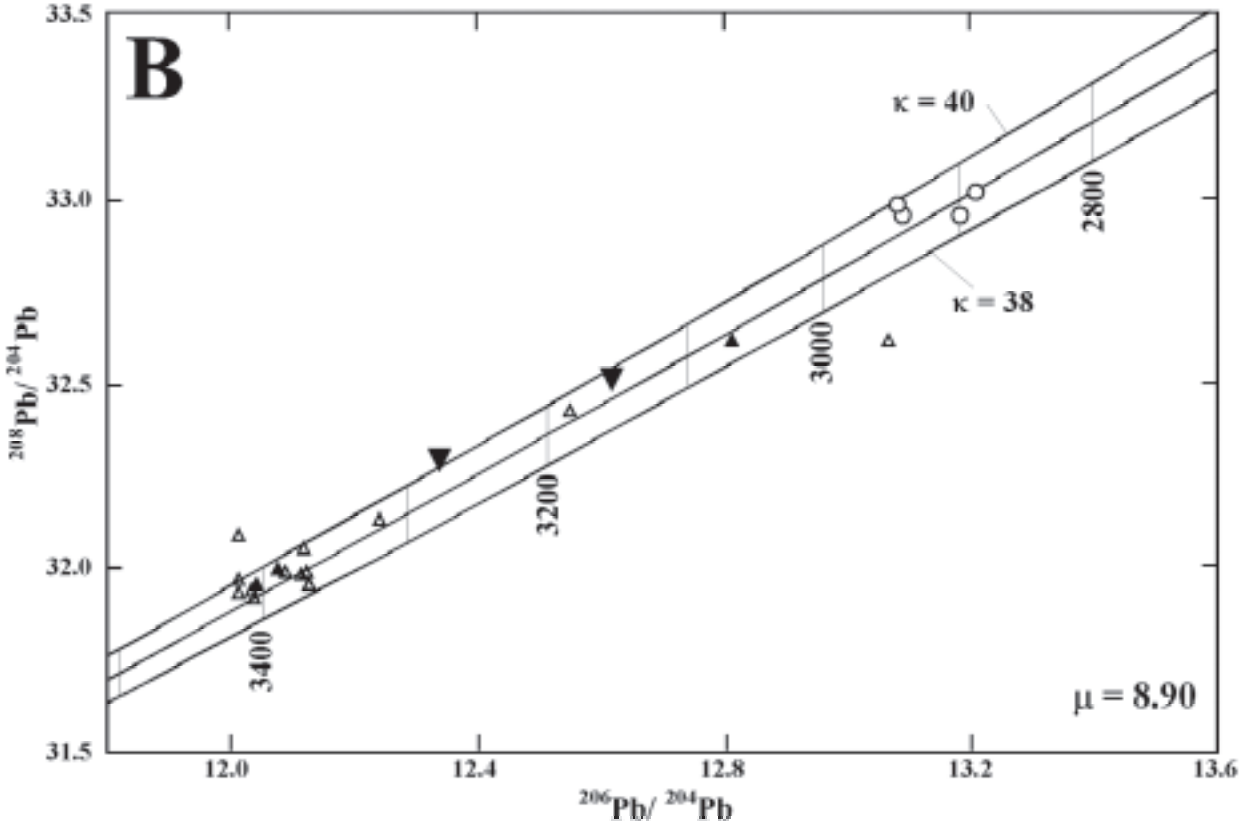
B
33.5
33.0
32.5
32.0
31.5
12.0
12.4
12.8
13.2
13.6
$^{208}Pb/^{204}Pb$
$^{206}Pb/^{204}Pb$
κ = 40
κ = 38
2800
3000
3200
3400
μ = 8.90

Figure 3

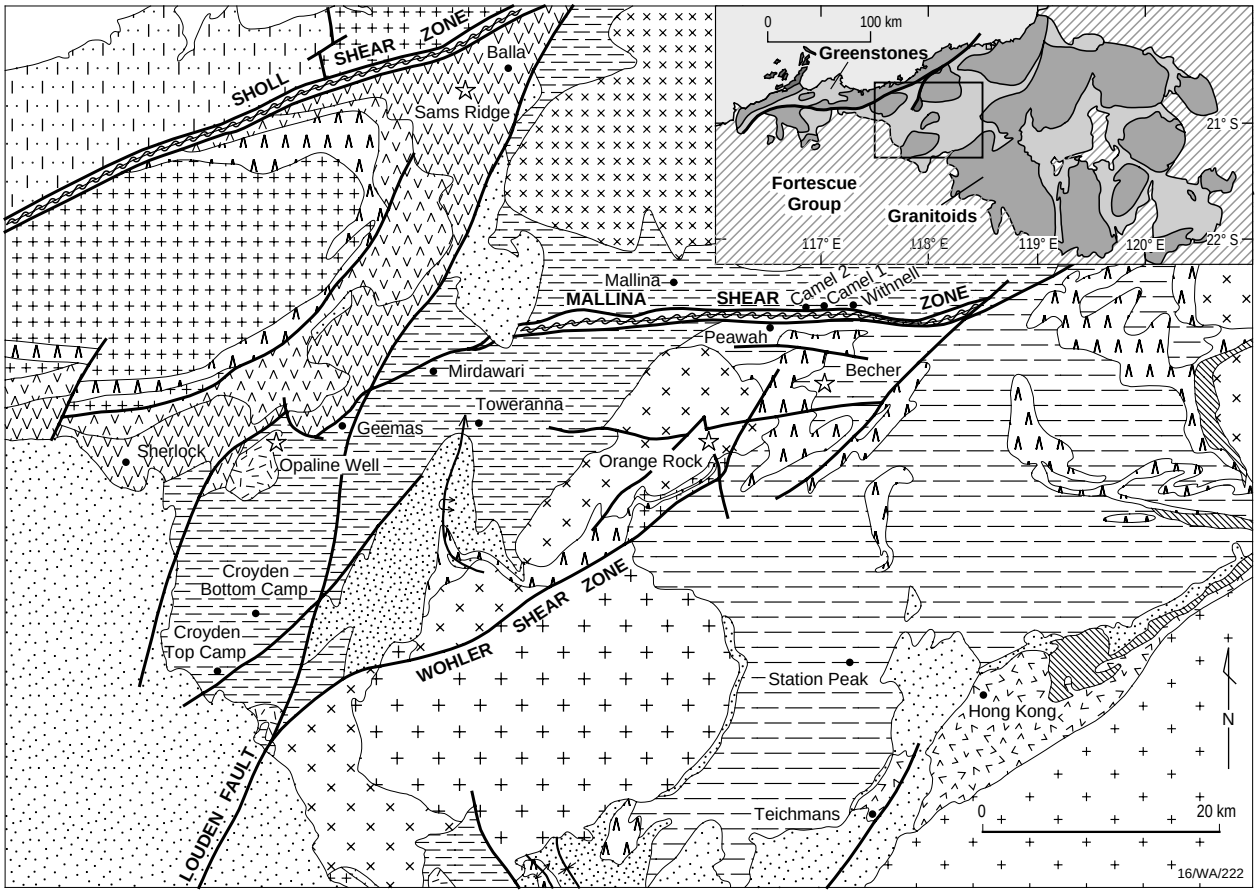

Shear Zone

Fortescue Group

Millindinna Complex

Louden and Negri Volcanics

Whim Creek Group

DeGrey Group

Unassigned shale, sandstone and mafic schist

Mallina Formation

Constantine Sandstone

Cleaverville Formation

Pilbara Well Greenstone Belt

GRANITOIDS

Opaline Well Granite (ca. 2765 Ma)

Satarist Granite (ca. 2940-2930 Ma)

Portree Granitoid Complex (ca. 2950 Ma)

Peawah Granodiorite (ca. 2950 Ma)

Forestier Bay Tonalite (ca. 3015 Ma)

Caines Well Granitoid Complex and Depuch Trondjemite (ca. 3093-2925 Ma)

Yule Granitoid Complex

Lode Au *and* Sb±Au *deposits*

Epithermal vein systems

Figure 4

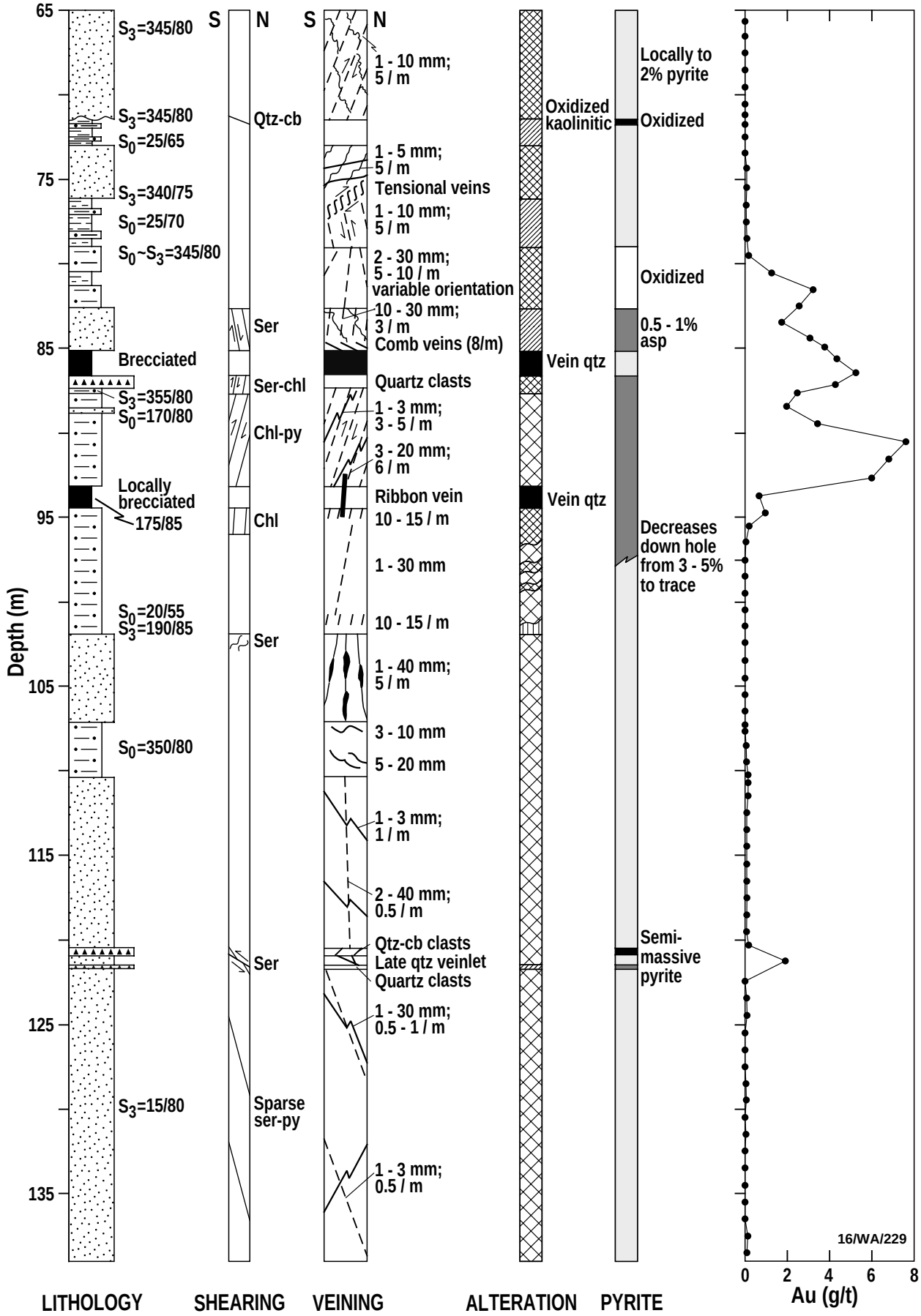
Depth (m)
65
75
85
95
105
115
125
135
S_3=345/80
S_3=345/80
S_0=25/65
S_3=340/75
S_0=25/70
S_0~S_3=345/80
Brecciated
S_3=355/80
S_0=170/80
Locally brecciated
175/85
S_0=20/55
S_3=190/85
S_0=350/80
S_3=15/80
S
N
S
N
Qtz-cb
Ser
Ser-chl
Chl-py
Chl
Ser
Ser
Sparse ser-py
1 - 10 mm; 5 / m
1 - 5 mm; 5 / m
Tensional veins
1 - 10 mm; 5 / m
2 - 30 mm; 5 - 10 / m variable orientation
10 - 30 mm; 3 / m
Comb veins (8/m)
Quartz clasts
1 - 3 mm; 3 - 5 / m
3 - 20 mm; 6 / m
Ribbon vein
10 - 15 / m
1 - 30 mm
10 - 15 / m
1 - 40 mm; 5 / m
3 - 10 mm
5 - 20 mm
1 - 3 mm; 1 / m
2 - 40 mm; 0.5 / m
Qtz-cb clasts
Late qtz veinlet
Quartz clasts
1 - 30 mm; 0.5 - 1 / m
1 - 3 mm; 0.5 / m
Oxidized kaolinitic
Vein qtz
Vein qtz
Locally to 2% pyrite
Oxidized
Oxidized
0.5 - 1% asp
Decreases down hole from 3 - 5% to trace
Semi-massive pyrite
16/WA/229
0
2
4
6
8
Au (g/t)
LITHOLOGY
SHEARING
VEINING
ALTERATION
PYRITE

Figure 5

Figure 6a– Poles to faults

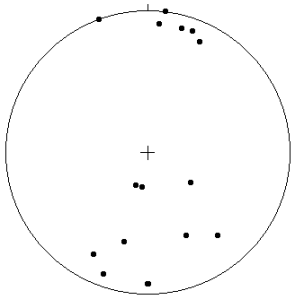

(n=16)

Figure 6b–Rose diagram of faults

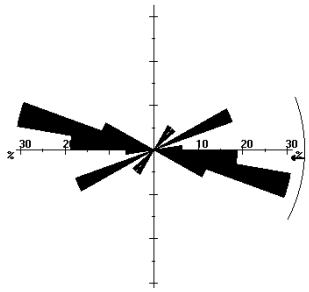

Figure 6c–Bedding plotted as great circles, dips steeply north and south.

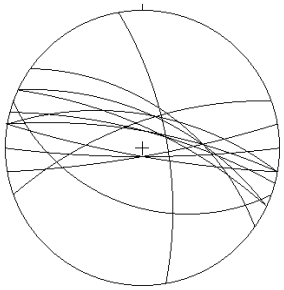

Figure 6

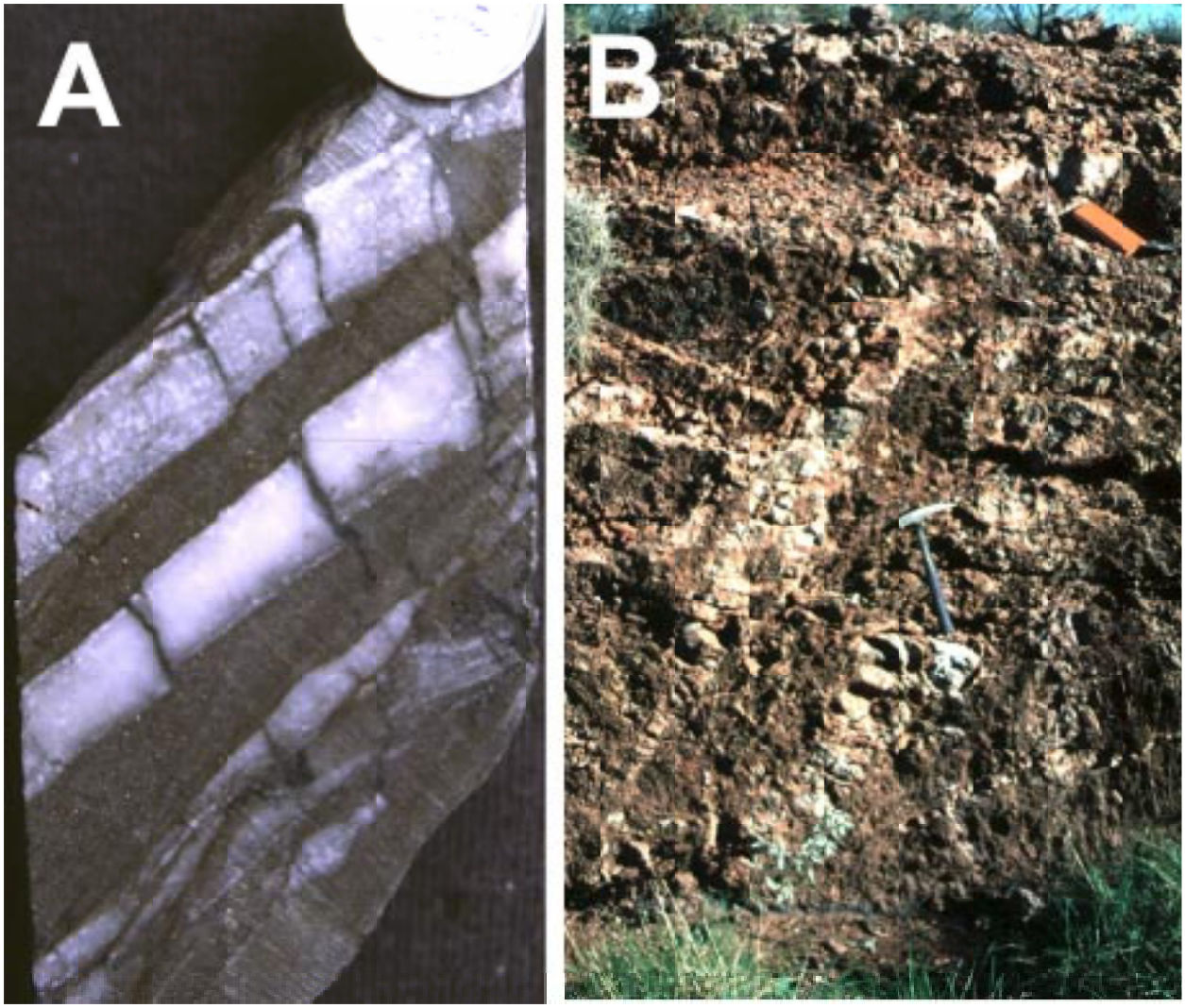

Figure 7

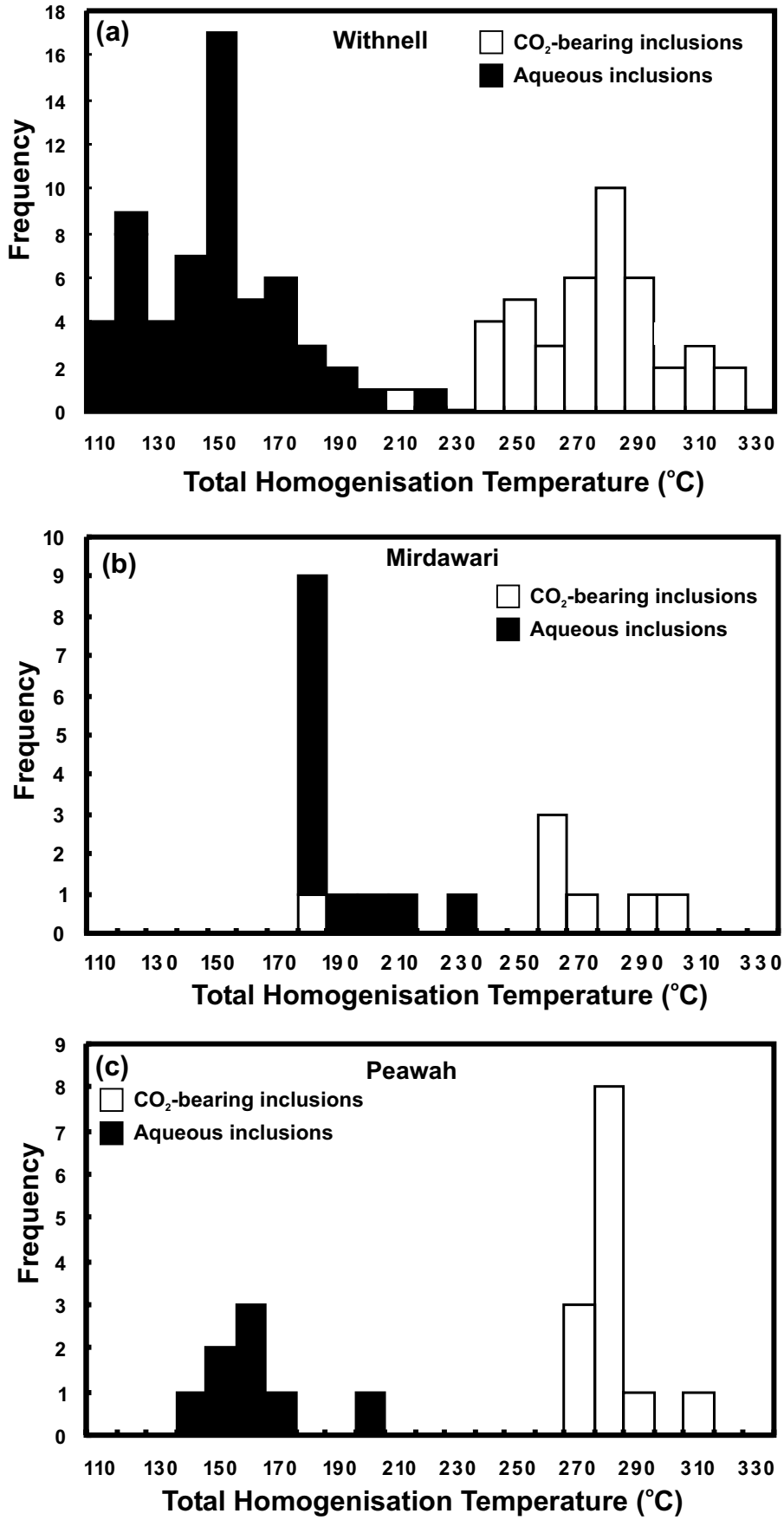
(a)
Withnell
CO2-bearing inclusions
Aqueous inclusions
Frequency
Total Homogenisation Temperature (°C)
(b)
Mirdawari
CO2-bearing inclusions
Aqueous inclusions
Frequency
Total Homogenisation Temperature (°C)
(c)
Peawah
CO2-bearing inclusions
Aqueous inclusions
Frequency
Total Homogenisation Temperature (°C)

Figure 8

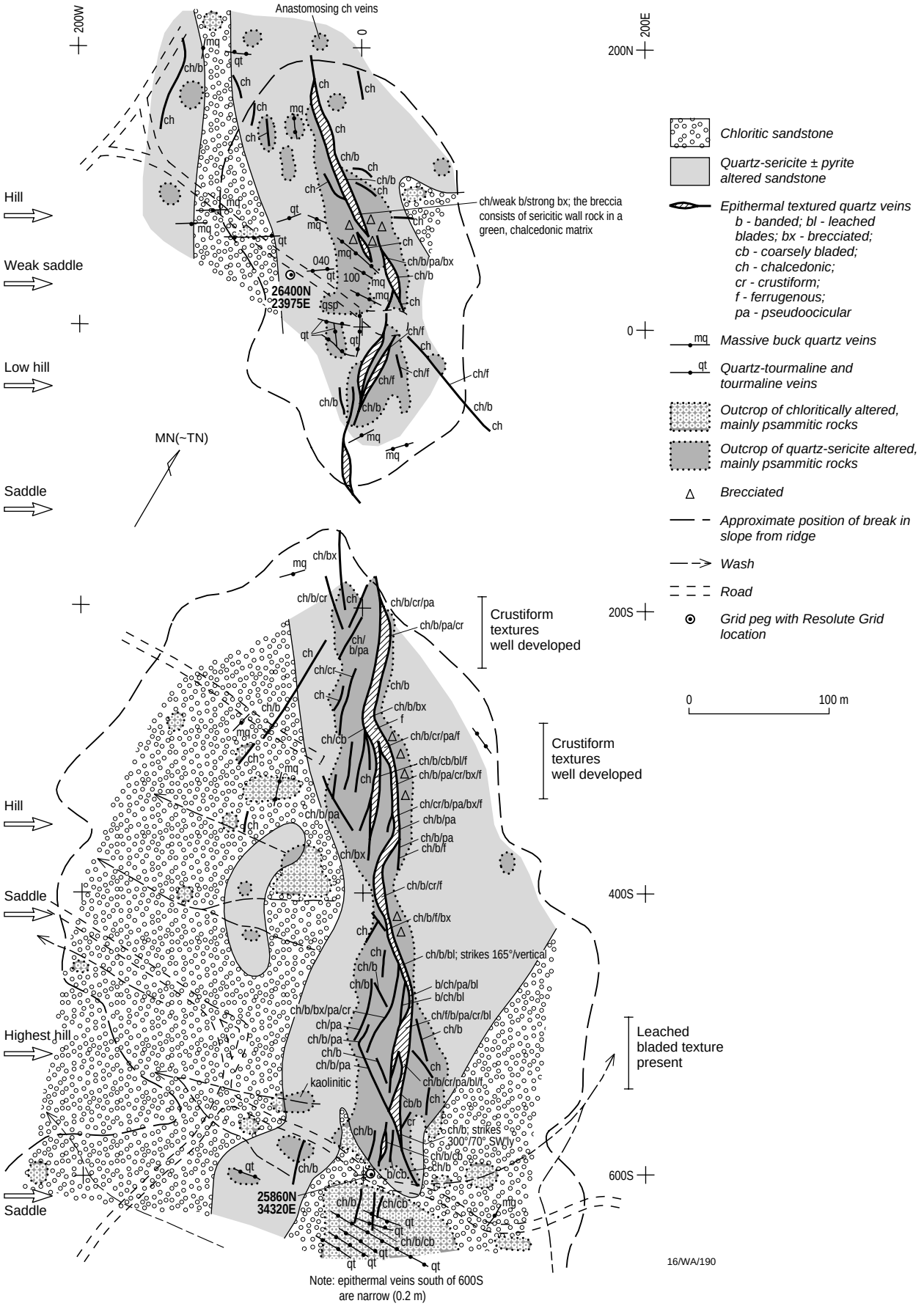
200W
0
200E
200N
0
200S
400S
600S
Hill
Weak saddle
Low hill
Saddle
Hill
Saddle
Highest hill
Saddle
MN(~TN)
Anastomosing ch veins
ch/weak b/strong bx; the breccia consists of sericitic wall rock in a green, chalcedonic matrix
26400N
23975E
25860N
34320E
Crustiform textures well developed
Crustiform textures well developed
Leached bladed texture present
kaolinitic
ch/b; strikes 300°/70° SW'ly
ch/b/bl; strikes 165°/vertical
Chloritic sandstone
Quartz-sericite ± pyrite altered sandstone
Epithermal textured quartz veins
b - banded; bl - leached blades; bx - brecciated; cb - coarsely bladed; ch - chalcedonic; cr - crustiform; f - ferrugenous; pa - pseudoocicular
Massive buck quartz veins
Quartz-tourmaline and tourmaline veins
Outcrop of chloritically altered, mainly psammitic rocks
Outcrop of quartz-sericite altered, mainly psammitic rocks
Brecciated
Approximate position of break in slope from ridge
Wash
Road
Grid peg with Resolute Grid location
0
100 m
16/WA/190
Note: epithermal veins south of 600S are narrow (0.2 m)

Figure 9

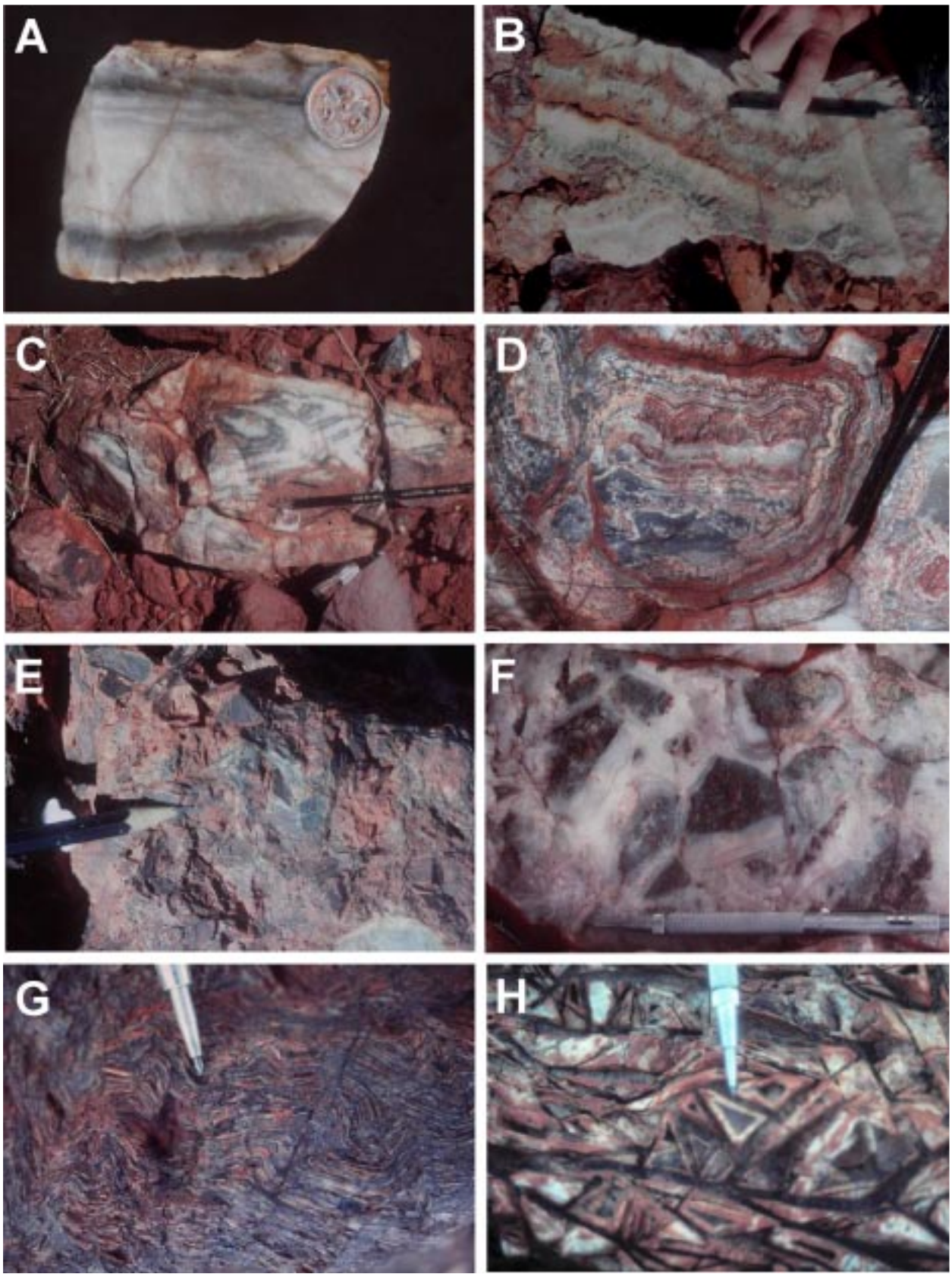

Figure 10

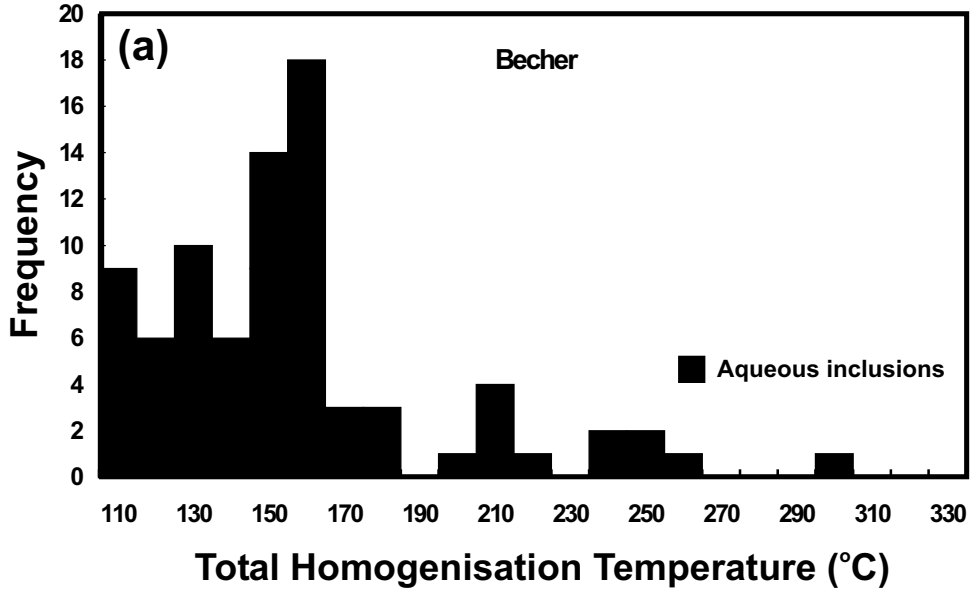
(a)
Becher
Frequency
Aqueous inclusions
Total Homogenisation Temperature (°C)

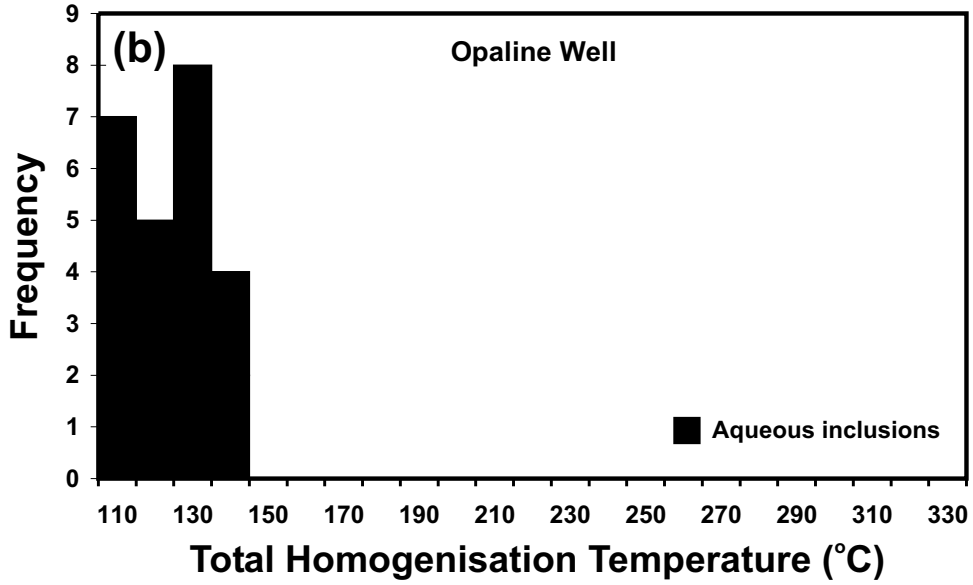
(b)
Opaline Well
Frequency
Aqueous inclusions
Total Homogenisation Temperature (°C)

Figure 11

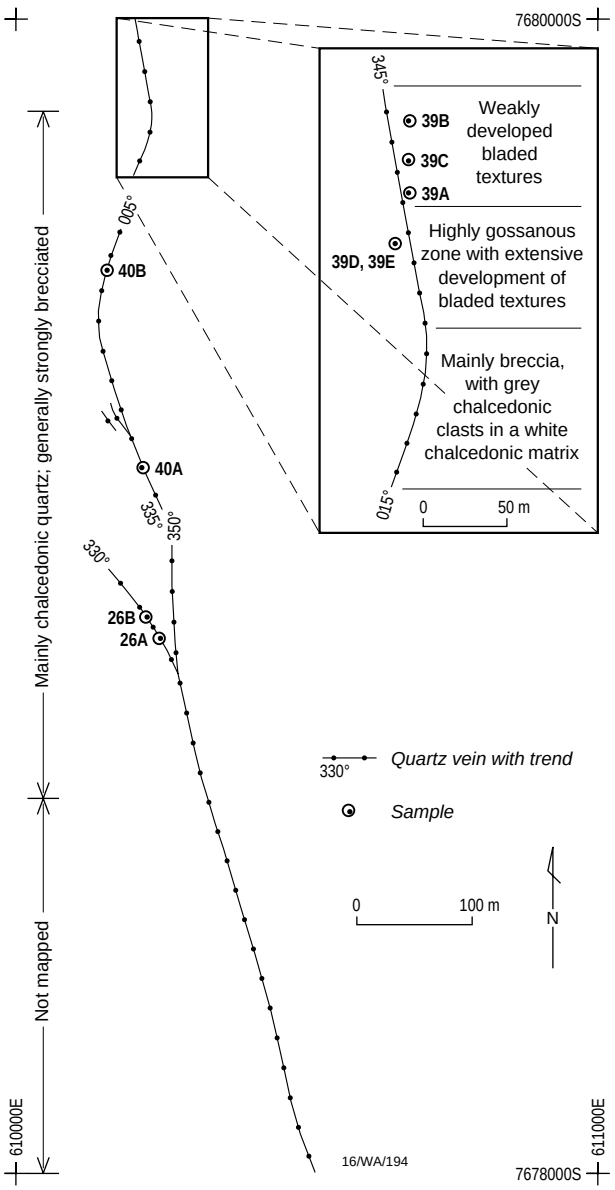
7680000S
345°
39B
39C
39A
Weakly developed bladed textures
Highly gossanous zone with extensive development of bladed textures
39D, 39E
Mainly breccia, with grey chalcedonic clasts in a white chalcedonic matrix
510°
0
50 m
500°
40B
40A
335°
350°
330°
26B
26A
Mainly chalcedonic quartz; generally strongly brecciated
Not mapped
Quartz vein with trend
330°
Sample
0
100 m
N
610000E
611000E
7678000S
16/WA/194

Figure 12

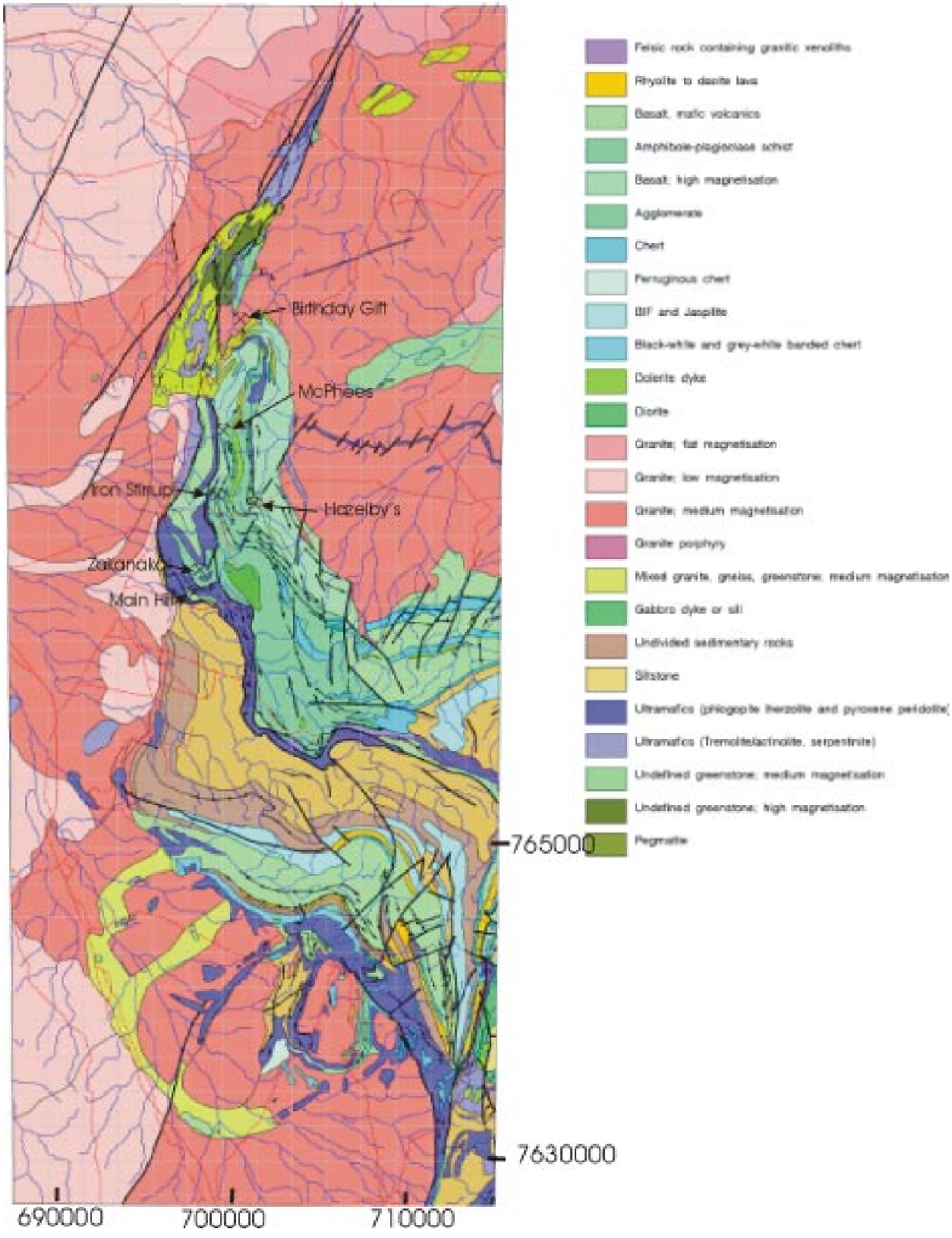
Birthday Gift
McPhees
Iron Stirrup
Hazelby's
Zafanaki
Main Hill
765000
7630000
690000
700000
710000
Felsic rock containing granitic xenoliths
Rhyolite to dacite lava
Basalt, mafic volcanics
Amphibole-plagioclase schist
Basalt, high magnetisation
Agglomerate
Chert
Ferruginous chert
BIF and Jaspilite
Black-white and grey-white banded chert
Dolerite dyke
Diorite
Granite; flat magnetisation
Granite; low magnetisation
Granite; medium magnetisation
Granite porphyry
Mixed granite, gneiss, greenstone; medium magnetisation
Gabbro dyke or sill
Undivided sedimentary rocks
Siltstone
Ultramafics (phlogopite herzolite and pyroxene peridotite)
Ultramafics (Tremolite/actinolite, serpentinite)
Undefined greenstone; medium magnetisation
Undefined greenstone; high magnetisation
Pegmatite

Figure 13

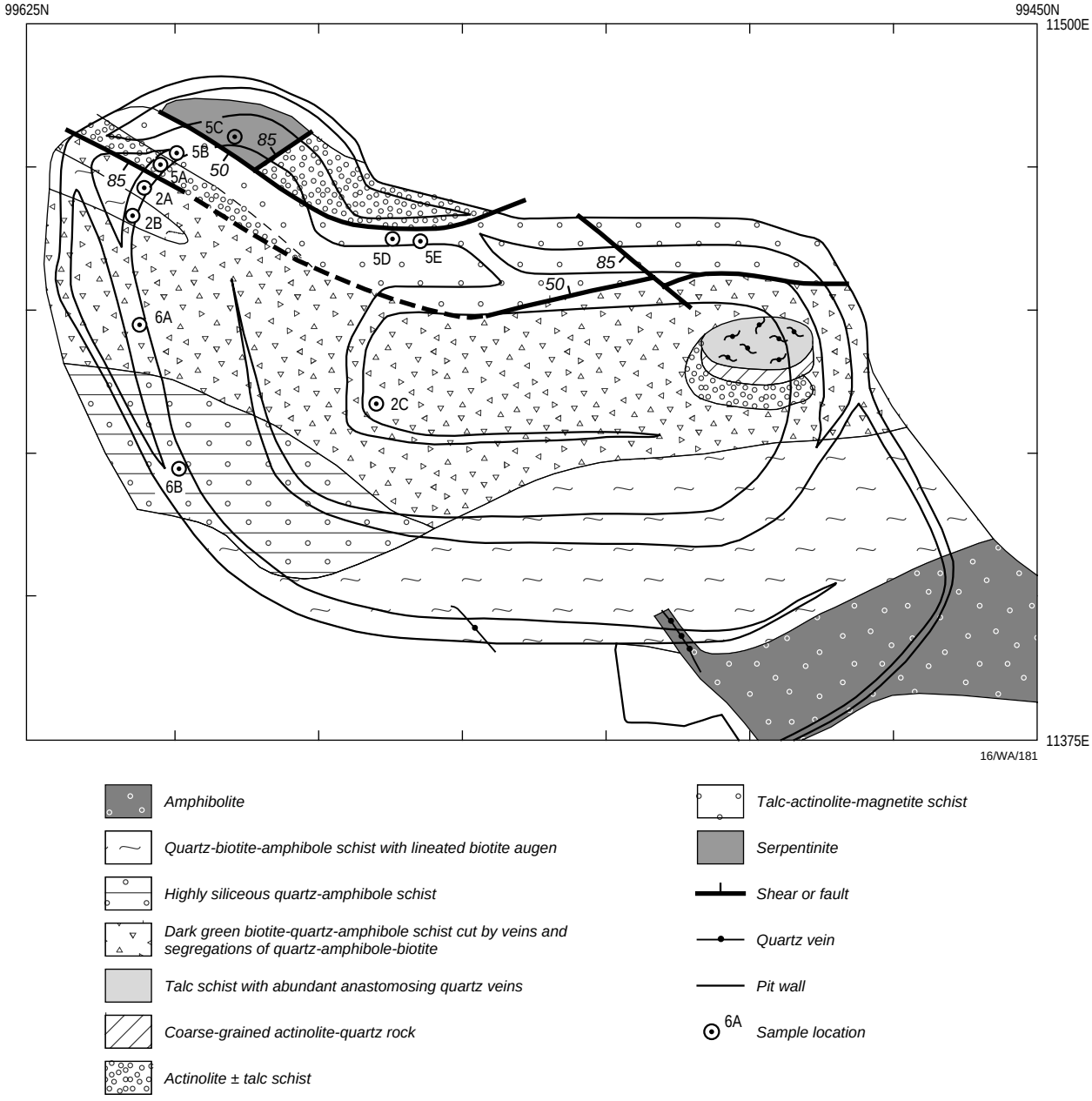
99625N
99450N
11500E
11375E
16/WA/181
5C
85
5B
50
5A
85
2A
2B
5D
5E
85
50
6A
2C
6B
Amphibolite
Quartz-biotite-amphibole schist with lineated biotite augen
Highly siliceous quartz-amphibole schist
Dark green biotite-quartz-amphibole schist cut by veins and segregations of quartz-amphibole-biotite
Talc schist with abundant anastomosing quartz veins
Coarse-grained actinolite-quartz rock
Actinolite ± talc schist
Talc-actinolite-magnetite schist
Serpentinite
Shear or fault
Quartz vein
Pit wall
6A
Sample location

Figure 14a

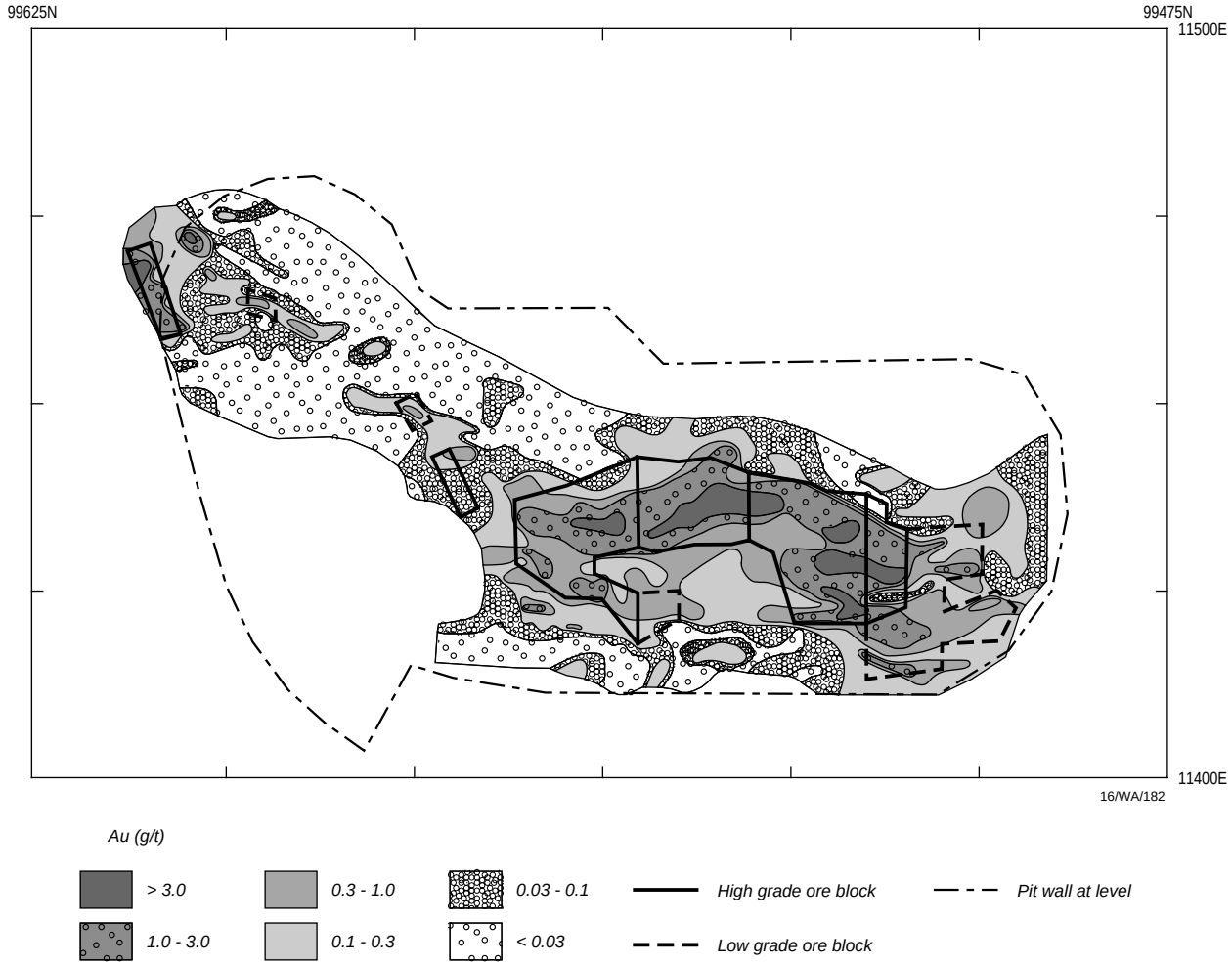
99625N
99475N
11500E
11400E
16/WA/182
Au (g/t)
> 3.0
1.0 - 3.0
0.3 - 1.0
0.1 - 0.3
0.03 - 0.1
< 0.03
High grade ore block
Low grade ore block
Pit wall at level

Figure 14b

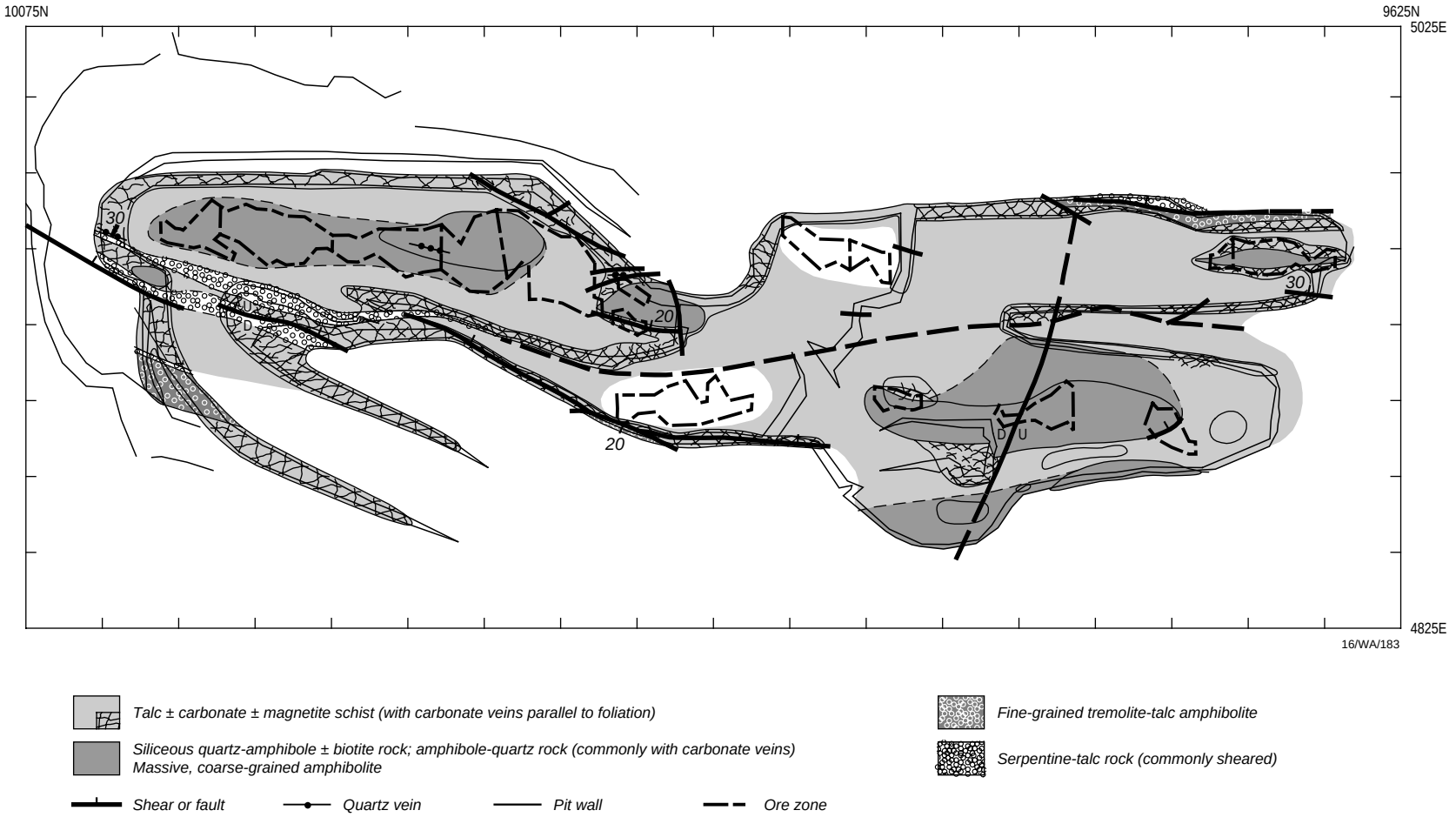
10075N
9625N
5025E
4825E
16/WA/183
30
20
20
30
D
U
D
U
Talc ± carbonate ± magnetite schist (with carbonate veins parallel to foliation)
Siliceous quartz-amphibole ± biotite rock; amphibole-quartz rock (commonly with carbonate veins)
Massive, coarse-grained amphibolite
Fine-grained tremolite-talc amphibolite
Serpentine-talc rock (commonly sheared)
Shear or fault
Quartz vein
Pit wall
Ore zone

Figure 15

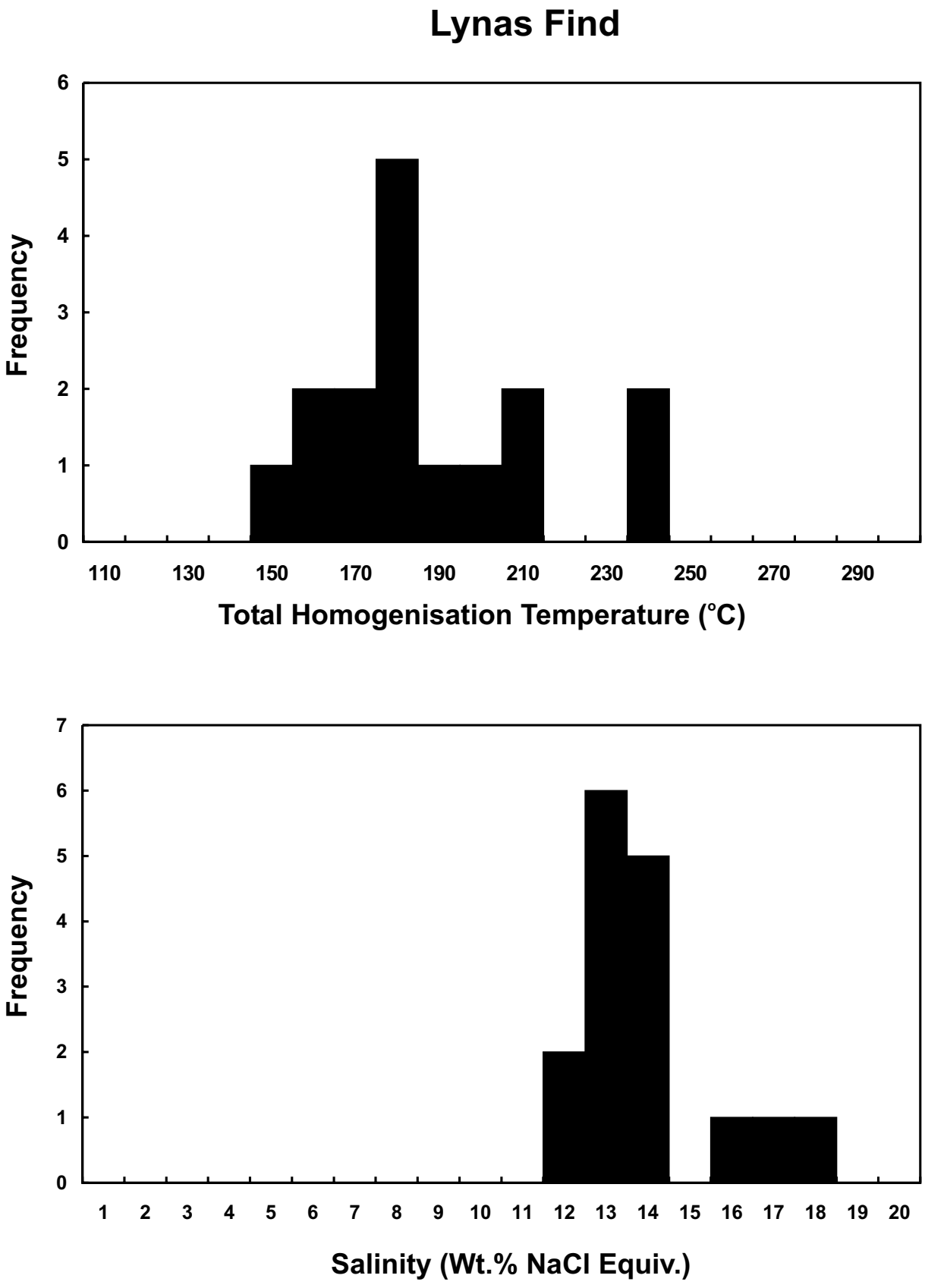
Lynas Find
Frequency
0
1
2
3
4
5
6
110
130
150
170
190
210
230
250
270
290
Total Homogenisation Temperature (°C)
Frequency
0
1
2
3
4
5
6
7
1
2
3
4
5
6
7
8
9
10
11
12
13
14
15
16
17
18
19
20
Salinity (Wt.% NaCl Equiv.)

Figure 16

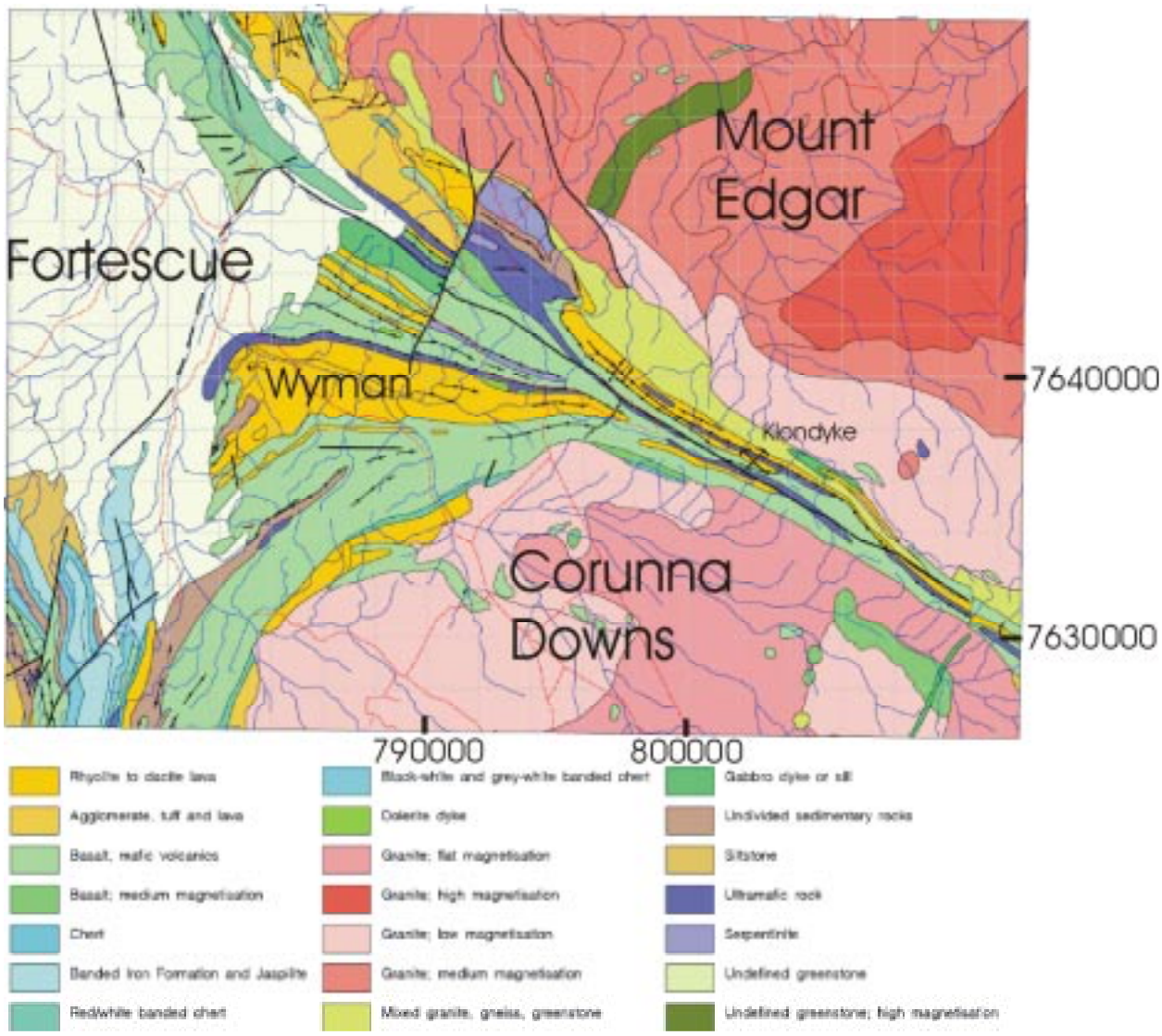
Mount
Edgar
Fortescue
Wyman
Klondyke
Corunna
Downs
7640000
7630000
790000
800000
Rhyolite to dacite lava
Agglomerate, tuff and lava
Basalt, mafic volcanics
Basalt; medium magnetisation
Chert
Banded Iron Formation and Jaspilite
Red/white banded chert
Black-white and grey-white banded chert
Dolerite dyke
Granite; flat magnetisation
Granite; high magnetisation
Granite; low magnetisation
Granite; medium magnetisation
Mixed granite, gneiss, greenstone
Gabbro dyke or sill
Undivided sedimentary rocks
Siltstone
Ultramafic rock
Serpentinite
Undefined greenstone
Undefined greenstone; high magnetisation

Figure 17

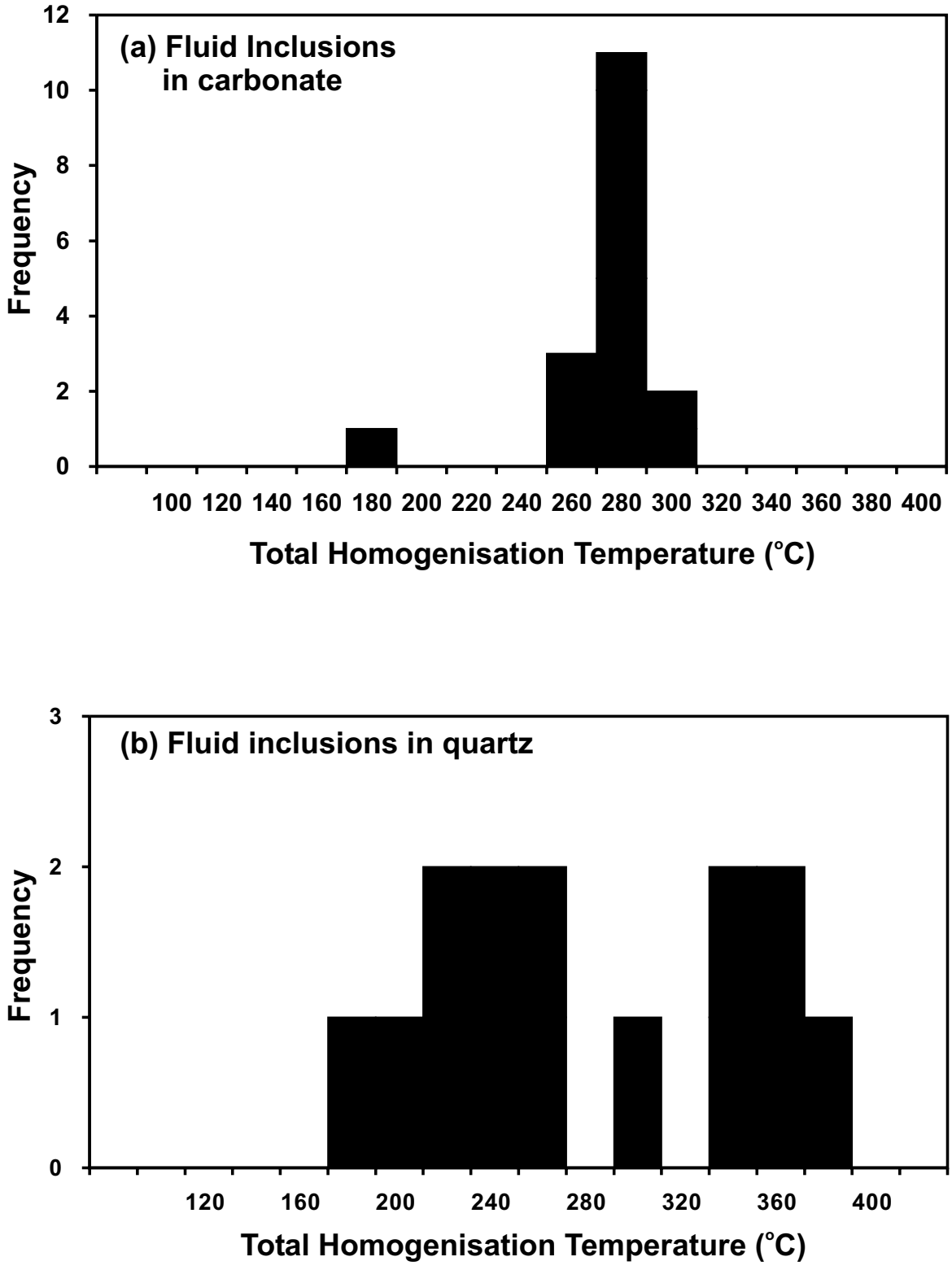
(a) Fluid Inclusions
in carbonate
Frequency
0
2
4
6
8
10
12
100 120 140 160 180 200 220 240 260 280 300 320 340 360 380 400
Total Homogenisation Temperature (°C)
(b) Fluid inclusions in quartz
Frequency
0
1
2
3
120 160 200 240 280 320 360 400
Total Homogenisation Temperature (°C)

Figure 18

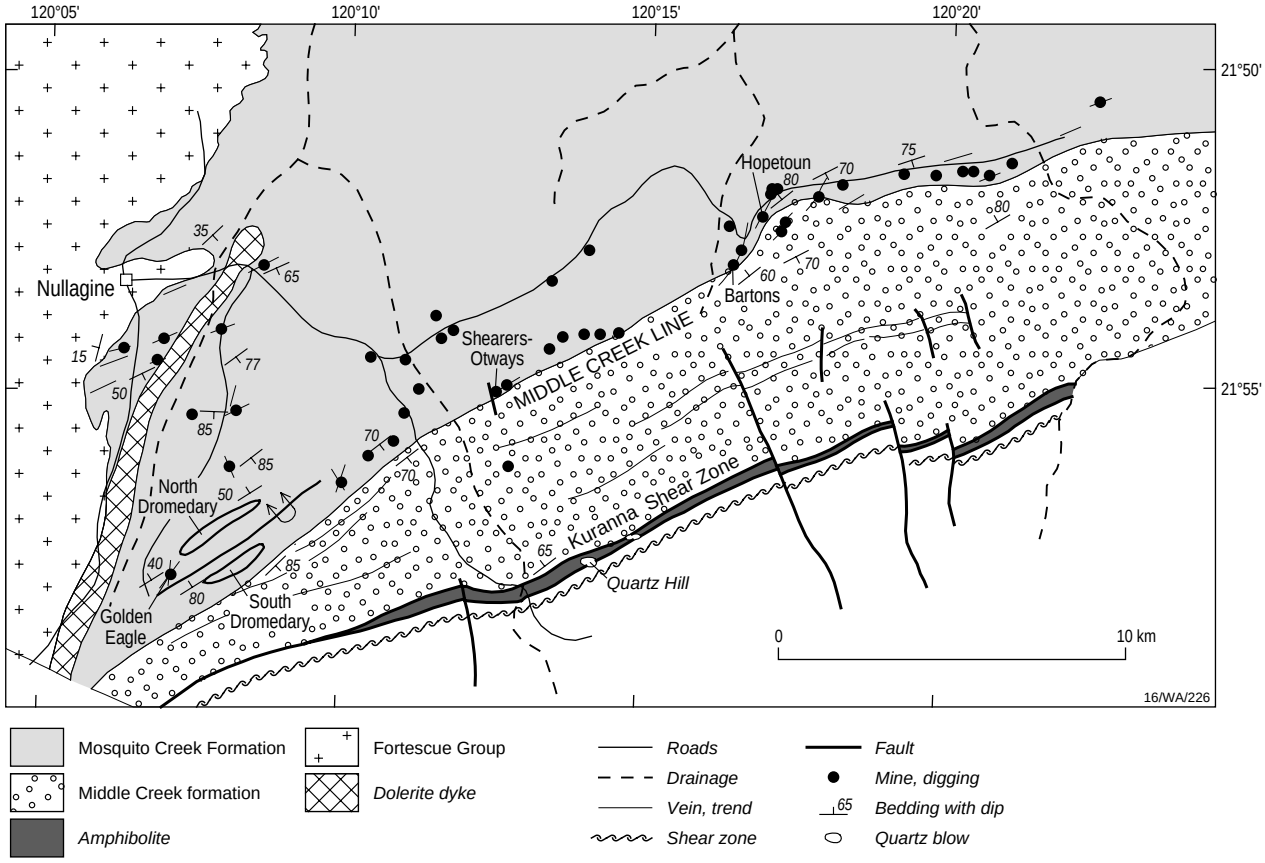
120°05'
120°10'
120°15'
120°20'
21°50'
21°55'
Nullagine
Hopetoun
Bartons
Shearers-
Otways
MIDDLE CREEK LINE
Kuranna Shear Zone
Quartz Hill
North
Dromedary
South
Dromedary
Golden
Eagle
0
10 km
16/WA/226
Mosquito Creek Formation
Middle Creek formation
Amphibolite
Fortescue Group
Dolerite dyke
Roads
Drainage
Vein, trend
Shear zone
Fault
Mine, digging
Bedding with dip
Quartz blow

Figure 19a

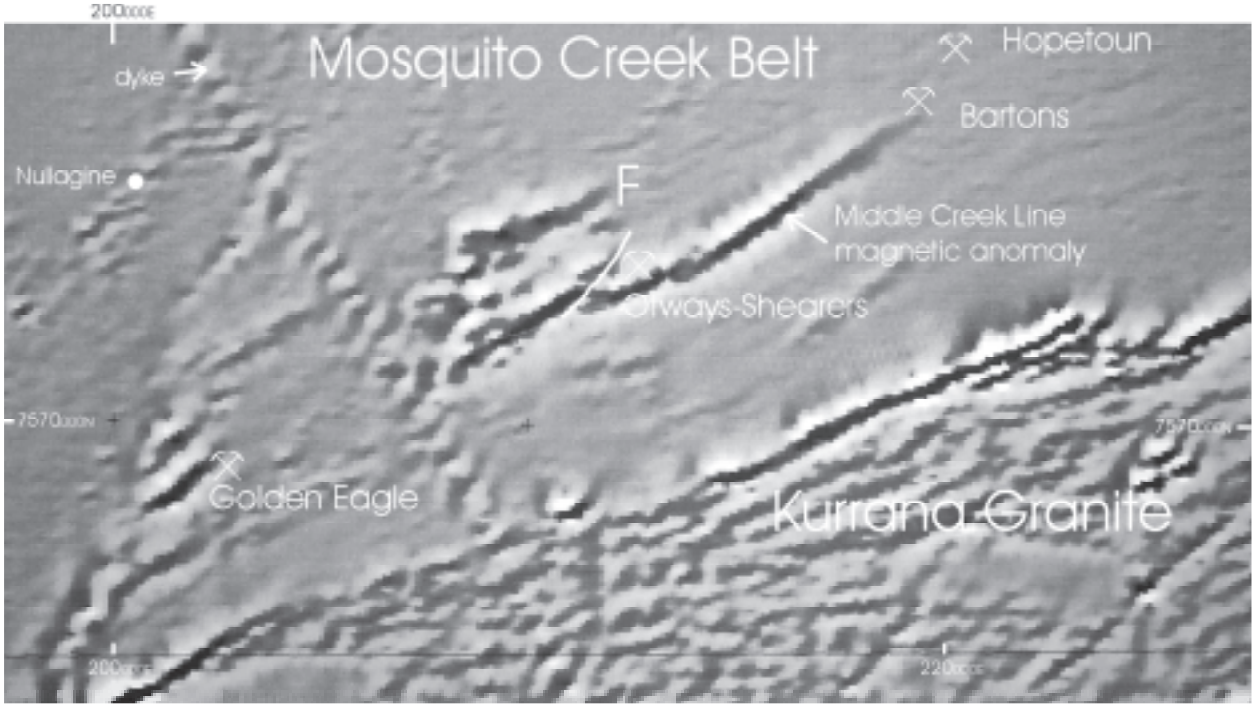
Mosquito Creek Belt
Hopetoun
Bartons
dyke
Nulagine
F
Middle Creek Line
magnetic anomaly
Orways-Shearers
Golden Eagle
Kurrana Granite

Figure 19b

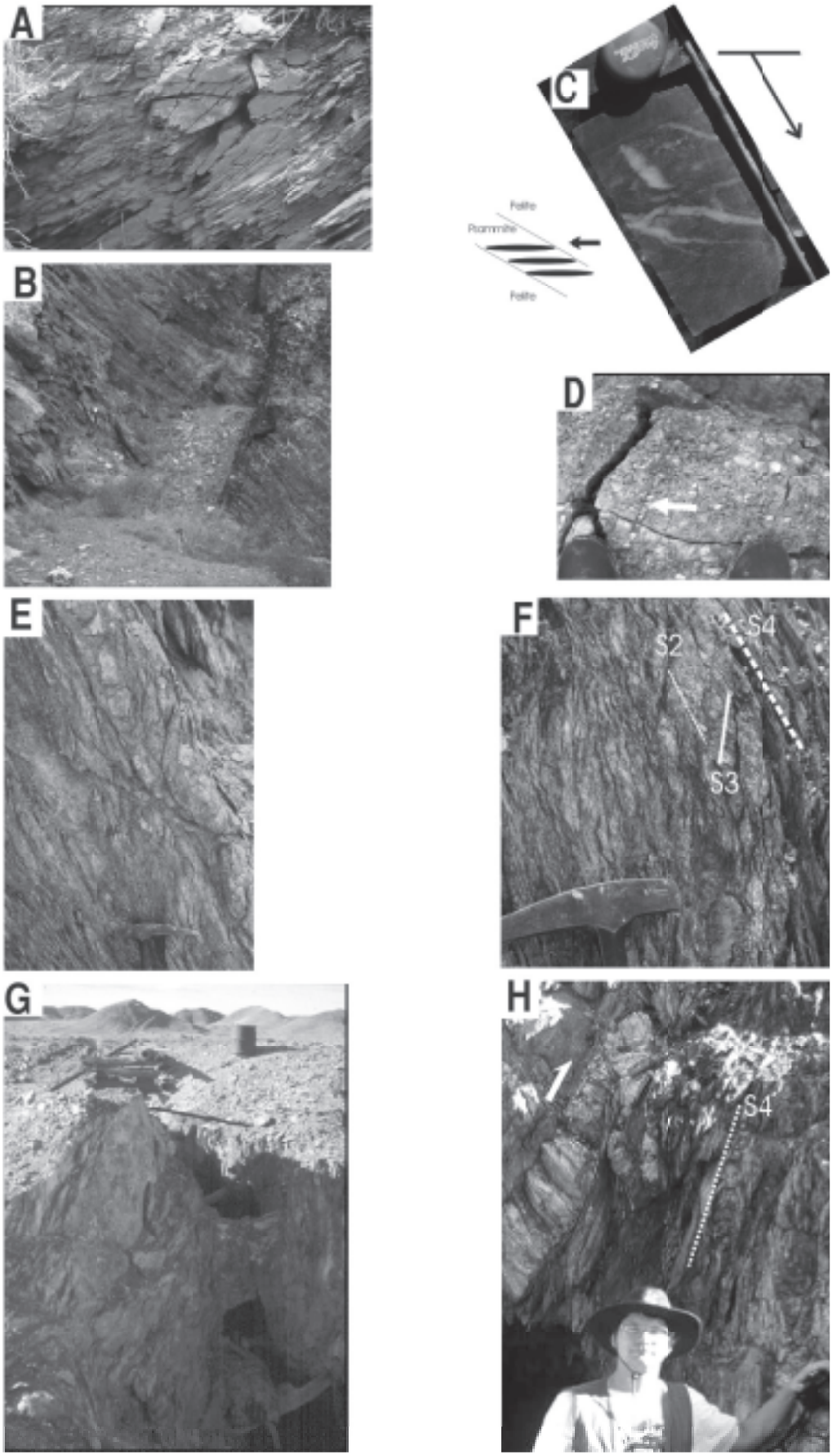

Figure 20

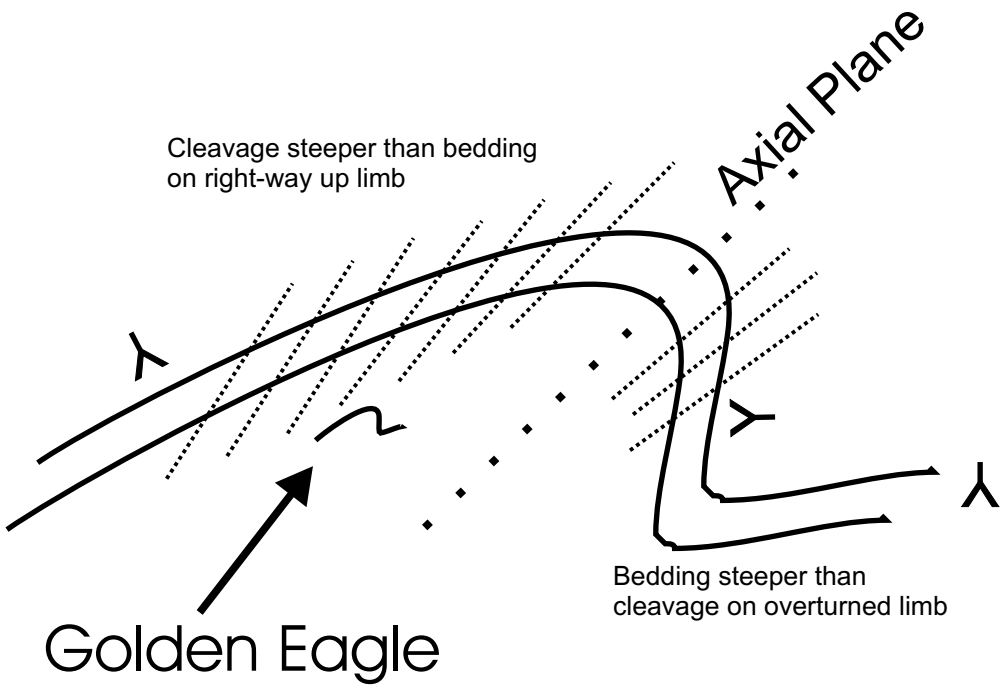
Cleavage steeper than bedding
on right-way up limb
Axial Plane
Bedding steeper than
cleavage on overturned limb
Golden Eagle

Figure 21

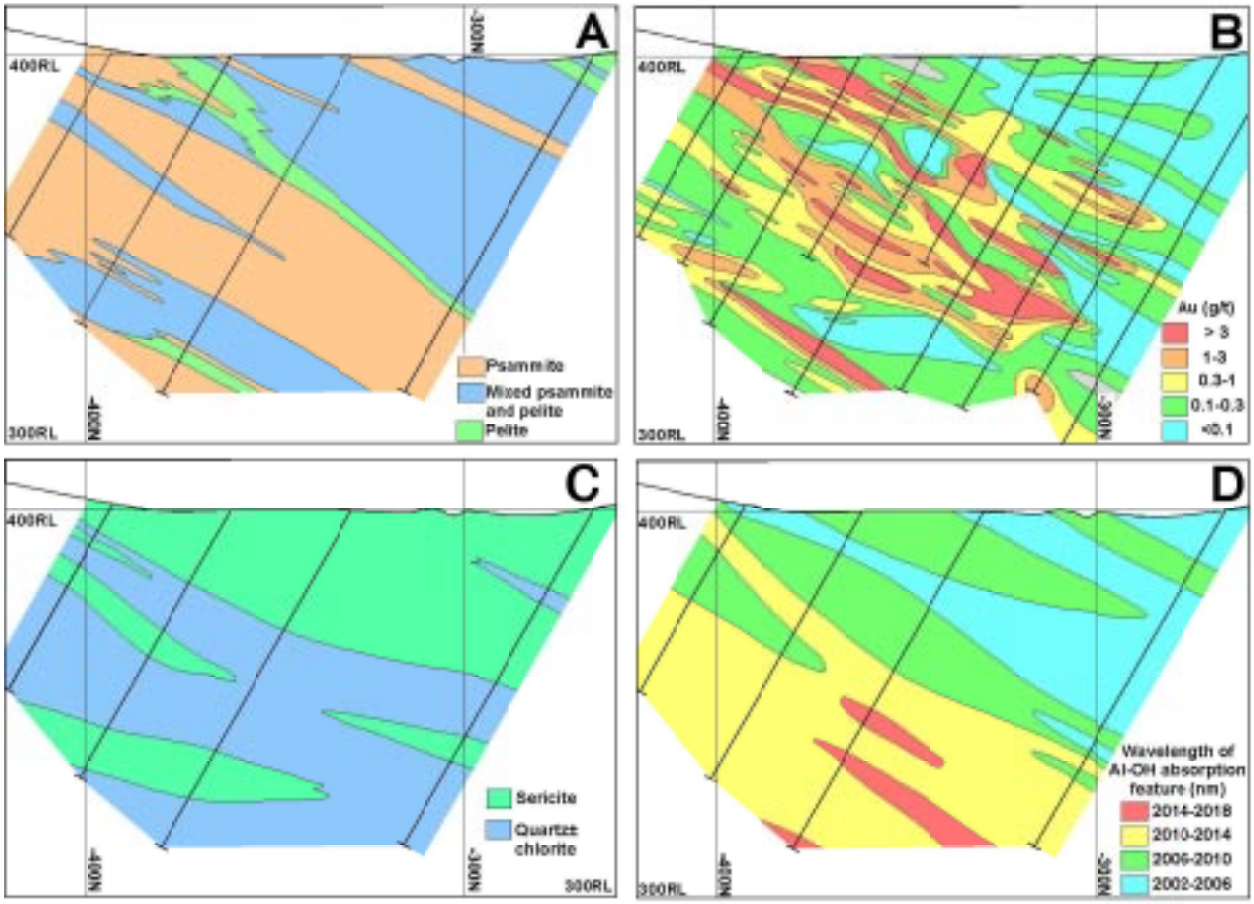
A
400RL
300RL
4100N
3900N
Psammite
Mixed psammite and pelite
Pelite
B
400RL
300RL
4100N
3900N
Au (g/t)
> 3
1-3
0.3-1
0.1-0.3
<0.1
C
400RL
300RL
4100N
3900N
Sericite
Quartz± chlorite
D
400RL
300RL
4100N
3900N
Wavelength of Al-OH absorption feature (nm)
2014-2018
2010-2014
2006-2010
2002-2006

Figure 22

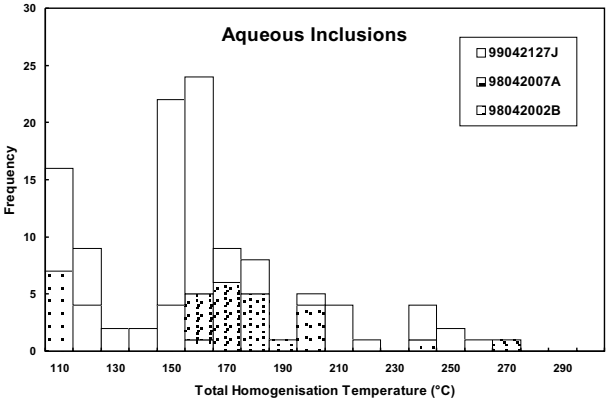
Aqueous Inclusions
99042127J
98042007A
98042002B
Frequency
0
5
10
15
20
25
30
110
130
150
170
190
210
230
250
270
290
Total Homogenisation Temperature (°C)

Figure 23

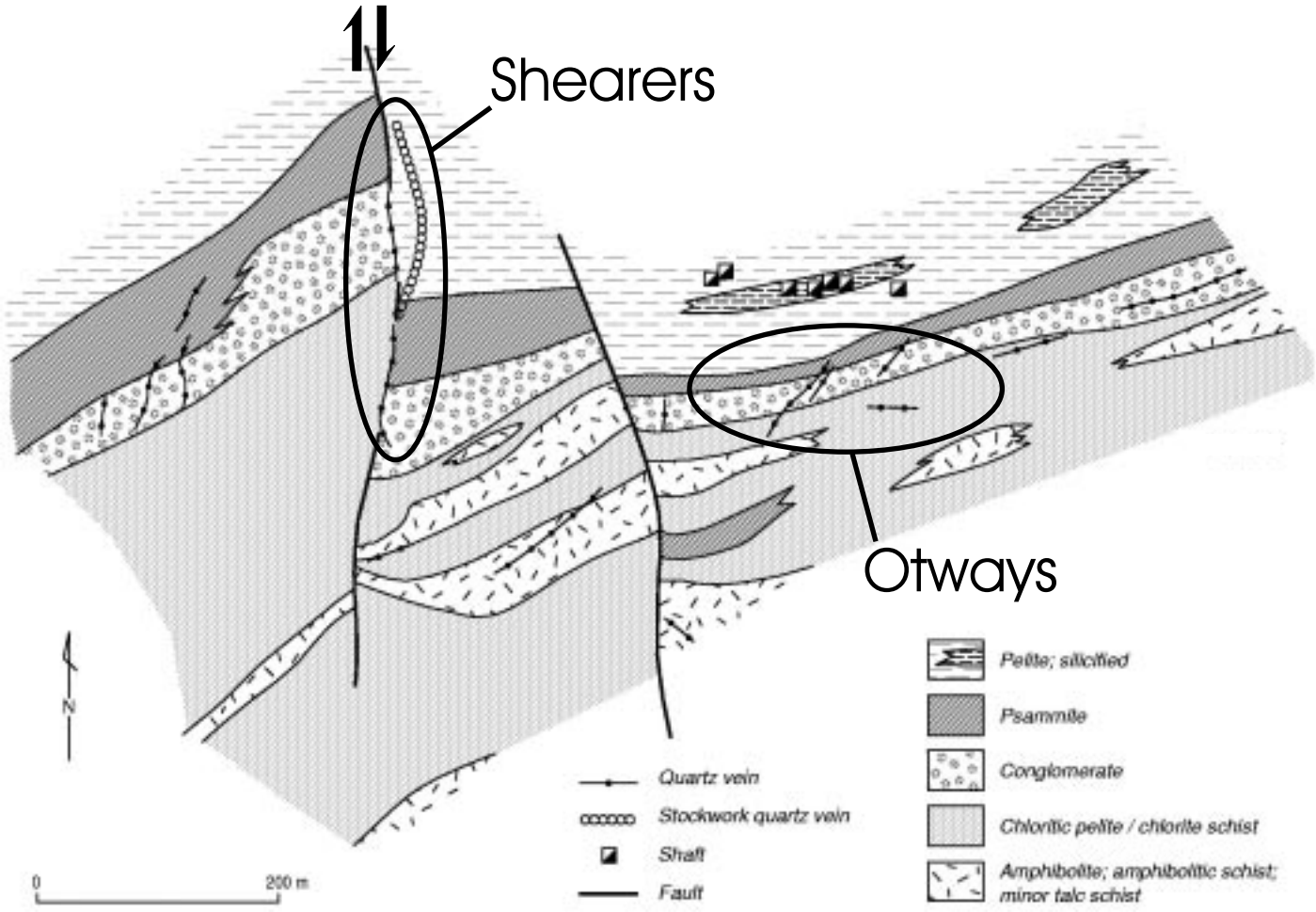
Shearers
Otways
N
0
250 m
Quartz vein
Stockwork quartz vein
Shaft
Fault
Pelite; silicified
Psammite
Conglomerate
Chloritic pelite / chlorite schist
Amphibolite; amphibolitic schist; minor talc schist

Figure 24